Supplementary Materials

Table of contents

Table S1. Global topological properties in dMRI studies included in case-control systematic review

Study Subjects' source	Sample characteristics	Methods of network construction	Main findings	Features	Included in meta-analysis
Abbasi et al. 2018[1] PPMI	PD: 132 HC: 61	Deterministic tractography, fractional anisotropy threshold 0.2, turning angular threshold 45°, fractional anisotropy weighted network, AAL atlas (90*90), sparsity range 0.1-0.3 with step 0.01.	Lower global measures (global efficiency and clustering coefficient) in PD *vs* HC, correlating positively with CSF levels of α-synuclein, amyloid-β42 and total tau. Characteristic path length significantly higher in PD *vs* HC. No significant difference in local efficiency in PD *vs* HC after false discovery rate correction.	Association between CSF biomarkers and graph theory metrics	Yes
Abbasi et al. 2020[2] PPMI	Mild-motor predominant PD: 82 Intermediate PD: 48 Diffuse-malignant PD: 14	Probabilistic tractography, number of tracts weighted network, Brainnetome atlas (246*246).	At baseline, diffuse-malignant PD *vs* mild-motor predominant and intermediate PD, had significantly lower global efficiency and higher characteristic path length. Lower global efficiency and higher characteristic path length at baseline significantly correlated with increase in global composite outcome, increase in postural instability gait difficulty score and decline in Montreal cognitive assessment score after 4.5-years follow-up.	Monitoring severity and progression	No No HC
Bergamino et al. 2023[3] PPMI	PD: 86 HC: 75	Tractography using *tckgen* (MRtrix3) with second-order integration over fiber orientation distribution algorithm, 5 million streamlines (length 4-200 mm, unidirectional tracking, maximum angle 45°), AAL atlas.	At baseline, network density was lower in PD *vs* HC, but not statistically significant after correction for multiple comparisons. No significant differences between PD *vs* HC in global efficiency, strength, or assortativity. After 1.5-years follow-up, PD still had lower network density, but the difference did not survive correction, with no significant differences in global efficiency, strength, or assortativity.	Monitoring progression	No Subjects overlap
Chen et al. 2022[4] PPMI	PD with probable RBD: 74 PD without probable RBD:97 HC: 73	Deterministic tractography, fractional anisotropy threshold of 0.2, turning angular threshold 45°, binary network (threshold: number of streamlines ≥ 3), AAL atlas (90*90).	PD with probable RBD had lower global efficiency and higher characteristic path length *vs* PD without probable RBD and HC. No significant differences in small-worldness among PD with and without probable RBD, and HC.	Rapid eye movement sleep behavior disorder	No Subjects overlap
Chen et al. 2023[5] PPMI	PD Q1 group (age rank: 0%~25%): 36 PD Q2-3 group (age rank: 26%~75%): 73 PD Q4 group (age rank: 76%~100%): 37	Deterministic tractography, fractional anisotropy threshold 0.2, turning angular threshold 45°, number of streamlines weighted network, AAL atlas (90*90), sparsity range 0.05-0.50 with step 0.05.	PD in Q4 had lower hierarchy, global efficiency, local efficiency, clustering coefficient, and higher characteristic path length, normalized characteristic path length, and small-worldness *vs* Q1 and Q2–3. No significant differences in network assortativity or synchronization across age quartiles. No significant differences in global graph theoretical metrics between male and female PD. Controlling for gender, years of education and duration, age was negatively associated with hierarchy, global efficiency, local efficiency, and clustering coefficient, and positively associated with characteristic path length, normalized characteristic path length, and small-worldness.	Age and gender differences in brain network topological measures in PD	No No HC in network analysis

Chung et al. 2022[6] South Korea	PD with high risk for developing dementia (5-year conversion from MCI): 38 PD with low risk for developing dementia: 37 HC: 23	Deterministic tractography, fractional anisotropy threshold 0.15, turning angular threshold 45°, length 30 mm to 300 mm, mean FA values of all generated fiber tracts weighted network, AAL atlas 2 (120*120), edges were retained if they appeared in >50% of participants.	PD with high risk for developing dementia had lower global efficiency, clustering coefficient and higher characteristic path length *vs* PD with low risk for dementia and HC. No significant differences in global topological metrics between PD with low risk for developing dementia and HC.	Predicting dementia conversion in PD with MCI	Yes
Colon-Perez et al. 2018[7] USA	PD without memory impairment (memory composite score ≤ −1.5): 31 PD with memory impairment: 9 HC: 40	Deterministic tractography, w(e_{ij}) weighted network, Desikan–Killiany and subcortical atlas (82*82), no threshold.	Lowest strength and characteristic path length in PD with memory impairment, followed by PD without memory impairment, highest in HC. No significant differences in density, clustering coefficient and small worldness among PD with and without memory impairment, and HC. Using the FA-weighted network, no differences in strength, clustering coefficient, or path length.	Memory impairment, edge weight	Yes - but PD with memory impairment excluded due to < 10 participants
Du et al. 2022[8] China	PD levodopa irresponsive (UPDRS-III score improvement rate < 30%): 22 PD levodopa responsive group (improvement rate ≥ 30%): 32	Deterministic tractography, fractional anisotropy threshold 0.2, turning angular threshold 45°, number of streamlines ≥ 3, number of streamlines or fractional anisotropy weighted network, AAL atlas modification (124*124).	For the number of streamlines weighted network, responsive PD had higher global efficiency and local efficiency, and lower characteristic path length *vs* irresponsive PD. No significant differences in clustering coefficient, normalized clustering coefficient, normalized characteristic path length, or small-worldness between the two groups. For the fractional anisotropy weighted network, only higher local efficiency was found in responsive PD.	Levodopa responsiveness	No No HC
Frigerio et al. 2024[9] Netherlands Brain Bank Normal Aging Brain Collection Amsterdam	PD: 19 HC: 15	Probabilistic tractography, binary network, Brainnetome and subcortical and cerebellum atlas (225*225), threshold: top 20% strongest connections retained for each subject.	PD had higher clustering coefficient *vs* HC. No significant difference in global efficiency between two groups.	Postmortem MRI and histopathology	No Post-mortem
Galantucci et al. 2017[10] Serbia	PD with MCI: 54 PD without MCI: 54 HC: 41	Deterministic tractography, fractional anisotropy threshold 0.15, turning angular threshold 45°, number of streamlines ≥3, edges were retained if they appeared in > 40% of participants, mean fractional anisotropy or mean diffusivity weighted network, Desikan–Killiany, subcortical and brainstem atlas (83*83).	PD without MCI had higher betweenness centrality and lower assortativity (MD network) *vs* HC, while other global metrics, including degree, clustering coefficient, density, global efficiency, characteristic path length, and small-worldness, had no significant differences. PD with MCI had higher betweenness centrality, assortativity (FA network), and characteristic path length, and lower degree, clustering coefficient, density, and global efficiency (FA network) *vs* HC. Compared to PD without MCI, those with MCI had lower clustering coefficient and global efficiency (FA network) and higher assortativity.	MCI	Yes

Gan et al. 2024[11] China	PD with impulse control disorders: 17 PD without impulse control disorders: 17 HC: 18	Deterministic tractography, number of streamlines ≥ 10, AAL atlas (116*116).	PD with impulse control disorders and HC had higher global efficiency and lower characteristic path length relative to PD without impulse control disorders. No differences in local efficiency, clustering coefficient, or small-worldness among the three groups. Questionnaire for Impulsive-Compulsive Disorders in Parkinson's Disease-Rating Scale scores were significantly correlated with characteristic path length ($r = -0.651$) and global efficiency ($r = 0.674$).	Impulse control disorders	Yes
Ge et al. 2024[12] China	PD with apathy: 47 PD without apathy: 37 HC: 40	Deterministic tractography, fractional anisotropy threshold 0.2, turning angular threshold 45°, number of streamlines > 10, AAL atlas (90*90).	PD without apathy had lower local efficiency and clustering coefficient *vs* HC. PD with apathy had lower local efficiency than HC and higher clustering coefficient than PD without apathy. No significant differences in global efficiency, characteristic path length or small-worldness among the three groups.	Apathy	Yes
Gou et al. 2018[13] PPMI	PD with depression: 28 PD without depression: 56 HC: 37	Deterministic tractography, fractional anisotropy threshold 0.2, turning angular threshold 45°, number of streamlines ≥3, number of streamlines weighted network, AAL atlas (90*90).	PD with depression had lower global efficiency and higher characteristic path length *vs* HC; also lower global and local efficiency and higher characteristic path length *vs* PD without depression. PD without depression had lower normalized characteristic path length and higher small-worldness *vs* HC. No significant differences in clustering coefficient, normalized clustering coefficient, or modularity among the three groups.	Depression	No Subjects overlap
Guan et al. 2019[14] China	PD: 90 HC:38	Deterministic tractography, fractional anisotropy threshold of 0.2, turning angular threshold 45°, fractional anisotropy weighted or binary network, AAL atlas (90*90), sparsity range 0.10-0.30 with step 0.02.	No significant differences in clustering coefficient, characteristic path length, local efficiency or global efficiency in PD *vs* HC in both weighted and binary networks.	Iron accumulation	Yes
Hu et al. 2020[15] China	PD with depression: 20 PD without depression: 47 HC: 46	Deterministic tractography, fractional anisotropy threshold of 0.2, turning angular threshold 45°, ROI-size-corrected fiber number weighted network, number of streamlines ≥ 1, 2, 3, 4, or 5, AAL atlas (90*90).	PD with depression had higher local efficiency, normalized clustering coefficient and small-worldness *vs* PD without depression; also higher characteristic path length, local efficiency, normalized characteristic path length, small-worldness, and lower global efficiency *vs* HC. PD without depression had lower local efficiency and normalized clustering coefficient *vs* HC. No significant differences in strength or clustering coefficient among the three groups.	Depression	Yes
Inguanzo et al. 2021[16] Spain	PD with MCI: 27 PD without MCI: 35 HC: 51	Probabilistic tractography, number of streamlines weighted network, number of streamlines ≥2, Desikan–Killiany and subcortical atlas (86*86), edges retained if they appeared in >50% of participants.	No significant differences in modularity, degree, small-worldness, normalized clustering coefficient or normalized characteristic path length among PD with and without MCI, and HC.	MCI	Yes
Jin et al. 2022[17] China	PD with freezing of gait: 21 PD without freezing of gait: 34	Deterministic tractography, fractional anisotropy threshold of 0.2, turning angular threshold 45°, number of streamlines ≥ 3, AAL atlas (90*90).	PD with freezing of gait had lower normalized clustering coefficient, small-worldness, clustering coefficient, and higher local efficiency *vs* HC. No significant differences in characteristic path length, global efficiency or normalized characteristic path length	Freezing of gait	Yes

	HC: 23		among the three groups. No significant correlation between freezing of gait questionnaire scores and global metrics.		
Kamagata et al. 2018[18] Japan	PD: 21 HC: 21	Probabilistic tractography or deterministic tractography, fiber orientation distribution threshold of 0.06 or 0.1, maximum curvature of 45°, length 4 mm to 200 mm, number of streamlines weighted network, Desikan–Killiany and subcortical atlas (84*84), sparsity range 0.10-0.30 with step 0.05.	PD had lower strength, clustering coefficient, global efficiency and small-worldness along with higher characteristic path length *vs* HC, using probabilistic MSMT-CSD tracking. Using probabilistic SSST-CSD tracking, only lower strength and small-worldness in PD *vs* HC. No significant differences in global metrics between the two groups with deterministic SSST-CSD. No correlations between global topological metrics and clinical measures.	Multi-shell, multi-tissue, constrained spherical deconvolution	Yes
Koirala et al. 2019[19] Germany	PD: 12 $HC_{middle\text{-}aged}$: 13	Probabilistic tractography, number of streamlines weighted network, AAL atlas (116*116), edges retained if they appeared in >5% of participants.	PD had lower characteristic path length and eccentricity *vs* middle-aged HC.	Age	Yes
Kok et al. 2020[20] Netherlands, Canada	Dutch dataset PD: 14 HC: 15 Canadian dataset PD: 19 HC: 18	Probabilistic tractography, fiber orientation distribution threshold of 0.1, maximum curvature of 30°, length 50 mm to 500 mm, fractional anisotropy- or number of streamlines- weighted network or binary network, Desikan–Killiany and subcortical atlas (87*87), edges retained if they appeared in >50% of participants.	No significant differences in local and global efficiency in PD *vs* HC in Dutch and Canadian datasets, using either fractional anisotropy- or number of streamlines- weighted network or binary network. However, in the Dutch dataset, local and global efficiency were negatively correlated with UPDRS motor scores using the fractional anisotropy-weighted network; in contrast, in the Canadian dataset no significant correlations between global metrics and UPDRS motor scores.		Yes
Li et al. 2017[21] China	PD: 35 HC: 26	Deterministic tractography, fractional anisotropy threshold 0.2, turning angular threshold 45°, fractional anisotropy weighted network, number of streamlines ≥ 0, 3, or 5, AAL atlas (90*90), Harvard-Oxford Structural Atlas (110*110), AAL atlas (1024*1024), edges retained if they appeared in >50% of participants.	PD had lower global efficiency and higher characteristic path length *vs* HC. Negative correlation between global efficiency and disease duration; positive correlation between characteristic path length and disease duration.	Robustness of atlas and threshold of number of streamlines	Yes
Li et al. 2024[22] China	PD with vertebrobasilar dolichoectasia: 16 PD without vertebrobasilar dolichoectasia: 158	Deterministic tractography, fractional anisotropy threshold 0.2, turning angular threshold 45°, binary number of streamlines*fractional anisotropy weighted network, number of streamlines ≥3, AAL atlas 3 (170*170), edges retained if they appeared in >80% of participants.	PD with vertebrobasilar dolichoectasia had lower global efficiency and local efficiency and higher hierarchy *vs* PD without vertebrobasilar dolichoectasia. No significant differences in characteristic path length, clustering coefficient, normalized characteristic path length, normalized clustering coefficient, rich club, assortativity and synchronization between the two groups.	Vertebrobasilar dolichoectasia	No No HC
Li et al. 2024[23] China	PD with postural instability/gait difficulty: 31 PD without postural instability/gait difficulty: 30	Deterministic tractography, fractional anisotropy threshold 0.2, turning angular threshold 45°, binary number of streamlines weighted network, number of streamlines ≥ 3, AAL atlas (116*116).	PD with postural instability/gait difficulty had lower local efficiency, clustering coefficient, global efficiency and higher characteristic path length, normalized clustering coefficient and small-worldness *vs* HC. Higher characteristic path length in PD with postural instability/gait difficulty *vs* PD without postural instability/gait difficulty.	Postural instability/gait difficulty	Yes

	HC: 35				
Liu et al. 2024[24] PPMI	PD: 127	Deterministic tractography, fractional anisotropy threshold 0.2, turning angular threshold 45°, number of streamlines (number of streamlines ≥ 3) or fractional anisotropy weighted network, AAL atlas 3 (170*170).	No correlations between global network metrics and semantic fluency test in either the fractional anisotropy- or number of streamlines- weighted networks.	Semantic dysfunction	No No HC
Mishra et al. 2020[25] PPMI	PD: 70 HC: 41	Deterministic tractography, fractional anisotropy threshold 0.2, turning angular threshold 35°, length threshold of 10 mm, number of streamlines*fractional anisotropy weighted network, number of streamlines ≥ 1, AAL and ATAG subcortex atlas (102*102).	PD had lower normalized clustering coefficient, modularity and small-worldness *vs* HC. No correlations between global network measures and clinical variables in either group.		No Subjects overlap
Nigro et al. 2016[26] Italy	PD: 21 HC: 30	Deterministic tractography, fractional anisotropy threshold 0.1, turning angular threshold 35°, number of streamlines*fractional anisotropy weighted network, number of streamlines ≥3, AAL atlas (90*90).	PD had lower global efficiency and clustering coefficient, strength and higher characteristic path length *vs* HC. No significant difference in density between the two groups. No correlations with UPDRS-ME, Hoehn and Yahr, HAMA, or Beck Depression Inventory scores and global metrics.		Yes
Ren et al. 2024[27] China	PD: 42 HC: 38	Probabilistic tractography, AAL atlas (90*90).	PD had lower global efficiency and local efficiency, and higher characteristic path length and normalized characteristic path length *vs* HC. Characteristic path length was correlated positively with MDS-UPDRS, HAMA, PDQ39, FOG-Q, and negatively with MoCA scores. Normalized characteristic path length was positively associated with MDS-UPDRS, MDS-UPDRS-III, PDQ39, FOG-Q, and negatively with MoCA scores. Global efficiency was negatively associated with MDS-UPDRS, HAMA and PDQ39.	Gait disturbance (FOG-Q)	Yes
Shah et al. 2017[28] India	PD: 65 HC: 65	Probabilistic tractography, number of streamlines weighted network, Desikan–Killiany and subcortical atlas (86*86), edges retained if they appeared in >50% of participants.	PD had lower clustering coefficient *vs* HC. No significant differences in global efficiency, characteristic path length, density and modularity between PD *vs* HC.		No No available data
Shang et al. 2023[29] China	PD: 69 HC: 70	Fractional anisotropy threshold 0.1, turning angular threshold 35°, fractional anisotropy or mean kurtosis weighted network, AAL atlas (90*90), sparsity range 0.05-0.30 with step 0.01.	PD had lower clustering coefficient, local efficiency, global efficiency, and higher characteristic path length and normalized characteristic path length *vs* HC. No significant differences in normalized clustering coefficient and small-worldness between PD *vs* HC.		Yes
Vriend et al. 2018[30] Netherlands	PD: 23 HC: 38	Probabilistic tractography, curvature threshold of 0.2, ROI corrected, number of streamlines weighted network, Brainnetome and subcortical atlas (224*224), sparsity range 0.10-0.20 with step 0.005, edges retained if they appeared in >60% of participants.	PD had lower clustering coefficient and global efficiency, and higher modularity *vs* HC. No correlations between age or UPDRS-III scores and global metrics in PD.		Yes
Wang et al. 2019[31]	PD with levodopa-induced dyskinesias: 21	Deterministic tractography, fractional anisotropy threshold 0.2, turning angular threshold 45°, number	PD without levodopa-induced dyskinesias had lower global efficiency and higher characteristic path length *vs* HC. No	Levodopa-induced dyskinesias	Yes

China	PD without levodopa-induced dyskinesias: 21 HC: 25	of streamlines*fractional anisotropy weighted network, number of streamlines ≥3, AAL atlas (90*90).	significant differences in global network metrics between PD with levodopa-induced dyskinesias *vs* HC. PD with levodopa-induced dyskinesias had higher local efficiency, global efficiency and clustering coefficient, and lower characteristic path length *vs* PD without levodopa-induced dyskinesias. No significant difference in small-worldness among the three groups. Negative correlation between characteristic path length and abnormal involuntary movement scale scores in PD with levodopa-induced dyskinesias.		
Wang et al. 2020[32] China	PD without MCI:43 PD with MCI: 28 HC: 31	Deterministic tractography, fractional anisotropy threshold 0.2, turning angular threshold 45°, number of streamlines weighted network, number of streamlines ≥3, AAL atlas (90*90).	PD with MCI had lower global efficiency and higher characteristic path length, normalized clustering coefficient and small-worldness *vs* HC. No significant differences in global network metrics between PD without MCI *vs* HC, or between PD without MCI *vs* patients with MCI.	MCI	Yes
Wang et al. 2023[33] China	PD with freezing of gait: 30 PD without freezing of gait: 40 HC: 25	Deterministic tractography, fractional anisotropy threshold 0.2, turning angular threshold 45°, number of streamlines weighted network, number of streamlines ≥10, AAL atlas (116*116).	PD with freezing of gait had lower global efficiency and higher normalized characteristic path length *vs* HC, and lower local efficiency and global efficiency *vs* PD without freezing of gait. No significant differences in normalized clustering coefficient and small-worldness among the three groups. In PD with freezing of gait, global and local efficiency were negatively correlated with FOG-Q scores.	Freezing of gait	Yes
Wen et al. 2017[34] PPMI	Prodromal PD: 20 de novo PD: 106 HC: 55	Deterministic tractography, quantitative anisotropy threshold 0.2, turning angular threshold 45°, the connection tract weighted network, AAL atlas (116*116).	Prodromal PD had higher clustering coefficient and small-worldness *vs* both HC and de novo PD, with no significant differences between the latter two. No significant differences in density, characteristic path length, global efficiency and assortativity among the three groups.	Prodromal PD (rapid eye movement sleep behavior disorder and olfactory dysfunction)	No Subjects overlap
Wen et al. 2017[35] PPMI	PD with hyposmia: 70 PD without hyposmia: 18 HC: 33	Deterministic tractography, quantitative anisotropy threshold 0.2, turning angular threshold 45°, fiber length ≥ 30 mm, product of the count of the connection tract weighted network, AAL atlas (116*116).	PD with hyposmia had lower local and global efficiency *vs* HC. PD without hyposmia had lower global efficiency and a trend towards lower local efficiency (P = 0.052) *vs* HC. No significant differences in density, clustering coefficient, small-worldness, or assortativity among the three groups.	Hyposmia	No Subjects overlap
Wen et al. 2018[36] PPMI	PD with tremor dominant: 52 PD with postural instability and gait difficulty: 13 HC: 61	Deterministic tractography, quantitative anisotropy threshold 0.2, turning angular threshold 45°, fiber length ≥ 30 mm, AAL atlas (116*116).	No significant differences in density, clustering coefficient, characteristic path length, local efficiency, global efficiency, small-worldness or assortativity among the three groups.	Motor subtype	No Subjects overlap
Wen et al. 2022[37] Singapore	PD without apathy: 28 PD with apathy: 31 HC: 32	Deterministic tractography, quantitative anisotropy threshold 0.02, turning angular threshold 45°, fiber length 30 mm to 450 mm, Destrieux atlas (168*168).	PD with apathy had lower global efficiency and longer characteristic path length *vs* both HC and PD without apathy, with no significant differences between the latter two. No significant	Apathy	Yes

			differences in clustering coefficient or local efficiency among the three groups.		
Zarkali et al. 2020[38] UK	PD with visual hallucinations: 19 PD without visual hallucinations: 81 HC: 34	Probabilistic tractography, number of streamlines*cross-sectional area weighted network, Glasser atlas (379*379).	No significant differences in clustering coefficient, characteristic path length or density among the three groups.	Visual hallucinations	Yes
Zhang et al. 2022[39] China	PD with left onset: 13 PD with right onset: 13 HC: 13	Deterministic tractography, fractional anisotropy threshold 0.2, turning angular threshold 45°, fractional anisotropy weighted network, AAL atlas (90*90), sparsity range 0.05-0.50 with step 0.05	No significant differences in local efficiency or global efficiency among the three groups. No correlations between network metrics and clinical scores.	Different sides of onset	Yes
Zhong et al. 2025[40] PPMI	PD with rest tremor (≥ 1 scores in the limb resting tremor part of section 3.17 of the MDS-UPDRS III): 42 PD without rest tremor: 27 HC: 56	Deterministic tractography, fractional anisotropy threshold 0.2, turning angular threshold 45°, fractional anisotropy weighted network, number of streamlines ≥3, AAL and SUIT atlas (124*124), edges retained if they appeared in > 80% of participants.	No significant differences in characteristic path length, clustering coefficient, global efficiency, local efficiency hierarchy, hierarchy (z-score), normalized clustering coefficient, normalized characteristic path length, and small-worldness among the three groups. In PD with rest tremor, tremor amplitude was positively correlated with small-worldness and normalized clustering coefficient, and negatively correlated with normalized characteristic path length. A positive correlation between hierarchy (z-score) and tremor amplitude was found in all PD.	Rest tremor	No Subjects overlap
Zhu et al. 2024[41] China	PD: 51 HC: 50	The definition of nodes: Pearson correlation coefficient between the residual kurtosis metric values of each paired node across groups, binary network, AAL atlas (90*90), sparsity range 0.10-0.50 with step 0.01.	PD had higher characteristic path length, clustering coefficient, local efficiency and normalized characteristic path length, and lower global efficiency *vs* HC. No significant differences in normalized clustering coefficient or small-worldness.		No No available data due to group-level network

Abbreviations: AAL, Automated Anatomical Labeling; dMRI, diffusion MRI; PD, Parkinson's disease; HC, healthy controls; PPMI, Parkinson's Progression Markers Initiative; RBD, REM sleep behavior disorder; MCI, mild cognitive impairment; UPDRS, Unified Parkinson's Disease Rating Scale; FA, fractional anisotropy; MD, mean diffusivity; ROI, region of interest; CSD, constrained spherical deconvolution; MSMT, multi-shell, multi-tissue; SSST, single-shell, single tissue; MDS, Movement Disorder Society; HAMA , Hamilton Anxiety Scale; PDQ39, Parkinson's Disease Questionnaire 39; FOG-Q, Freezing of Gait Questionnaire; MoCA, Montreal Cognitive Assessment.

Table S2. Global topological properties in fMRI studies in case-control systematic review

Study Subjects' source	Sample characteristics	Methods of network construction	Main findings	Features	Included in meta-analysis
Albano et al. 2022[42] Serbia	PD with candidates for DBS: 19 PD with non-candidates for DBS: 41 HC: 60	Rs-fMRI, Gaussian Kernel of FWHM 6 mm, high-pass temporal filter of 0.01 Hz, edge definitions: Pearson correlation, Fisher's r-to-z transformation, removing negative connection; Desikan–Killiany and subcortical atlas (83*83), functional connections retained when also present in structural network of HC.	No significant differences in strength, characteristic path length, local efficiency or clustering coefficient between PD vs HC. Among PD, DBS candidates had progressive changes in global network metrics over time (4 years), while non-candidates did not.	PD candidates for DBS, progression	Yes
Baagil et al. 2023[43] PPMI	PD with impulse control disorders: 21 PD without impulse control disorders: 44 HC: 23	Rs-fMRI, temporal bandpass filter 0.01-0.15 Hz, pairwise correlation weighted network, AAL atlas 3 (166*166).	PD without impulse control disorders had lower characteristic path length *vs* HC. No significant differences between PD with and without impulse control disorders.	Impulse control disorders	No Subjects overlap
Baggio et al. 2014[44] Spain	PD with MCI: 23 PD without MCI: 43 HC: 36	Rs-fMRI, edge definitions: Pearson correlation, removing negative connection; weighted network, AAL atlas (90*90), sparsity range 0.05-0.25 with step 0.025 (0.15 for primary statistical analysis).	No significant differences in clustering coefficient, modularity and small-worldness between collapsed PD *vs* HC. PD with MCI had higher small-worldness and modularity *vs* HC and patients without MCI. No significant differences in clustering coefficient, characteristic path length and global efficiency among the three groups.	MCI	Yes
Berman et al. 2016[45] USA	PD: 19 HC: 16	Rs-fMRI, regression for nuisance covariates: head motion, CSF, WM & global signal, simultaneous surface electromyography; Gaussian Kernel of FWHM 6 mm, temporal bandpass filter of 0.01 to 0.1 Hz, edge definitions: absolute value of the correlation of BOLD signal, binary network, Power atlas (226*226), sparsity range 0.09-0.50 with step 0.01.	PD on-medication had lower local efficiency and a trend toward reduced global efficiency *vs* PD off-medication. No significant differences between either PD group and HC. Local and global efficiency did not correlate with duration or MDS-UPDRS.	On-medication and off-medication	Yes
Borchert et al. 2019[46] UK	PD: 30 HC: 75	Rs-fMRI, edge definitions: wavelet correlations, binary network, random atlas (473*473), sparsity range 0.01-0.10 (0.06 for primary statistical analysis).	PD on placebo had lower clustering coefficient *vs* HC, with no significant differences in characteristic path length and modularity. No significant main effect of atomoxetine on global clustering coefficient, path length, or modularity, *vs* placebo. Similarly, citalopram did not alter these global network metrics at group level; however, its effects on clustering coefficient, characteristic path length, and modularity correlate with disease severity by UPDRS-III scores.	Atomoxetine and citalopram drug	No No available data
Chen et al. 2020[47] PPMI	PD without MCI: 22 PD with MCI: 45 HC: 18	Rs-fMRI, correction: head motion, susceptibility distortions; Gaussian Kernel of FWHM 6 mm, inter-regional correlation coefficient, binary network, Schaefer atlas (100*100), sparsity range 0.01-0.50 with step 0.01.	In a specific sparsity range, PD with MCI had lower clustering and small-worldness and higher characteristic path length *vs* those without MCI. PD with MCI *vs* HC had lower clustering coefficient. No significant differences in global metrics between PD without MCI and HC.	MCI	No Subjects overlap
Chen et al. 2022[48]	iRBD: 21	Rs-fMRI, regression for nuisance covariates: head motion, whole-brain, WM & CSF signal; Gaussian Kernel of	Both iRBD patients and PD without RBD had lower local efficiency and global efficiency, and higher characteristic path length *vs* HC.	Rapid eye movement sleep	No

China	PD without RBD: 23 HC: 22	FWHM 4 mm, temporal bandpass filter of 0.01 to 0.08 Hz, edge definition: Pearson correlation coefficient, removing negative connection; weighted network, AAL atlas (90*90)., sparsity range 0.05-0.50 with step 0.05.	However, no significant differences in global metrics between iRBD patients and PD.	behavior disorder	No available data.
Chen et al. 2023[49] China	MSA-P: 76 PD: 53 HC: 88	Rs-fMRI, regression for nuisance covariates: head motion, WM & CSF signal; temporal bandpass filter of 0.01 to 0.08 Hz, edge definition: Pearson correlation coefficient, removing negative connection; binary network, AAL atlas (116*116), sparsity range 0.05-0.50 with step 0.01.	MSA-P patients had lower clustering coefficient and local efficiency *vs* HC. Similarly, PD had lower clustering coefficients *vs* HC. However, no significant differences among the groups in global efficiency, characteristic path length, or small-worldness.	Multiple system atrophy with predominant parkinsonism	Yes
Chen et al. 2023[5] PPMI	Q1 group (age rank: 0%~25%): 36 Q2-3 group (age rank: 26%~75%): 73 Q4 group (age rank: 76%~100%): 37 Male PD: 124 Female PD: 74	Rs-fMRI, regression for nuisance covariates: head motion, WM & CSF signal; Gaussian Kernel of FWHM 4 mm, temporal bandpass filter of 0.01 to 0.1 Hz, edge definition: Pearson correlation coefficient, Fisher's r-to-z transformation; AAL atlas (90*90), sparsity range 0.05-0.50 with step 0.05.	No significant differences in global network metrics among the three age quartile groups or between male and female PD.	Age and gender differences in brain network topological measures in PD	No No HC in network properties analysis
Dan et al. 2024[50] China	PD with probable RBD: 36 PD without probable RBD: 57 HC: 71	Rs-fMRI, regression for nuisance covariates: head motion, WM & CSF signal; temporal bandpass filter of 0.01 to 0.1 Hz, edge definition: Pearson correlation coefficient, Fisher's r-to-z transformation; Dosenbach atlas (160*160), sparsity range 0.10-0.34 with step 0.01.	PD with probable RBD had lower global efficiency, local efficiency, and clustering coefficient, and higher characteristic path length, assortativity, and modularity *vs* HC, and lower global efficiency *vs* PD without probable RBD. Negative correlation between assortativity and MoCA scores in PD with probable RBD.	Probable rapid eye movement sleep behavior disorder (RBD Q-HK score ≥19, and subscale ≥8)	Yes
De Micco et al. 2021[51] Italy	Combined PD: 147 early/mild PD: 77 early/severe PD: 70 HC: 38	Rs-fMRI, regression for nuisance covariates: head motion, WM & ventricular CSF signal; temporal bandpass filter of 0.01 to 0.08 Hz, edge definition: Pearson correlation coefficient, Fisher's r-to-z transformation, removing negative connections; AAL based (K-means) atlas (220*220), functional connections retained only if also present in the structural network of HC.	Combined PD had lower strength and higher characteristic path length than HC, whereas no significant differences in global network metrics among early/mild PD, early/severe PD and HC. In the combined PD group, cognitive COS changes negatively correlated with characteristic path length. For early/severe PD, cognitive COS changes positively correlated with strength, local efficiency, and clustering coefficient, while negatively correlating with characteristic path length. No correlations between cognitive COS changes and global metrics in early/mild PD.	Progression, PD subtype (early/mild and early/mild)	Yes
Devignes et al. 2022[52] France Netherlands	PD with frontostriatal cognition: 14 PD with posterior cortical cognition: 20 PD with mixed cognition: 30 PD with normal cognition: 31 HC: 24	Rs-fMRI, regression for nuisance covariates: WM & CSF signal; Gaussian Kernel of FWHM 6 mm, temporal bandpass filter 0.01-0.10 Hz, edge definition: Pearson correlation coefficient, weighted network, group-level parcellation (ICA) atlas (590*590).	Global and local efficiency did not differ significantly across the five groups.	Cognition subtypes (frontostriatal, posterior cortical and mixed cognitive subtype)	Yes
Diao et al. 2024[53] China	PD: 80	Rs-fMRI, edge definition: correlations of the time series, Fisher's r-to-z transformation; AAL atlas (90*90).	Clustering coefficient negatively correlated with standard deviation of F0, while local efficiency positively correlated with average	Acoustic assessment	No. No case-control

			diadochokinesis rate. Speech features: PD had higher standard deviation of F0 and lower average diadochokinesis rate *vs* HC.		comparison of global metrics
Engels et al. 2018[54] Netherlands	PD: 24 HC: 27	Rs-fMRI, Gaussian Kernel of FWHM 5 mm, temporal bandpass filter > 0.01 Hz, edge definition: Pearson correlation coefficient, Fisher's r-to-z transformation, removing negative connections; Power atlas (264*264).	PD in on-state had higher global efficiency *vs* HC, while patients in off-state had a trend of higher global efficiency.	Drug	Yes
Fang et al. 2017[55] China	PD: 26 HC: 19	Rs-fMRI, regression for nuisance covariates: head motion, WM & CSF signal; Gaussian Kernel of FWHM 4 mm, temporal bandpass filter 0.01 to 0.08 Hz, edge definition: Pearson correlation coefficient, binary network, Shen atlas (278*278), sparsity range 0.05-0.50 with step 0.05.	PD had lower clustering coefficient and characteristic path length *vs* HC.		Yes
Filippi et al. 2021[56] Italy	Mild PD: 86 Moderate-to-severe PD: 60 Mild motor-predominant PD: 43 Mild-diffuse PD:43 HC: 60	Rs-fMRI, head motion correction, Gaussian Kernel of FWHM 6 mm, temporal bandpass filter > 0.01 Hz, edge definition: Pearson correlation coefficient, Fisher's r-to-z transformation, removing negative connections; binary network, Desikan–Killiany, subcortical and brainstem atlas (83*83), functional connections retained only if also present in the structural network of HC.	No significant differences in strength, clustering coefficient, local efficiency or characteristic path length among mild PD, moderate-to-severe PD and HC, as well as among mild motor-predominant, mild-diffuse PD and HC. Moderate-to-severe PD had progressive changes with decreased strength, local efficiency and clustering coefficient, and increased characteristic path length than mild PD, while mild PD, mild motor-predominant and mild-diffuse PD had no alterations in global metrics over time.	Progression. PD subtypes including mild, moderate-to-severe, mild motor-predominant and mild-diffuse	Yes
Geng et al. (2024)[57] OpenfMRI, ds000245, Japan	PD with severe hyposmia: 15 PD with no/mild hyposmia: 15 HC: 15	Rs-fMRI, Gaussian Kernel of FWHM 4 mm, temporal bandpass filter 0.01 to 0.1 Hz, AAL atlas (116*116), sparsity range 0.10-0.34 with step 0.01.	Both PD with severe hyposmia and PD with no/mild hyposmia had lower clustering coefficient and local efficiency, and higher normalized characteristic path length, *vs* HC.	Hyposmia	No Subjects overlap
Göttlich et al. 2013[58] Germany	PD: 37 HC: 20	Rs-fMRI, regression for nuisance covariates: head motion, WM & ventricular CSF signal; Gaussian Kernel of FWHM 6 mm, temporal bandpass filter 0.01 to 0.08 Hz, edge definition: Pearson correlation coefficient, Fisher's r-to-z transformation, keeping 30% of strongest weights; binary network, AAL atlas modification (343*343), sparsity range 0.10-0.35 with step 0.05.	In low sparsity values (S = 0.1 and 0.15), PD had lower characteristic path length and normalized characteristic path length, and higher clustering coefficient *vs* HC. No significant difference in normalized clustering coefficient between the two groups.		Yes
Guan et al. 2019[14] China	PD: 90 HC:38	Rs-fMRI, regression for nuisance covariates: head motion, WM & CSF signal; Gaussian Kernel of FWHM 6 mm, temporal bandpass filter 0.01 to 0.1 Hz, edge definition: Pearson correlation coefficient, Fisher's r-to-z transformation; binary or weighted network, AAL atlas (90*90), sparsity range 0.05-0.50 with step 0.05.	In weighted network, PD had lower global efficiency, local efficiency and clustering coefficient, and higher characteristic path length *vs* HC. In binary network, PD had higher global efficiency, and lower characteristic path length and clustering coefficient. Moreover, global efficiency was positively correlated with PDQ-39 in binary networks, while in weighted networks, both global and local efficiency were negatively correlated with PDQ-39.		Yes
Holtbernd et al. 2024[59] PD from Germany iRBD and HC from PPMI	iRBD: 18 PD: 18 HC: 34	Rs-fMRI, regression for nuisance covariates: head motion, temporal bandpass filter 0.01-0.15 Hz, edge definition: pairwise correlations coefficients, weighted network, AAL atlas 3.1 (142*142), proportional threshold 0.254.	PD and iRBD patients had lower small-worldness *vs* HC, with no significant difference between the two patient groups. Characteristic path length did not differ significantly among the three groups. No correlations between global metrics and UPDRS-III.	Rapid eye movement sleep behavior disorder	Yes

Hou et al. 2018[60] China	PD with rigidity-dominant: 20 HC: 20	Rs-fMRI, regression for nuisance covariates: head motion, WM, CSF signal & global signal; temporal bandpass filter 0.01 to 0.08 Hz, edge definition: Pearson correlation coefficient, binary network, AAL atlas (90*90), sparsity range 0.10-0.34 with step 0.01.	No significant differences in global efficiency, local efficiency and clustering coefficient and characteristic path length between PD with rigidity-dominant *vs* HC.	Rigidity-dominant	Yes
Hou et al. 2020[61] China	PD without MCI: 19 PD with MCI: 22 HC: 28	Rs-fMRI, regression for nuisance covariates: head motion, WM, CSF & global signal; temporal bandpass filter 0.01 to 0.08 Hz, edge definition: Pearson correlation coefficient, binary network, Dosenbach atlas (160*160), sparsity range 0.10-0.34 with step 0.01.	Both PD subgroups (with and without MCI) had lower clustering coefficient, local efficiency, and characteristic path length, but higher global efficiency, *vs* HC. No significant differences in global metric between PD subgroups.	MCI	Yes
Hou et al. 2023[62] China	PD with glucocerebrosidase mutation: 11 PD with noncarriers: 11 HC: 18	Rs-fMRI, regression for nuisance covariates: head motion, WM & CSF signal; temporal bandpass filter 0.01 to 0.08 Hz, edge definition: Pearson correlation coefficient, binary network, Dosenbach atlas (160*160), sparsity range 0.10-0.34 with step 0.01.	PD with glucocerebrosidase mutation had lower characteristic path length and higher global efficiency *vs* HC, while PD with noncarriers had lower clustering coefficient. No significant difference in local efficiency among the three groups.	Mutations of glucocerebrosidase gene	Yes
Klobušiaková et al. 2019[63] Czech Republic	PD without MCI: 17 PD with MCI: 22 HC: 51	Rs-fMRI, regression for nuisance covariates: head motion, WM & CSF signal; Gaussian Kernel of FWHM 5 mm, edge definition: Pearson correlation coefficient, Fisher's r-to-z transformation, removing negative connection; weighted network, AAL atlas modification (78*78).	At baseline, PD without MCI had lower strength, clustering coefficient, and global efficiency, and higher characteristic path length *vs* HC, whereas PD with MCI did not differ significantly from either HC or PD without MCI. No significant differences in normalized clustering coefficient, normalized characteristic path length or modularity among the three groups. After 1 year follow-up, although trends emerged in the PD-all group, no significant differences were detected in either PD or HC.	MCI, progression	Yes
Li et al. 2020[64] China	PD with probable RBD: 30 PD without probable RBD: 62 HC: 20	Rs-fMRI, Gaussian Kernel of FWHM 6 mm, temporal bandpass filter 0.01 to 0.1 Hz, edge definition: pairwise correlations coefficients, binary network, AAL atlas (90*90), sparsity range 0.05-0.5 with step 0.05.	No significant differences in small-world, global efficiency, assortativity, synchronization and hierarchy among PD with and without RBD, and HC.	Rapid eye movement sleep behavior disorder	No No available data.
Li et al. 2021[65] China	PD with freezing of gait: 37 PD without freezing of gait: 38	Rs-fMRI, regression for nuisance covariates: head motion, WM, CSF & global signal; Gaussian Kernel of FWHM 4 mm, temporal bandpass filter 0.01 to 0.08 Hz, edge definition: Pearson correlation coefficient, binary network, AAL atlas (116*116), sparsity range 0.10-0.35 with step 0.01.	PD with freezing of gait, *vs* PD without freezing of gait, had lower normalized clustering coefficient and small-worldness, with no significant differences in clustering coefficient, characteristic path length, normalized characteristic path length, local efficiency or global efficiency.	Freezing of gait	No No HC
Li et al. 2022[66] China	Combined PD: 40 PD with freezing of gait-transition (5-years follow-up): 20 PD without freezing of gait-transition: 20 HC: 20	Rs-fMRI, regression for nuisance covariates: head motion, WM, CSF & global signal; Gaussian Kernel of FWHM 4 mm, temporal bandpass filter 0.01 to 0.08 Hz, edge definition: Pearson correlation coefficient, binary network, AAL atlas (116*116), sparsity range 0.05-0.35 with step 0.01.	No significant differences in clustering coefficient, characteristic path length, normalized clustering coefficient, normalized characteristic path length, local efficiency global efficiency or small-worldness between combined PD *vs* HC, or among PD with and without freezing of gait transition, and HC.	Freezing of gait- transition	Yes
Li et al. 2024[67] China	PD with normal cognition: 46	Rs-fMRI, Gaussian Kernel of FWHM 6 mm, edge definition: Pearson correlation coefficient, removing	Both PD with normal cognition and MCI had higher global efficiency and lower characteristic path length *vs* HC, while PD with	Cognition	Yes

	PD with MCI: 43 PD with dementia: 19 HC: 34	negative connection; binary network, independent component analysis-based ROIs (22*22), correlation threshold range 0.1-0.5 with step 0.05.	dementia did not differ. No significant differences among the four groups in clustering coefficient, normalized clustering coefficient, normalized characteristic path length, local efficiency, or small-worldness.		
Lin et al. 2018[68] PPMI	PD: 31 HC: 19	Rs-fMRI, edge definition: Partial correlation analysis, binary network, Desikan–Killiany atlas (68*68), sparsity = 0.15.	No significant differences in graph measures between PD *vs* HC. Symbol Digit Modality Test scores significantly positively associated with characteristic path length and negatively correlated with global efficiency.	Cognition	No Subjects overlap
Lopes et al. 2017[69] France Netherlands	PD cognitively intact (G1): 31 PD with slight mental slowing (G2): 31 PD with mild to moderate deficits mainly in executive functions (G3): 43 PD with severe deficits in all cognitive domains (G4): 14 HC: 25	Rs-fMRI, temporal bandpass filter < 0.10 Hz, edge definition: linear correlation, regressed out age, formal education duration and participating centre; weighted network, Destrieux and subcortical atlas (164*164).	PD in G1 had lower global efficiency *vs* G2, G3 and G4, and higher characteristic length path, local efficiency and clustering coefficient *vs* G4, and higher clustering coefficient *vs* G3. PD in G2 had higher clustering coefficient and local efficiency *vs* G4, and lower global efficiency *vs* G4. PD in G3 had lower global efficiency *vs* G4. Cognitive scores were positively related to characteristic length path, local efficiency and clustering coefficient and negatively associated with global efficiency.	Cognitive phenotypes	Yes
Luo et al. 2015[70] China	PD: 47 HC: 47	Rs-fMRI, regression for nuisance covariates: head motion, WM & CSF signal; Gaussian Kernel of FWHM 6 mm, temporal bandpass filter 0.01 to 0.08 Hz, edge definition: Pearson correlation coefficients, binary network, Craddock atlas (200*200), sparsity range 0.10-0.45 with step 0.01.	PD had lower clustering coefficient and local efficiency *vs* HC, while characteristic path length and global efficiency did not differ. Visuospatial function (visuospatial subscore of Addenbrooke's Cognitive Examination-Revised) was positively related to strength clustering coefficient and local efficiency.		No No available data
Ma et al. 2017[71] China	PD: 32 HC: 31	Rs-fMRI, regression for nuisance covariates: head motion, WM & CSF signal (not regress global signal); no spatial smoothing, temporal bandpass filter 0.01 to 0.08 Hz, edge definition: Pearson correlation coefficients, removing negative connection; weighted network, Zalesky's random atlas (1024*1024).	PD had lower clustering coefficient and higher characteristic path length *vs* HC. No significant differences in normalized clustering coefficient, normalized characteristic path length, small-worldness and modularity between PD *vs* HC.		Yes
Oltra et al. 2021[72] Spain	PD with probable RBD: 27 PD without probable RBD: 32 HC: 30	Rs-fMRI, temporal bandpass filter > 0.01 Hz, Brainnetome atlas (246*246), sparsity range 0.05-0.25 with step 0.025.	PD with probable RBD, *vs* PD without probable RBD, had higher normalized characteristic path length. Further, PD with probable RBD-MCI (n = 14) had higher normalized characteristic path length *vs* PD without probable RBD-MCI (n = 13). Normalized characteristic path length was negatively associated with Stroop Word, Stroop Color, Symbol Digits Modalities Test-Oral version and Rey Auditory Verbal Learning Test total in PD with probable RBD	Rapid eye movement sleep behavior disorder, MCI	No No available data
Prajapati et al. 2021[73] PD from PPMI HC from Atlanta and Baltimore datasets	PD: 51 HC: 51	Rs-fMRI, regression for nuisance covariates: head motion, WM & CSF signal (not regress global signal); Gaussian Kernel of FWHM 4 mm, temporal bandpass filter 0.01 to 0.1 Hz, edge definition: Pearson correlation coefficients, binary network, Dosenbach atlas (160*160), sparsity range 0.05-0.5 with step 0.05.	At specific sparsity, PD had higher assortativity, synchronization, betweenness centrality, characteristic path length and lower hierarchy, clustering coefficient *vs* HC, with no significant difference in degree centrality. Male *vs* female PD had higher assortativity, synchronization and betweenness centrality, and lower clustering coefficient, while hierarchy, degree centrality and characteristic path length did not differ.		Yes

Qian et al. 2017[74] China	PD with depression: 20 PD without depression: 47 HC: 46	Rs-fMRI, regression for nuisance covariates: head motion, WM, ventricular & global signal; no spatial smoothing, five frequencies, edge definition: Pearson correlation coefficients, removing negative connection; weighted network, AAL atlas (90*90), sparsity range 0.10-0.35 with step 0.01.	In IMF1, PD with depression had lower normalized clustering coefficient *vs* PD without depression at low sparsity. In IMF2, PD with depression had higher characteristic path length *vs* HC, and both PD with depression and patients without depression had lower normalized characteristic path length *vs* HC over a wide range of sparsity. In IMF3, PD without depression had lower normalized clustering coefficient, normalized characteristic path length and higher characteristic path length *vs* HC, while PD with depression only had lower normalized characteristic path length *vs* HC over a wide range of sparsity. In IMF4 and IMF5, global network metrics did not differ among the three groups.	Depression, different frequency: IMF1, 0.12-0.22 Hz; IMF2, 0.05-0.12 Hz; IMF3, 0.02-0.05 Hz; IMF4, 0.01-0.03 Hz; IMF5, 0-0.02 Hz;	No No available data
Qiu et al. 2021[75] China	PD with depression: 22 PD without depression: 23 HC: 25	Rs-fMRI, regression for nuisance covariates: head motion, WM & CSF signal; Gaussian Kernel of FWHM 4 mm, temporal bandpass filter 0.01 to 0.1 Hz, edge definition: Pearson correlation coefficients, Fisher's r-to-z transformation; binary network, AAL atlas (90*90), sparsity range 0.05-0.50 with step 0.01.	PD with depression had lower local efficiency *vs* HC. No significant differences in global efficiency, characteristic path length, clustering coefficient, normalized characteristic path length, normalized clustering coefficient, small-worldness or modularity among the three groups.	Depression	Yes
Ruan et al. 2020[76] China	PD with freezing of gait: 23 PD without freezing of gait: 33 HC: 24	Rs-fMRI, regression for nuisance covariates: head motion, WM, CSF & global signal; Gaussian Kernel of FWHM 6 mm, temporal bandpass filter 0.01 to 0.08 Hz, edge definition: Pearson correlation coefficients, binary network, AAL atlas (90*90), sparsity range 0.10-0.40 with step 0.05.	Characteristic path length, clustering coefficient, normalized characteristic path length, normalized clustering coefficient, small-worldness, global efficiency and local efficiency did not differ significantly among the three groups.	Freezing of gait	No No available data
Sako et al. 2019[77] Japan	MSA: 11 PD: 23 HC: 11	Rs-fMRI, regression for nuisance covariates: head motion, WM & CSF signal; Gaussian Kernel of FWHM 8 mm, temporal bandpass filter 0.01 to 0.08 Hz, edge definition: Fisher-transformed correlation coefficients, binary network, AAL atlas (132*132).	Characteristic path length, transitivity, degree, and assortativity did not differ significantly among the three groups. In PD, transitivity correlated positively with levodopa equivalent dose, while in MSA, characteristic path length correlated positively with Hoehn-Yahr stage.	Multiple system atrophy	Yes
Sang et al. 2015[78] China	PD: 26 HC: 30	Rs-fMRI, regression for nuisance covariates: head motion, WM &CSF signal; no spatial smoothing, temporal bandpass filter 0.01 to 0.08 Hz, edge definition: Pearson correlation coefficients, Fisher's r-to-z transformation; binary network, AAL atlas (90*90), sparsity range 0.11-0.34 with step 0.01.	PD had lower global efficiency and normalized global efficiency *vs* HC at high sparsity, with no significant differences in local efficiency, normalized local efficiency or modularity. Global network metrics did not correlate with UPDRS.		Yes - but some sparsity was not extracted due to overlapping bars and symbols
Sarasso et al. 2022[79] Serbia	PD with freezing of gait: 30 PD with freezing of gait converters: 11 PD with freezing of gait non-converters: 11 HC: 30	Rs-fMRI, Gaussian Kernel of FWHM 6 mm, temporal bandpass filter >0.01 Hz, edge definition: Pearson correlation coefficients, Fisher's r-to-z transformation, removing negative connection; binary network, Desikan–Killiany and subcortical atlas (83*83), functional connections retained only if also present in the structural network of HC.	PD with freezing of gait converters had higher clustering coefficient and local efficiency *vs* both HC and PD with freezing of gait. Lower local efficiency and clustering coefficient at baseline correlated with worsening of executive functions at 2-year follow-up.	Freezing of gait, progression	Yes
Schill et al. 2023[80] Germany	PD: 14 HC: 23	Task-fMRI, Gaussian Kernel of FWHM 4 mm, edge definition: normalized mutual information coefficients, weighted network, Eickhoff-Zilles cytoarchitectonic probabilistic atlas (212*212), percolation thresholding.	Under both neutral and disgusted conditions, PD had lower degree, strength, clustering coefficient, and global efficiency *vs* HCs, with no significant difference in density.	Task-fMRI, neutral condition and disgusted condition	Yes - only neutral condition

Shang et al. 2023[81] China	PD: 51 HC: 60	Rs-fMRI, regression for nuisance covariates: head motion, WM & CSF signal (not global signal); no spatial smoothing, temporal bandpass filter 0.01 to 0.08 Hz, edge definition: Pearson correlation coefficients, removing negative connection; binary network, AAL atlas (90*90), sparsity range 0.10-0.50 with step 0.01.	In low-order functional connectivity network, no significant differences between PD *vs* HC in local efficiency, global efficiency, clustering coefficient, characteristic path length, normalized clustering coefficient, normalized characteristic path length, or small-worldness. In contrast, in high-order networks, PD had lower global efficiency, normalized clustering coefficient, and small-worldness, and higher characteristic path length. UPDRS-III scores were negatively correlated with both normalized clustering coefficient and small-worldness.	Low-order functional connectivity network (temporal series Pearson correlation) and High-order functional connectivity network (Pearson correlation of low-order)	Yes - only lower-order
Shang et al. 2023[29] China	PD: 69 HC: 70	Rs-fMRI, regression for nuisance covariates: head motion, WM &CSF signal (not global signal); no spatial smoothing, temporal bandpass filter 0.01 to 0.08 Hz, edge definition: Pearson correlation coefficients, Fisher's r-to-z transformation; weighted network, AAL atlas (90*90), sparsity range 0.05-0.30 with step 0.01.	PD had lower characteristic path length and normalized characteristic path length, and higher global efficiency and small-worldness *vs* HC. No significant differences in clustering coefficient, normalized clustering coefficient and local efficiency between PD *vs* HC.		Yes
Siva et al. 2024[82] OpenfMRI, ds000245, Japan	PD with severe hyposmia: 15 PD with no/mild hyposmia: 15 HC: 15	Rs-fMRI, no spatial smoothing, edge definition: Pearson correlation coefficients, Fisher's r-to-z transformation; Dosenbach atlas (160*160), sparsity range 0.10-0.50 with step 0.05.	PD with severe hyposmia had lower clustering coefficient, local efficiency and small-worldness *vs* HC and PD with no/mild hyposmia. PD with no/mild hyposmia had lower clustering coefficient *vs* HC. No significant differences in characteristic path length, modularity, network centrality, assortativity, and strength among the three groups.	Hyposmia	Yes
Skidmore et al. 2011[83] USA	PD: 14 HC: 15	Rs-fMRI, no spatial smoothing, 0.06 to 0.12 Hz frequency range, edge definition: wavelet correlation, weighted network, AAL atlas (116*116), retained 10% of strongest connections.	PD had lower global efficiency *vs* HC.		Yes
Sreenivasan et al. 2019[84] PPMI	PD: 20 HC: 16	Rs-fMRI, regression for nuisance covariates: head motion, WM & CSF signal; 8mm 3D-Gaussian filter, temporal bandpass filter 0.008 to 0.1 Hz, edge definition: Pearson correlation coefficients, weighted network, AAL atlas (90*90), sparsity range 0.10-0.50 with step 0.01.	PD had lower small-worldness, normalized clustering coefficient, global efficiency, local efficiency and strength, and higher normalized characteristic path length *vs* HC. Negative correlation between normalized clustering coefficient and duration in PD.		No Subjects overlap
Sreenivasan et al. 2023[85] CNTN	PD with freezing of gait: 16 PD without freezing of gait: 16 HC: 16	Rs-fMRI, regression for nuisance covariates: head motion, WM & CSF signal; temporal bandpass filter 0.008 to 0.1 Hz, edge definition: Pearson correlation coefficients, weighted network, Brainnetome atlas (246*246), sparsity range 0.10-0.50 with step 0.01.	PD with freezing of gait had lower assortativity *vs* PD without freezing of gait. No significant differences in small-worldness, characteristic path length, clustering coefficient, global efficiency, local efficiency and strength among the three groups.	Freezing of gait	Yes
Suo et al. 2017[86] China	PD: 153 HC: 81	Rs-fMRI, regression for nuisance covariates: head motion, WM, CSF & global signal; temporal bandpass filter 0.01 to 0.08 Hz, edge definition: Pearson correlation coefficients, binary network, AAL atlas (90*90), sparsity range 0.10-0.34 with step 0.01.	PD had lower clustering coefficient, global efficiency, local efficiency and higher characteristic path length *vs* HC, with no significant differences in normalized clustering coefficient, normalized characteristic path length or small-worldness.		Yes

Suo et al. 2022[87] China	PD with MCI: 24 PD with normal cognition: 17 HC: 24	Rs-fMRI, regression for nuisance covariates: head motion, WM, CSF & global signal; Gaussian Kernel of FWHM 4 mm, temporal bandpass filter 0.01 to 0.08 Hz, edge definition: Pearson correlation coefficients, removing negative connection; weighted network, AAL atlas (116*116), sparsity range 0.05-0.40 with step 0.01.	Both PD with MCI and PD with normal cognition had lower clustering coefficient, local efficiency and global efficiency, and higher characteristic path length, *vs* HC. No significant differences in global metrics between PD *vs* MCI and PD with normal cognition. Wechsler adult intelligence scale-IV Similarities correlated positively with global efficiency and negatively with characteristic path length.	MCI	Yes
Tang et al. 2017[88] China	Familial PD: 31 Sporadic PD: 36 HC: 38	Rs-fMRI, regression for nuisance covariates: head motion, WM & CSF signal (not regressing global signal); no spatial smoothing, temporal bandpass filter >0.01 Hz, edge definition: wavelet correlation, weighted network, Brainnetome atlas (246*246).	At the fourth wavelet scales (0.016 to 0.031 Hz), sporadic PD had lower assortativity *vs* familial PD and HC, while clustering coefficient, global efficiency, and characteristic path length did not differ significantly among familial and sporadic PD and HC.	Genetics	Yes
Tuovinen et al. 2018[89] Austria	PD: 16 HC: 16	Rs-fMRI, regression for nuisance covariates: head motion, WM & CSF signal; high-pass filtering of 100 s, edge definition: Pearson correlation coefficients, Fisher's r-to-z transformation; AAL atlas (116*116), sparsity range 0.05-0.50 with step 0.01.	At baseline, PD had higher global efficiency *vs* HC. However, at follow-up, PD global efficiency declined while HC remained unchanged.	Progression	Yes
van Balkom et al. 2022[90] Netherlands	PD with cognition training: 37 PD with active control: 34	Rs-fMRI, regression for nuisance covariates: head motion, WM & CSF signal (not regress global signal); Gaussian Kernel of FWHM 6 mm, temporal bandpass filter 0.009-0.13 Hz, edge definition: wavelet correlation (replicated by Pearson correlation); Schaefer and subcortical atlas (300*300), no threshold for network construction.	No significant differences in global efficiency, modularity and participation coefficient between PD with cognition training *vs* PD with active control after 8-week multi-domain cognitive training.	Eight-week multi-domain cognitive training	No No HC
Vancea et al. 2019[91] USA	PD: 16 HC: 16	Rs-fMRI, regression for nuisance covariates: head motion, WM & ventricles signal; spatial smoothing, edge definition: Pearson correlation coefficients, Fisher's r-to-z transformation; weighted network, Eickhoff-Zilles cytoarchitectonic probabilistic atlas (206*206), sparsity range 0.15-0.95 with step 0.05, removing edges when <10% of maximum weight in the network.	PD had lower clustering coefficient *vs* HC at sparsity range 4-7, with no significant difference in characteristic path length.		Yes
Wang et al. 2023[92] China	PD with depression: 20 PD without depression: 37 HC: 41	Rs-fMRI, regression for nuisance covariates: head motion, WM & CSF signal; temporal bandpass filter 0.01-0.08 Hz, edge definition: Pearson correlation coefficients, binary network, Brainnetome atlas (246*246), sparsity range 0.05-0.34 with step 0.01.	No significant differences in clustering coefficient, characteristic path length, normalized clustering coefficient, normalized characteristic path length, local efficiency, global efficiency and small-worldness among the three groups.	Depression	Yes
Wang et al. 2023[33] China	PD with freezing of gait: 30 PD without freezing of gait: 40 HC: 25	Rs-fMRI, regression for nuisance covariates: head motion, WM, CSF & global signal; Gaussian Kernel of FWHM 6 mm, temporal bandpass filter 0.01 to 0.08 Hz, edge definition: Pearson correlation coefficients, Fisher's r-to-z transformation, removing negative connections; weighted network, AAL atlas (116*116), sparsity range 0.05-0.40 with step 0.01.	PD with freezing of gait had higher local efficiency *vs* PD without freezing of gait. No significant differences in normalized clustering coefficient, normalized characteristic path length among the three groups. No correlations between global metrics and FOG-Q in PD with freezing of gait.	Freezing of gait	Yes
Wright et al. 2020[93] Canada	PD with low cognition (MoCA < 26): 8 PD with normal cognition: 10	Rs-fMRI, regression for nuisance covariates: head motion, WM, CSF & global signal; Gaussian Kernel of FWHM 8 mm, temporal bandpass filter 0.008 to 0.09 Hz, binary network, AAL and pons atlas (118*118), cost range 0.15-0.25.	No significant differences in clustering coefficient, characteristic path length, local efficiency, global efficiency and small-worldness among the three groups.	Cognition	Yes - but PD with low cognition group was excluded

	HC: 10				due to <10 participants
Wu et al. 2021[94] UK	PD: 18	Rs-fMRI, regression for nuisance covariates: head motion, WM & CSF signal; Gaussian Kernel of FWHM 8 mm, temporal bandpass filter > 0.0078 Hz, edge definition: Bivariate correlation coefficients, binary network, independent component analysis-based atlas (25*25), sparsity range 0.10-0.34 with step 0.01.	Deep brain stimulation of the subthalamic nucleus was not correlated with global efficiency, assortativity, clustering coefficient, or betweenness centrality.	Deep brain stimulation of the subthalamic nucleus	No No HC.
Yuan et al. 2024[95] China	PD with end-of-dose wearing-off: 61 PD without end-of-dose wearing-off: 39	Rs-fMRI, spatial smoothing, edge definition: Pearson correlation coefficients, Fisher's r-to-z transformation; weighted network, AAL atlas (90*90), sparsity range 0.1-0.5 with step 0.05.	No significant differences in global efficiency and local efficiency between PD with and without end-of-dose wearing-off. Positive correlation between degree centrality and daily dopamine or dopamine agonist therapy in control group.	End-of-dose wearing-off	No No HC.
Zhang et al. 2014[96] China	PD with tremor-dominant: 15 PD with non-tremor-dominant: 10 HC: 20	Rs-fMRI, regression for nuisance covariates: head motion, WM & CSF signal (not global signal); Gaussian Kernel of FWHM 4 mm, temporal bandpass filter 0.01-0.1 Hz, edge definition: Pearson correlation coefficients, Fisher's r-to-z transformation, removing negative connection; weighted network, Zalesky's random cere-AAL and AAL atlas (1024*1024).	Local efficiency and global efficiency can differentiate both tremor-dominant and non-tremor-dominant PD *vs* HC, and this discrimination ability was influenced by the cerebellum.	Tremor-dominant, classification	Yes
Zhang et al. 2015[97] China	PD with resting tremor: 16 HC: 20	Rs-fMRI, regression for nuisance covariates: head motion, WM & CSF signal; Gaussian Kernel of FWHM 6 mm, temporal bandpass filter 0.01-0.1 Hz, edge definition: wavelet correlation, weighted network, Power atlas (264*264).	PD had lower local efficiency and higher global efficiency *vs* HC. Normalized local efficiency negatively correlated with tremor level.	Resting tremor	No No available data
Zhang et al. 2022[39] China	PD with left onset: 13 PD with right onset: 13 HC: 13	Rs-fMRI, Gaussian Kernel of FWHM 6 mm, edge definition: Pearson correlation coefficients, binary network, AAL atlas (90*90), sparsity range 0.05-0.5 with step 0.05.	No significant differences in local efficiency or global efficiency among the three groups. No correlations between global metrics and clinical scores.	Different sides of onset	Yes
Zhu et al. 2021[98] PPMI	PD with impulse control disorders: 18 PD without impulse control disorders: 18 HC: 16	Rs-fMRI, Gaussian Kernel of FWHM 6 mm, temporal high-pass filter 128s, binary network, Schaefer atlas (100*100), sparsity range 0.10-0.50 with step 0.01.	Within a specific sparsity range, PD with impulse control disorders had higher clustering coefficient and characteristic path length, and lower small-worldness *vs* patients without impulse control disorders. HC had higher clustering coefficient *vs* PD without impulse control disorders and lower characteristic path length than PD with impulse control disorders.	Impulse control disorders	No Subjects overlap

Abbreviations: AAL, Automated Anatomical Labeling; CSF, cerebrospinal fluid; WM, white matter; fMRI, functional MRI; PD, Parkinson's disease; HC, healthy control; DBS, deep brain stimulation; Rs-fMRI, resting-state functional MRI; FWHM, full width at half maxima; PPMI, Parkinson's Progression Markers Initiative; MCI, mild cognitive impairment; BOLD, blood oxygen level dependent; RBD, REM sleep behavior disorder; MDS, Movement Disorder Society; UPDRS, Unified Parkinson's Disease Rating Scale; MSA-P, Multiple System Atrophy with Predominant Parkinsonism; MoCA, Montreal Cognitive Assessment; COS, clinical outcome scores; ICA, Independent Component Analysis; PDQ39, Parkinson's Disease Questionnaire 39; ROI, region of interest; IMF, intrinsic mode function.

Table S3. Global topological properties in sMRI studies in case-control systematic review

Study Subjects' source	Sample characteristics	Methods of network construction	Main findings	Features	Included in meta-analysis
Chen et al. 2023[5] PPMI	Q1 group (age rank: 0%~25%): 36 Q2-3 group (age rank: 26%~75%): 73 Q4 group (age rank: 76%~100%): 37	VBM, spatial smoothing, individual structural covariance network, edge definitions: Pearson correlation, Fisher's r-to-z transformation, AAL atlas (90*90).	No significant differences in global network metrics among the three age quartile groups. Female PD had higher characteristic path length and normalized characteristic path length *vs* male PD, with no significant differences in clustering coefficient, normalized clustering coefficient and small-worldness.	Age and gender differences in the brain network topological measures in PD	No No HC in network analysis
Diao et al. 2024[99] China	PD: 138 HC: 40	VBM (CAT12), individual differential structural covariance network, edge definitions: partial Pearson correlation coefficient (PCC, calculated between gray matter volumes of brain regions) in HC group, added one patient to the HC group, computed ΔPCCn = PCCn+1 – PCCn to quantify network changes induced by the patient, assigned Z-scores of ΔPCCn of as edge weights in the network; AAL atlas 3 (156*156), sparsity range 0.14-0.50 with step 0.01.	No correlation between global network metrics and long-term DBS outcomes.	Bilateral subthalamic nucleus -DBS	No No HC in network analysis
Guo et al. 2018[100] PPMI	PD with possible RBD: 51 PD with non-possible RBD: 140 HC: 76	VBM (CAT12), Gaussian Kernel of FWHM 8 mm, group-level structural covariance network, edge definitions: Pearson correlation coefficient of gray matter volume, AAL atlas (116*116), sparsity range 0.1-0.50 with step 0.02.	No significant differences in normalized clustering coefficient, normalized characteristic path length, small-worldness, local efficiency and global efficiency among the three groups.	Rapid eye movement sleep behavior disorder	No No available data due to group-level network
Pereira et al. 2015[101] PPMI	PD with MCI: 33 PD with normal cognition: 90 HC: 56	SBM (Freesurfer v5.3), group-level structural covariance network, edge definitions: Pearson correlation coefficient of cortical thickness and subcortical volume, Destrieux and subcortical atlas (162*162), weighted or binary network, sparsity range 0.02-0.12 with step 0.005.	PD with MCI had lower global efficiency and higher characteristic path length *vs* HC; results were robust in weighted and binary network, in Destrieux and Desikan atlas and removing subcortical volume. No significant differences in clustering coefficient and small-worldness among the three groups.	MCI	No No available data due to group-level network
Samantaray et al. 2024[102] PPMI	PD with subtype A (based on structural gray matter): 21 PD with subtype B: 31 PD with subtype AB: 44	VBM (CAT12), Gaussian Kernel of FWHM 8 mm, group-level structural covariance network, edge definitions: Pearson correlation coefficient of gray matter volume, binary network, LONI probabilistic brain atlas (56*56), sparsity range 0.55-0.90 with step 0.0025.	Significant differences in clustering coefficient, local efficiency, betweenness centrality and participation coefficient among the three groups at specific sparsity.	Subtyping PD using biclustering based on gray matter.	No No available data due to group-level network

Suo et al. 2021[103] China	PD with MCI: 24 PD with normal cognition: 17 HC: 29	VBM, Gaussian Kernel of FWHM 6 mm, individual structural covariance network, edge definitions: Kullback–Leibler divergence similarity of gray matter volume, binary network, AAL atlas (116*116), sparsity range 0.05-0.38 with step 0.01.	PD with normal cognition had lower normalized characteristic path length *vs* HC, while PD with MCI had higher local efficiency and small-worldness. In PD with MCI, local efficiency was positively correlated with clock drawing scores.	MCI	Yes
Suo et al. 2021[104] China	PD: 54 HC: 54	VBM, Gaussian Kernel of FWHM 6 mm, individual structural covariance network, edge definitions: Kullback–Leibler divergence similarity of gray matter volume, binary network, AAL atlas (90*90), sparsity range 0.10-0.34 with step 0.01.	PD had higher clustering coefficient and local efficiency *vs* HC, with no significant differences in characteristic path length, normalized clustering coefficient, normalized characteristic path length and global efficiency. No significant differences in global metrics between tremor-dominant and akinetic-rigid motor subtypes.		Yes
Tang et al. 2024[105] China	PD with high Glial cell-derived neurotrophic factor: 19 PD with high Glial cell-derived neurotrophic factor: 19 HC: 25	SBM (Freesurfer), group-level structural covariance network, edge definitions: Pearson correlation coefficient, Desikan–Killiany atlas (68*68), binary network, sparsity range 0.10-0.40 with step 0.01.	PD with high GDNF had lower clustering coefficient and small-worldness *vs* HC. PD with low GDNF had lower clustering coefficient, normalized clustering coefficient and small-worldness, and higher characteristic path length *vs* HC. PD with high GDNF had lower small-worldness than PD with low GDNF.	GDNF (subtyping by K-means cluster analysis)	No No available data due to group-level network
Wang et al. 2020[106] China	PD: 60 HC: 56	SBM (CAT12), group-level structural covariance network, edge definitions: Pearson correlation coefficient of sulcal depth, Desikan–Killiany atlas (68*68), binary network, sparsity range 0.26-0.50 with step 0.02.	PD had higher normalized clustering coefficient, normalized characteristic path length and assortativity *vs* HC, based on AUC analysis at multiple sparsity levels.		No No available data due to group-level network
Wu et al. 2018[107] China	PD: 48 HC: 50	VBM, group-level structural covariance network, edge definitions: Pearson correlation coefficient of gray matter volume, binary network, AAL atlas (90*90), sparsity range 0.1-0.4.	Within a specific sparsity range, PD had higher clustering coefficient and characteristic path length *vs* HC. AUC analysis found a between-group difference in normalized clustering coefficient.		No No available data due to group-level network
Xie et al. 2022[108] China	PD with levodopa challenge test high improvement: 25 PD with levodopa challenge test low improvement: 13	VBM (CAT12), Gaussian Kernel of FWHM 6 mm, individual structural covariance network, edge definitions: Jensen–Shannon divergence similarity, AAL atlas (90*90), sparsity range 0.02-0.5 with step 0.01.	No significant differences between the two groups in clustering coefficient, characteristic path length, normalized clustering coefficient, normalized characteristic path length, local efficiency, global efficiency, assortativity, modularity, synchronization, hierarchy and small-worldness.	Predicts levodopa responsiveness to identify candidates for DBS	No No HC.
Xu et al. 2017[109] China	PD: 37 HC: 34	SBM (Freesurfer), group-level structural covariance network, edge definitions: Pearson correlation coefficient of local gyrification index, Desikan–Killiany atlas (68*68), binary network, sparsity range 0.15-0.40 with step 0.01.	PD had higher clustering coefficient and characteristic path length, and lower global efficiency *vs* HC.		Yes

Xu et al. 2018[110] China	PD (Hoehn-Yahr stage 1 or 1.5): 31 HC: 37	VBM (CAT12), Gaussian Kernel of FWHM 8 mm, group-level structural covariance network, edge definitions: Pearson correlation coefficient of gray matter volume, binary network, AAL atlas (116*116), sparsity range 0.01-0.5 with step 0.02.	No significant differences PD *vs* HC in clustering coefficient, characteristic path length, normalized clustering coefficient, normalized characteristic path length, local efficiency, global efficiency and small-worldness.	Hemiparkinsonism (Hoehn-Yahr stage 1 or 1.5)	No No available data due to group-level network
Yadav et al. 2016[111] China	PD: 64 HC: 46	SBM (Freesurfer), Gaussian Kernel of FWHM 15 mm, group-level structural covariance network, edge definitions: Pearson correlation coefficient, Desikan–Killiany atlas (68*68), sparsity range 0.42-0.50 with step 0.01.	No significant differences in global metrics in male *vs* female PD.	Gender	No No available data due to group-level network
Yan et al. 2024[112] China	PD: 50 HC: 46	SBM (CAT12), Gaussian Kernel of FWHM 15 mm, individual structural covariance network, edge definitions: Jensen-Shannon divergence-based similarity of cortical thickness, local gyrification index, fractional dimension and sulcal depth; binary network, Desikan–Killiany atlas (68*68), sparsity range 0.13-0.50 with step 0.01.	In local gyrification index-based morphological brain networks, PD had lower local efficiency, normalized characteristic path length and clustering coefficient *vs* HC. UPDRS-III scores negatively correlated with local efficiency and clustering coefficient. No significant differences in network based on cortical thickness, fractional dimension and sulcal depth.		Yes
Zhang et al. 2015[97] China	PD with resting tremor: 16 HC: 20	VBM, Gaussian Kernel of FWHM 6 mm, individual structural covariance network, edge definitions: seed cube similarity approach, removing negative correlation; binary network, Desikan–Killiany atlas (68*68), sparsity range 0.02-0.4 with step 0.02.	PD had higher global efficiency, normalized global efficiency and local efficiency *vs* HC. Normalized local efficiency negatively correlated with tremor level. No correlations between global metrics and clinical scores (including tremor, UPDRS and duration).	Resting tremor	No No available data

Abbreviations: AAL, Automated Anatomical Labeling; sMRI, structural MRI; PPMI, Parkinson's Progression Markers Initiative; PD, Parkinson's disease; HC, healthy controls; DBS, deep brain stimulation; RBD, REM sleep behavior disorder; FWHM, full width at half maxima; MCI, mild cognitive impairment; GDNF, glial cell line-derived neurotrophic factor; UPDRS, Unified Parkinson's Disease Rating Scale; SBM, Surface-based morphometry; VBM, voxel-based morphometry.

Table S4. Global topological properties in EEG studies in case-control systematic review

Study Subjects' source	Sample characteristics	Methods of network construction	Main findings	Features	Included in meta-analysis
Bočková et al. 2021[113] Czech Republic	PD with DBS optimal responders: 12 PD with DBS suboptimal responders: 6 PD with DBS non-responders: 14	Task-EEG: target stimuli, frequent stimuli and distractors stimuli, 204 channels, temporal bandpass filter: 1-8 Hz, 8-20 Hz, 20-45 Hz and 55-80 Hz; edge definitions: phase lag index, Fisher's r-to-z transformation; weighted network, AAL atlas (90*90).	In 1-8 Hz, PD with DBS suboptimal responders in DBS on state had lower strength and higher clustering coefficient and characteristic path length *vs* PD in DBS off state with and target stimuli. In 55-80 Hz, different global network metrics significant differences between DBS on-state *vs* off-state in PD with DBS suboptimal responders and patients with DBS non-responders in target, frequent and distractors stimuli, while no significant differences in PD with DBS optimal responders. There were no significant differences in 8-20 Hz, 20-45 Hz.	Deep brain stimulation of subthalamic nucleus	No No HC
Bosch et al. 2022[114] USA	Combined PD: 83 PD with freezing of gait: 42 PD without freezing of gait: 41 HC: 42	Rs-EEG, 64 channels, frequency bands: theta 4-7 Hz, edge definitions: phase locking value, the definition of nodes: electrode positioning (59*59), the top 20% of weighted links computed using Pearson correlation were kept in the final graph.	PD had higher strength and clustering coefficient *vs* HC, while no significant differences between PD with and without freezing of gait.	Freezing of gait	Yes
Fogelson et al. 2013[115] Spain	PD: 15 HC: 15	Task-EEG: predicted and random targets, predictive sequence and random standards; 64 channels, frequency bands: theta band (4-8 Hz), alpha band (8-12 Hz) and beta band (12-28 Hz); edge definitions: synchronization likelihood; binary network, the definition of nodes: electrode positioning (64*64), global degree threshold range 8-15 with step 0.5.	In the alpha and theta frequency band, PD had higher clustering coefficient and characteristic path length *vs* HC with predicted targets. In the theta frequency band, PD had higher clustering coefficient *vs* HC in predictive sequence. No significant differences between PD *vs* HC in random targets and standard condition.		Yes
Formaggio et al. 2021[116] Italy	PD: 15 HC: 10	Rs-EEG, 32 channels, temporal bandpass filter: 1-30 Hz, edge definitions: Granger coefficients, directed and weighted network, the definition of nodes: Brodmann atlas (8*8).	No significant difference in global efficiency between PD *vs* HC.	Granger causality	Yes
Hassan et al. 2017[117] France Netherlands	PD with cognitively intact: 63 PD with mild cognitive deficits (G2): 46 PD with severe cognitive deficits: 15	Rs-EEG, 128 channels, frequency bands: delta band (0.5-4 Hz), theta band (4-8 Hz), alpha 1 band (8-10 Hz), alpha 2 band (10-13 Hz), beta band (13-30 Hz) and gamma band (30-45 Hz); edge definitions: phase locking value; weighted network, the definition of nodes: Desikan-Killiany atlas (68*68).	Across all frequency bands, worsening cognitive impairment was associated with declines in strength, clustering coefficient, characteristic path length, and global efficiency, though no differences reached significance.		No No HC
Li et al. 2021[118] China	PD after DBS: 20 HC: 21	Rs-EEG, 256 channels, frequency bands: theta band (4-8 Hz), alpha band (8-13 Hz), beta 1 band (13-20 Hz) and beta 2 band (20-30 Hz); edge definitions: phase locking value; weighted network, the definition of nodes: Desikan-Killiany atlas (68*68), sparsity range 0.05-0.5 with step 0.05.	In alpha, beta 1 and beta 2 frequency bands, both PD with DBS-o and DBS-ON conditions had lower local efficiency and clustering coefficient in the sparsity 0.05. No significant differences in global metrics between PD with DBS-OFF and DBS-ON states.	Effect of acute deep brain stimulation	No After DBS surgery

Mehraram et al. 2020[119] UK	PD with dementia: 21 Alzheimer's disease (AD): 32 Dementia with Lewy bodies (DLB): 25 HC: 18	Rs-EEG, 128 channels, frequency bands: theta band (4-7.5 Hz), alpha band (8-13.5 Hz) and beta band (14-20.5 Hz); edge definitions: weighted phase lag index; weighted network, the definition of nodes: electrode positioning, sparsity range 0.03-0.60 with step 0.01.	In theta frequency band, both PD with dementia and DLB had higher small-worldness and modularity *vs* AD. In alpha frequency band, both PD with dementia and DLB had lower degree and clustering coefficient, and higher characteristic path length and modularity, *vs* HC. Furthermore, PD with dementia had higher modularity *vs* AD. In beta frequency band, DLB had lower degree, clustering coefficient, and higher characteristic path length, small-worldness and modularity *vs* AD. DLB had lower clustering coefficient *vs* HC.	Dementia including PD, DLB and AD	Yes
Peláez Suárez et al. 2021[120] Cuba	PD with MCI: 15 PD without MCI: 15 HC: 26	Rs-EEG, frequency bands: delta band (1-4 Hz), theta band (4-7 Hz), alpha band (8-12 Hz) and beta band (13-20 Hz); edge definitions: synchronization likelihood probability, the definition of nodes: electrode positioning (45*45).	PD with MCI had lower clustering coefficient (alpha band) and characteristic path length (theta and delta bands) *vs* HC. PD without MCI had lower clustering coefficient (beta band), local efficiency (beta and theta bands) and characteristic path length (beta and theta bands) *vs* HC.	MCI	Yes
Rajagopal et al. 2025[121] India	PD: 26 HC: 13	Task-EEG: lower-limb pedaling motor task, 64 channels, frequency bands: delta band (1-4 Hz), theta band (4-8 Hz), alpha band (8-13 Hz), beta band (13-30 Hz) and gamma band (30-50 Hz); edge definitions: phase lag index, the definition of nodes: electrode positioning (59*59).	In motor task, PD had lower clustering coefficient (delta band) and global efficiency (delta band), and higher clustering coefficient (gamma band) and characteristic path length (delta band) *vs* HC. In contrast, in rest-state, no significant differences in global metrics between PD and HC across all frequency bands.		Yes
Revankar et al. 2021[122] Japan	PD with pareidolia: 10 PD without pareidolia: 11 HC: 10	Task-EEG, 32 channels, frequency bands: theta band (4-7 Hz), low alpha band (IAF-2 Hz), high alpha band (IAF+2 Hz); edge definitions: weighted phase lag index, binary network, the definition of nodes: electrode positioning (32*32), sparsity of 0.3.	In the low alpha band, PD with pareidolia had higher normalized clustering coefficient *vs* PD without pareidolia and HC. No significant differences in global network metrics in theta and high alpha bands.	Pareidolia	No No available data for theta band
Stylianou et al. 2022[123] Openneuro: ds002778	PD: 15 HC: 16	Rs-EEG, 32 channels, frequency filter: 0.5-45 Hz, edge definitions: generalized Hurst exponent and bivariate focus-based multifractal, binary network, the definition of nodes: electrode positioning (32*32).	PD on-medication had lower clustering coefficient and characteristic path length, and higher degree *vs* PD off-medication and HC in the network based on bivariate focus-based multifractal, with no significant differences in the network by generalized Hurst exponent. In the network by generalized Hurst exponent, the North American Adult Reading Test scores positive correlated with degree and clustering coefficient, and negative with characteristic path length.	Dopaminergic treatment: on- and off-medication	No No available data
Utianski et al. 2016[124] USA	PD with dementia: 18 PD with MCI: 13 PD with normal cognition: 57 HC: 57	Rs-EEG, 21 channels, frequency bands: delta band (2.5-4 Hz), theta band (4-8 Hz), alpha 1 band (8-10 Hz), alpha 2 band (10-13 Hz) and beta band (13-30 Hz); edge definitions: phase lag index, weighted network, the definition of nodes: electrode positioning (21*21).	PD with normal cognition had higher normalized clustering coefficient, normalized characteristic path length and modularity *vs* HC in delta, theta, alpha 1 and 2 bands, and lower weighted degree divergence in delta and alpha bands but higher in theta and beta bands in patients than HC. PD with dementia had lower normalized clustering coefficient, normalized characteristic path length and weighted degree divergence in alpha 1 band and higher modularity in alpha 1 and 2 bands *vs* PD with normal cognition. PD with MCI had lower normalized clustering coefficient and weighted degree divergence *vs* PD with normal cognition in alpha 1 band		No No available data

Vecchio et al. 2021[125] Italy	PD: 13 HC: 13	Rs-EEG, 19 channels, frequency bands: delta band (2-4 Hz), theta band (4-8 Hz), alpha 1 band (8-10.5 Hz), alpha 2 band (10.5-13 Hz) and beta 1 band (13-20 Hz), beta 2 band (20-30 Hz) and gamma band (30-45 Hz); edge definitions: Lagged Linear Connectivity values, weighted network, the definition of nodes: Brodmann atlas (84*84).	PD had lower small-worldness in theta band but higher small-worldness in alpha 2 band *vs* HC.		Yes
Wang et al. 2024[126] China	PD: 32 MSA: 35 HC: 30	Rs-EEG, 64 channels, frequency bands: delta band (1-4 Hz), theta band (4-8 Hz), alpha band (8-13 Hz), beta band (13-30 Hz) and gamma band (30-60 Hz); edge definitions: weighted phase lag index, the definition of nodes: AAL atlas (90*90).	Both PD and MSA had lower modularity, and higher degree and global efficiency *vs* HC in theta band. PD had higher local efficiency *vs* HC in both theta and gamma bands, and higher degree and global efficiency in gamma band.	Multiple system atrophy	Yes
Yin et al. 2023[127] China	PD with freezing of gait: 15 PD without freezing of gait: 13 HC: 16	Rs-EEG, 32 channels, frequency bands: delta band (1-4 Hz), theta band (4-8 Hz), alpha band (8-13 Hz), beta band (13-30 Hz) and gamma band (30-40 Hz); edge definitions: transfer entropy, directed and binary network, the definition of nodes: electrode positioning (30*30), threshold: maximum threshold without isolated nodes and the constructed brain network satisfied the small-world property	PD without freezing of gait had higher characteristic path length, and lower global efficiency, clustering coefficient and transitivity *vs* PD with freezing of gait and HC in theta band, with no significant differences in delta, alpha, alpha, beta and gamma bands. Characteristic path length positively correlated with freezing of gait scale score.	Freezing of gait	Yes
Zhang et al. 2022[128] Germany	PD: 15	Rs-EEG, 32 channels, frequency bandpass filter: 1-35 Hz, beta band (13-30 Hz); edge definitions: lagged coherence, the definition of nodes: electrode positioning (32*32), sparsity range 0.04-0.36 with step 0.02.	No significant differences in global efficiency and clustering coefficient between PD on-medication *vs* off-medication.	On- and off-medication	No No HC
Zhang et al. 2022[129] China	PD: 29 HC: 22	Rs-EEG, 19 channels, frequency bands: delta band (1-4 Hz), theta band (4-8 Hz), alpha band (8-13 Hz) and beta band (13-30 Hz); edge definitions: phase lag index, the definition of nodes: electrode positioning (19*19), sparsity 0.3.	PD had higher clustering coefficient (delta, theta, alpha and beta bands), characteristic path length (theta and alpha bands), local efficiency (delta, alpha and beta bands) and global efficiency (delta, alpha and beta bands) *vs* HC.		Yes

Abbreviations: AAL, Automated Anatomical Labeling; EEG, electroencephalography; PD, Parkinson's disease; HC, healthy control; MEG, magnetic encephalography; DBS, deep brain stimulation; Rs, resting-state; MCI, mild cognitive impairment; MSA, multiple system atrophy.

Table S5. Global topological properties in other-modality studies in case-control systematic review

Study Subjects' source	Sample characteristics	Methods of network construction	Main findings	Features	Included in meta-analysis
Chen et al. 2019[130] China	PD with dementia: 18 Alzheimer's disease (AD): 22 Dementia with Lewy bodies (DLB): 22 HC: 22	PET (^{18}F-FDG), Gaussian Kernel of FWHM 10 mm, group-level glucose metabolism network, edge definitions: partial correlation of intensity value (exclude age and gender interference), binary network, AAL atlas (90*90), sparsity range 0.06-0.40.	In specific sparsity: DLB patients had higher clustering coefficient, characteristic path length and normalized characteristic path length, and lower global efficiency, normalized clustering coefficient and small-worldness *vs* HC. PD with dementia had higher clustering coefficient, local efficiency and normalized characteristic path length *vs* HC. AD had higher local efficiency *vs* HC.	Dementia	No No available data due to group-level network
Ji et al. 2019[131] China	PD: 57 HC: 52	Rs-fMRI (white matter), regression for nuisance covariates: head motion and CSF signal (not regressed WM & global signal); Gaussian Kernel of FWHM 6 mm, temporal bandpass filter of 0.01-0.1 Hz, edge definition: Pearson correlation coefficient, Fisher's r-to-z transformation; Zalesky's random atlas (128*128, 256*256 or 512*512), sparsity range 0.04-0.40.	PD had higher normalized clustering coefficient and small-worldness *vs* HC, with no significant differences in strength, normalized characteristic path length, local efficiency and global efficiency; results robust in networks of 128, 256 and 512 nodes.		Yes
Ko et al. 2018[132] USA	PD1: 33 PD2: 33 PD3: 33 PD4: 21 HC1: 33 HC2: 33	PET (^{18}F-FDG), Gaussian Kernel of FWHM 10 mm, group-level glucose metabolism network, edge definitions: absolute values of pairwise regional correlation coefficients, binary network, AAL atlas (95*95), sparsity range 0.28-0.50 in PD1 and HC1, 0.12-0.50 in PD2, PD3, PD4 and HC2.	No significant group differences in global metrics in whole brain, but PD1, PD2 and PD3 patients had higher clustering coefficient and small-worldness and lower characteristic path length *vs* HC1 and HC2 in PD-related metabolic network.		No No available data due to group-level network
Li et al. 2023[133] China	PD: 49 HC: 49	PET (^{18}F-FDG), individual glucose metabolism network, edge definitions: Jensen-Shannon divergence similarity estimation, binary network, AAL atlas (90*90), sparsity range 0.02-0.50 with step 0.01.	PD had higher assortativity, modularity, normalized characteristic path length and characteristic path length, and lower global efficiency and synchronization *vs* HC, with no significant differences in clustering coefficient, local efficiency, normalized clustering coefficient, hierarchy and small-worldness.		Yes
Liu et al. 2020[134] China	PD1: 20 PD2: 15 HC: 20	PET (^{18}F-FDG), Gaussian Kernel of FWHM 8 mm, group-level glucose metabolism network, edge definitions: partial correlation coefficients (exclude age and gender interference), binary network, AAL and metabolism atlas (95*95), sparsity range 0.38-0.50 with step 0.01.	No significant group differences in global metrics in whole brain. However, in PD-related metabolic network, PD1 had higher clustering coefficient and characteristic path length *vs* HC while PD2 had higher clustering coefficient and small-worldness *vs* HC.		No No available data due to group-level network
Olde Dubbelink et al. 2014[135] Netherlands	At baseline de novo PD: 12 HC: 14 After follow-up PD: 43 HC: 14	Rs-MEG, frequency bands: delta band (0.5-4 Hz), theta band (4-8 Hz), alpha 1 band (8-10 Hz), alpha 2 band (10-13 Hz), beta band (13-30 Hz) and gamma band (30-48 Hz); edge definitions: phase lag index, weighted network, the definition of nodes: AAL atlas (78*78).	In delta band, de novo PD had lower normalized clustering coefficient *vs* HC, with no significant difference in normalized characteristic path length. Normalized clustering coefficient (theta, alpha 1 and alpha 2 bands) and normalized characteristic path length (alpha 2 only) decreased over time in PD.	Progression	Yes

Wang et al. 2022[136] USA	PD: 11 HC: 34	Rs-MEG, 204 gradiometers and 102 magnetometers, frequency bandpass filter: 26-50 Hz, edge definitions: phase locking values, the definition of nodes: Glasser atlas (360*360).	PD in DBS-ON state had higher strength, global efficiency and clustering coefficient *vs* PD in DBS-OFF state and HC, and lower modularity than patients in DBS-OFF state. Both PD in DBS-ON and DBS-OFF states had lower transitivity *vs* HC.	After deep brain stimulation	No After DBS surgery

Abbreviations: AAL, Automated Anatomical Labeling; CSF, cerebrospinal fluid, PET, positron emission tomography; FDG, fluorodeoxyglucose; PD, Parkinson's disease; HC, health control; FWHM, full width at half maxima; Rs, resting-state; fMRI, functional MRI; MEG, magnetic encephalography; DBS, deep brain stimulation.

Table S6. Demographic and clinical characteristics in dMRI studies in case-control meta-analysis

Study	Subgroup	PD n	PD male n	PD age years	HC n	HC male n	HC age years	Education years	Duration years	UPDRS-III	H&Y	MMSE	Drug state	LEDD mg
Abbasi et al. 2018	Non-subgroup	132	84	61.3	61	38	60.2	15.3	NA	10.4	NA	NA	Naïve/off-state	NA
Chung et al. 2022	PDD-H	38	22	72.4	23	13	70.1	8.51	1.7	27.9	NA	NA	Naïve/off-state	NA
Chung et al. 2022	PDD-L	37	22	70.9	23	13	70.1	9.15	1.6	26.8	NA	NA	Naïve/off-state	NA
Colon-Perez et al. 2018	PD-Well	31	NA	67.3	40	NA	68.2	16.8	7.9	18.2	NA	NA	On-state	NA
Galantucci et al. 2017	PD-NC	54	29	63	41	15	63	11.8	4.6	26.3	1.6	28.6	On-state	447
Galantucci et al. 2017	PD-MCI	54	29	64	41	15	63	10.9	6.2	37.2	2.1	27.6	On-state	691
Gan et al.2024	PD-NICD	17	9	60.1	18	14	64.1	11.1	6.8	35.4	2.2	28.1	On-state	620
Gan et al.2024	PD-ICD	17	11	58.9	18	14	64.1	12.1	9.5	35.5	2.3	28.5	On-state	765
Ge et al.2024	PD-non-Apathy	37	24	66.5	40	25	63.9	11.5	3	23.9	2	29	Naïve/off-state	450
Ge et al.2024	PD-Apathy	47	31	65.7	40	25	63.9	11.0	4	25.5	2	29	Naïve/off-state	450
Guan et al. 2019	Non-subgroup	90	50	59.4	38	16	57.9	8.4	4.0	25.9	1.9	27.0	Naïve/off-state	NA
Hu et al. 2020	PD-non-Depression	47	25	57.9	46	22	57.8	10.8	6.3	26.2	1.6	NA	On-state	554
Hu et al. 2020	PD-Depression	20	9	58.1	46	22	57.8	11.2	5.4	27.7	1.4	NA	On-state	501
Inguanzo et al. 2021	PD-NC	35	27	63	51	23	66	14	7	15	2	NA	On-state	527
Inguanzo et al. 2021	PD-MCI	20	9	68	51	23	66	11	8	15	2.4	NA	On-state	575
Jin et al. 2022	PD-NFOG	34	17	64.7	23	9	64.2	10.4	3.1	22.3	2.1	25.8	Naïve/off-state	NA
Jin et al. 2022	PD-FOG	21	10	65.5	23	9	64.2	9.46	5.9	23.4	2.4	25.6	Naïve/off-state	NA
Kamagata et al. 2018	Non-subgroup	21	12	64.5	21	8	63.7	NA	5	14.4	1.5	NA	On-state	NA
Koirala et al. 2019	Non-subgroup	12	4	66.8	13	8	53.2	NA	13.6	34.5	3.8	NA	On-state	622
Kok et al. 2020	Data NL	14	10	65	15	10	61.4	NA	5.2	18.4	NA	NA	Naïve/off-state	NA
Kok et al. 2020	Data CA	19	12	60.7	18	4	56.9	NA	4.8	25.4	NA	NA	Naïve/off-state	NA
Li et al. 2017	Non-subgroup	35	18	61.3	26	16	62.8	NA	2.1	30.0	2.1	27.0	Naïve/off-state	NA
Li et al. 2024	PD-NPIGD	30	18	65.9	35	23	64.8	9	5.5	30.1	2.7	28.2	Naïve/off-state	NA
Li et al. 2024	PD-PIGD	31	20	66.2	35	23	64.8	12	4	29.3	2.6	27.9	Naïve/off-state	NA
Nigro et al. 2016	Non-subgroup	21	15	57.9	30	20	60.6	NA	1.6	16.0	1.5	28.4	Naïve/off-state	NA
Ren et al. 2024	Non-subgroup	42	21	63.6	38	18	62.3	8.3	5.7	17.7	1.9	26.8	On-state	NA
Shang et al. 2023b	Non-subgroup	69	30	63.9	70	NA	NA	11.3	3.7	27.4	1.5	23.	Naïve/off-state	315
Vriend et al. 2018	Non-subgroup	23	17	58.9	38	20	57.9	NA	0.2	21.8	1.9	28.6	Naïve/off-state	NA
Wang et al. 2019	PD-non-dyskinetic	21	14	63.2	25	17	62.9	10.5	6.0	34.4	2.2	28.1	Naïve/off-state	718
Wang et al. 2019	PD-dyskinetic	21	13	60.3	25	17	62.9	9.9	9	35.7	2.5	27.9	Naïve/off-state	745
Wang et al. 2020	PD-NC	43	16	60.2	31	16	57	12	2	28.6	2	29	NA	NA
Wang et al. 2020	PD-MCI	28	23	63.9	31	16	57	9	2	30.8	2.5	26	NA	NA
Wang et al. 2023a	PD-nFOG	40	25	61.8	25	NA	NA	11.3	6.4	29.8	2.2	28	Naïve/off-state	687
Wang et al. 2023a	PD-FOG	30	17	62.3	25	NA	NA	9.7	6.3	33.5	2.4	28	Naïve/off-state	646
Wen et al. 2022	PD-non-Apathy	28	15	60.4	32	23	62.1	13	5.3	12.7	2	NA	On-state	439
Wen et al. 2022	PD-Apathy	31	23	62.7	32	23	62.1	12.1	6.8	18.9	2	NA	On-state	506
Zarkali et al. 2020	Non-subgroup	100	53	64.3	34	16	66.4	16.9	4.1	15.4	NA	28.9	On-state	449
Zhang et al. 2022	PD-L	13	7	60.6	13	NA	NA	NA	3.9	24.1	1.7	27.9	Naïve/off-state	NA
Zhang et al. 2022	PD-R	13	8	59.2	13	NA	NA	NA	3.6	24.5	1.8	27.4	Naïve/off-state	NA

Abbreviations: PD, Parkinson's disease; HC, healthy controls; PDD-H, PD with dementia high-risk group; PDD-L, PD with dementia low-risk group; PD-Well, cognitively well PD; PD-NC, PD with normal cognition; PD-MCI, PD with mild cognitive impairment; PD-ICD, PD with impulse control disorders; PD-NICD, PD without impulse control disorders; PD-FOG, PD with freezing of gait; PD-NFOG, PD without freezing of gait; Data NL, Dutch dataset; Data CA, Canadian dataset; PD-PIGD, PD with postural instability/gait difficulty; PD-NPIGD, PD with without postural instability/gait difficulty; PD-L, left-onset PD; PD-R, right-onset PD; UPDRS, Unified Parkinson's Disease Rating Scale; H&Y, Hoehn and Yahr; MMSE, Mini-mental state examination; LEDD, levodopa-equivalent daily dose; dMRI, diffusion MRI; NA, not available.

Table S7. Demographic and clinical characteristics in fMRI studies in case-control meta-analysis

Study	Subgroup	PD n	PD male n	PD age years	HC n	HC male n	HC age years	Education years	Duration years	UPDRS-III	H&Y	MMSE	Drug state	LEDD mg
Albano et al. 2022	PD-Candidates for DBS	19	11	61.1	60	29	61.8	11.2	8.9	43.7	2.3	NA	On-state	883
Albano et al. 2022	PD-Non-candidates	41	25	62.0	60	29	61.8	12.3	7.4	34.7	1.9	NA	On-state	680
Berman et al. 2016	Non-subgroup	19	11	61.7	16	9	61.3	NA	5.7	24.4	2.2	NA	Naïve/off-state	547
Chen et al. 2023	Non-subgroup	53	28	60.2	88	37	61.1	10.3	2	17.3	1.8	27	Naïve/off-state	390
Dan et al. 2024	PD with probable RBD	36	19	61.2	71	32	60.5	11	3	17.5	NA	NA	Naïve/off-state	NA
Dan et al. 2024	PD without probable RBD	57	26	58.4	71	32	60.5	9	2	16	NA	NA	Naïve/off-state	NA
De Micco et al. 2021	PD-all	147	85	63.2	38	18	61.3	10.5	1.4	19.4	1.5	NA	Naïve/off-state	NA
Devignes et al. 2022	PD-FS	14	13	67.3	24	10	62.1	14.8	8.9	26.6	2.3	NA	On-state	782
Devignes et al. 2022	PD-MS	30	15	67.2	24	10	62.1	10.2	8.2	22.4	2.3	NA	On-state	815
Devignes et al. 2022	PD-NC	31	26	63.3	24	10	62.1	13.6	9.5	22.1	2.0	NA	On-state	728
Devignes et al. 2022	PD-PC	20	12	63.3	24	10	62.1	11.9	6.8	21	2	NA	On-state	731
Engels et al. 2018	Non-subgroup	24	17	63.4	27	16	59.4	5.3	4.1	17.7	NA	NA	Naïve/off-state	797
Fang et al. 2017	Non-subgroup	26	13	62.2	19	8	56.2	NA	2.2	20.9	1.6	27	Naïve/off-state	106
Filippi et al. 2021	Moderate to severe-PD	60	37	63.6	60	29	61.8	11.4	8.8	43.3	2.5	NA	On-state	480
Filippi et al. 2021	Mild-PD	86	48	60.2	60	29	61.8	13.2	2.0	17.2	1.1	NA	On-state	149
Guan et al. 2019	Non-subgroup	90	50	59.4	38	16	57.9	8.4	4.0	25.9	1.85	27.0	Naïve/off-state	NA
Holtbernd et al. 2024	Non-subgroup	18	9	65.4	39	28	64.4	NA	5.2	24.7	1.7	29	On-state	936
Hou et al. 2020	PD-NC	19	8	54.9	28	8	55.4	12.5	1.9	20.8	1.9	NA	Naïve/off-state	NA
Hou et al. 2020	PD-MCI	22	11	55.8	28	8	55.4	8.1	1.5	20.2	1.8	NA	Naïve/off-state	NA
Hou et al. 2023	PD-GBA	11	5	46.3	18	8	49.9	8.9	3.9	31.1	2.1	NA	Naïve/off-state	276
Hou et al. 2023	PD-noncarriers	11	7	47.9	18	8	49.9	10.6	2.6	27.4	2	NA	Naïve/off-state	282
Klobušiaková et al. 2019	PD-NC	17	13	61	51	15	68	17	4	14	2	28	On-state	610
Klobušiaková et al. 2019	PD-MCI	22	15	68	51	15	68	13	5	14	2	27	On-state	895
Li et al. 2022	Non-subgroup	40	20	53.3	20	10	53.3	9.2	2.4	20	1.7	27.4	Naïve/off-state	485
Li et al. 2024	PD-Dementia	19	10	68	34	15	64.5	9	5	38.5	2.5	NA	On-state	450
Li et al. 2024	PD-NC	46	21	61	34	15	64.5	12	5	21.4	2	NA	On-state	388
Li et al. 2024	PD-MCI	43	20	61	34	15	64.5	9	3	18.3	2	NA	On-state	300
Lopes et al. 2017	Group 2	31	24	64.6	25	16	62.0	13.8	8.3	22.6	2.1	28.5	On-state	728
Lopes et al. 2017	Group 4	14	10	69.8	25	16	62.0	9.4	10.4	22.0	2.2	24.14	On-state	839
Lopes et al. 2017	Group 3	43	26	66.7	25	16	62.0	11.3	8.7	21.3	2.2	27.0	On-state	863
Lopes et al. 2017	Group 1	31	21	60.2	25	16	62.0	13.5	7.5	19.1	1.9	28.8	On-state	753
Ma et al. 2017	Non-subgroup	32	13	59.3	31	12	61.9	NA	3.3	29.3	2.1	27.1	Naïve/off-state	NA
Qiu et al. 2021	PD-Depression	22	13	64.5	25	9	55	9.5	3	30.6	2	28	Naïve/off-state	0
Qiu et al. 2021	PD-non-Depression	23	16	66	25	9	55	10.1	3	27.3	2	28	Naïve/off-state	0

Sako et al. 2019	Non-subgroup	23	12	67	11	6	67	NA	4.7	NA	2	NA	Naïve/off-state	255
Sarasso et al. 2022	PD-FOG	30	22	63.8	30	21	63.7	11.9	9.9	47.1	2.6	NA	On-state	956
Sarasso et al. 2022	PD- FOG-converters	11	7	61.9	30	21	63.	11.6	10.9	43.6	2.5	NA	On-state	89
Sarasso et al. 2022	PD- non converters	11	6	63.8	30	21	63.7	12.1	7.7	32.8	1.9	NA	On-state	691
Schill et al. 2023	Non-subgroup	14	9	59.6	23	11	64.1	18.0	2.9	11.1	1.3	NA	On-state	539
Shang et al. 2023a	Non-subgroup	51	31	60.7	60	35	61.6	12.1	3.4	28.9	1.5	28.6	Naïve/off-state	NA
Shang et al. 2023b	Non-subgroup	69	30	63.9	70	34	63.3	11.3	3.7	27.4	1.5	23.2	Naïve/off-state	315
Siva et al. 2024	PD-no/mild hyposmia	15	6	64.4	15	7	63.3	NA	6.1	15.8	2	29	On-state	395
Siva et al. 2024	PD-severe hyposmia	15	7	70.7	15	7	63.3	NA	5.9	14.2	2	29.1	On-state	456
Skidmore et al. 2011	Non-subgroup	14	12	62	15	9	65	NA	NA	39	NA	27	Naïve/off-state	NA
Sreenivasan et al. 2023	PD-FOG	16	13	69.4	16	9	68.5	14.9	9.5	19.4	2.2	NA	On-state	1052
Sreenivasan et al. 2023	PD-nFOG	16	10	67.6	16	9	68.5	16.2	7.3	13.2	2	NA	On-state	491
Suo et al. 2017	Non-subgroup	153	67	55.7	81	36	53.7	8.5	5.5	27.8	2.4	27	Naïve/off-state	788
Suo et al. 2022	PD-MCI	24	9	54.3	24	11	55.4	9.6	3.3	24.3	1.9	27.7	Naïve/off-state	291
Suo et al. 2022	PD-NC	17	10	54	24	11	55.4	11.4	2.2	17.1	1.8	28.8	Naïve/off-state	241
Tang et al. 2017	PD-Familial	31	17	53.1	38	21	53.4	NA	5.7	NA	2.4	28.1	Naïve/off-state	434
Tang et al. 2017	PD-Sporadic	36	21	53.8	38	21	53.4	NA	4.7	NA	2.3	25.6	Naïve/off-state	333
Tuovinen et al. 2018	Non-subgroup	16	11	65.4	16	11	59.8	NA	2.2	29.7	2.3	29.1	Naïve/off-state	377
Vancea et al. 2019	Non-subgroup	16	8	62.3	16	8	62.8	15.2	10.0	18.1	1.9	28.5	Naïve/off-state	964
Wang et al. 2023a	PD-FOG	30	17	62.3	25	17	62.3	9.7	6.3	33.5	2.4	28	Naïve/off-state	645
Wang et al. 2023a	PD-nFOG	40	25	61.8	25	17	62.3	11.3	6.4	29.8	2.2	28	Naïve/off-state	687
Wang et al. 2023b	PD-Depression	20	8	59.2	41	21	60.1	9.0	NA	28.7	NA	27	Naïve/off-state	NA
Wang et al. 2023b	PD-non-Depression	37	20	58.7	41	21	60.1	9.3	NA	24.9	NA	29	Naïve/off-state	NA
Wright et al. 2020	PD-NC	10	8	66.5	10	2	62.8	NA	9.4	13.1	NA	NA	On-state	576
Zhang et al. 2014	PD-non-tremor-dominant	10	6	63.1	20	11	59.2	7.8	2.6	NA	2.2	30	Naïve/off-state	NA
Zhang et al. 2014	PD-tremor-dominant	15	8	60.5	20	11	59.2	9.8	2.5	NA	2.3	29.8	Naïve/off-state	NA
Zhang et al. 2022	PD-R	13	8	59.2	13	5	61.4	NA	3.6	24.5	1.8	27.4	Naïve/off-state	NA
Zhang et al. 2022	PD-L	13	7	60.6	13	5	61.4	NA	3.9	24.1	1.7	27.9	Naïve/off-state	NA
Baggio et al. 2014	PD-NC	43	23	64	36	19	63.4	10.8	6.1	14.1	1.6	29.4	On-state	647
Baggio et al. 2014	PD-MCI	23	14	66.7	36	19	63.4	9.7	9	18.6	2.0	28.52	On-state	940
Gottlich et al. 2013	Non-subgroup	37	22	65	20	10	63	NA	6.5	22.3	NA	NA	On-state	NA
Hou et al. 2018	PD-AR	20	10	54.3	20	9	53.2	10.6	2.4	20.6	2	NA	Naïve/off-state	NA
Prajapati et al. 2020	Non-subgroup	51	22	48.4	51	NA	NA	NA	NA	NA	NA	NA	Naïve/off-state	NA
Sang et al. 2015	Non-subgroup	26	12	54.3	30	NA	NA	NA	2.2	19.0	1.3	28.4	Naïve/off-state	318

Abbreviations: PD, Parkinson's disease; HC, health control; DBS, deep brain stimulation; RBD, REM sleep behavior disorder; PD-FS, PD with frontostriatal cognitive subtype; PD-MS, PD with mixed cognitive subtype; PD-NC, PD with normal cognition; PD-PC, PD with posterior cortical cognitive subtype; PD-MCI, PD with mild cognitive impairment; PD-GBA, PD with glucocerebrosidase mutation; Group 1/2/3/4, PD with intact cognition(G1), only slight mental slowing

(G2), mild to moderate deficits mainly in executive functions (G3), severe deficits in all cognitive domains (G4); PD-FOG, PD with freezing of gait; PD-nFOG, PD without freezing of gait; PD-L, left-onset PD; PD-R, right-onset PD; PD-AR, rigidity-dominant PD; UPDRS, Unified Parkinson's Disease Rating Scale; H&Y, Hoehn and Yahr; MMSE, Mini-mental state examination; LEDD, levodopa-equivalent daily dose; fMRI, functional MRI; NA, not available.

Table S8. Demographic and clinical characteristics in sMRI studies in case-control meta-analysis

Study	Subgroup	PD n	PD male n	PD age years	HC n	HC male n	HC age years	Education years	Duration years	UPDRS-III	H&Y	MMSE	Drug state	LEDD mg
Suo et al. 2021a	Non-subgroup	54	19	56	54	18	56	9	1.5	17.4	1.6	27.9	Naïve/off-state	129
Suo et al. 2021b	PD-N	17	10	54	29	12	53	11	2.2	17.1	1.8	28.8	Naïve/off-state	241
Suo et al. 2021b	PD-M	24	9	54	29	12	53	10	3.3	24.3	1.9	27.7	Naïve/off-state	291
Xu et al. 2017	Non-subgroup	37	20	59	34	12	56	NA	3.9	19.2	NA	NA	NA	325
Yan et al. 2024	Non-subgroup	50	27	59	46	21	58	8	6.1	25.0	2.6	27.8	On-state	478

Abbreviations: PD, Parkinson's disease; HC, healthy controls; PD-N, PD with normal cognition; PD-M, PD with mild cognitive impairment; UPDRS, Unified Parkinson's Disease Rating Scale; H&Y, Hoehn and Yahr; MMSE, Mini-mental state examination; LEDD, levodopa-equivalent daily dose; sMRI, structural MRI; NA, not available.

Table S9. Demographic and clinical characteristics in EEG studies in case-control meta-analysis

Study	Subgroup	PD n	PD male n	PD age years	HC n	HC male n	HC age years	Education years	Duration years	UPDRS-III	H&Y	MMSE	Drug state	LEDD mg
Bosch et al. 2022	Non-subgroup	83	58	68.6	42	24	71.4	NA	5.1	13.4	NA	NA	On-state	863
Fogelson et al. 2013	Non-subgroup	15	8	58.8	15	8	58.3	NA	5.6	20.2	2.2	NA	On-state	NA
Formaggio et al. 2021	Non-subgroup	15	9	69.93	10	3	NA	11.5	6.1	33.1	NA	NA	Naïve/off-state	450
Mehraram et al. 2020	Non-subgroup	21	20	73.4	18	11	76.3	NA	NA	24.5	NA	23.4	On-state	806
Peláez Suárez et al. 2021	PD-NC	15	12	58.4	26	NA	NA	NA	7.7	31.73	NA	NA	On-state	568.3
Peláez Suárez et al. 2021	PD-MCI	15	12	62.7	26	NA	NA	NA	8.1	36	NA	NA	On-state	588
Rajagopal et al. 2025	Non-subgroup	26	17	NA	13	8	69	NA	NA	NA	NA	NA	On-state	NA
Vecchio et al. 2021	Non-subgroup	13	5	61.5	13	5	61.5	NA	NA	NA	NA	NA	NA	NA
Wang et al. 2024	Non-subgroup	32	18	65.8	30	14	63.3	12.1	5.1	31.4	NA	27.3	NA	NA
Yin et al. 2023	PD-NFOG	13	10	64.6	16	7	63.9	9.6	5.6	18.3	1.4	26.2	NA	NA
Yin et al. 2023	PD-FOG	15	10	64.6	16	7	63.9	9.8	5.7	26.3	1.5	26.5	NA	NA
Zhang et al. 2022	Non-subgroup	29	9	NA	22	11	NA	NA	3.2	NA	NA	NA	Naïve/off-state	NA

Abbreviations: PD, Parkinson's disease; HC, healthy controls; PD-NC, PD with normal cognition; PD-MCI, PD with mild cognitive impairment; PD-FOG, PD with freezing of gait; PD-nFOG, PD without freezing of gait; UPDRS, Unified Parkinson's Disease Rating Scale; H&Y, Hoehn and Yahr; MMSE, Mini-mental state examination; LEDD, levodopa-equivalent daily dose; EEG, electroencephalography; NA, not available.

Table S10. Overview of graph theory methods in dMRI studies in case-control meta-analysis

Study	Subgroup	Parcellation	Template	Template_cerebellum	Nodes	Tractography	Edge weighting	Direction	Threshold
Abbasi et al. 2018	Non-subgroup	AAL	AAL	Cerebellum-excluded	90	DT	FA	64	Proportional threshold
Chung et al. 2022	PDD-H	AAL2	AAL	Contain cerebellum	120	DT	FA	45	Non-proportional threshold
Chung et al. 2022	PDD-L	AAL2	AAL	Contain cerebellum	120	DT	FA	45	Non-proportional threshold
Colon-Perez et al. 2018	PD-Well	Desikan–Killiany	Non-AAL	Cerebellum-excluded	82	DT	NA	6/64	Non-proportional threshold
Galantucci et al. 2017	PD-NC	Desikan–Killiany	Non-AAL	Cerebellum-excluded	83	DT	FA	65	Non-proportional threshold
Galantucci et al. 2017	PD-MCI	Desikan–Killiany	Non-AAL	Cerebellum-excluded	83	DT	FA	65	Non-proportional threshold
Gan et al.2024	PD-NICD	AAL	AAL	Contain cerebellum	116	DT	NA	30	Non-proportional threshold
Gan et al.2024	PD-ICD	AAL	AAL	Contain cerebellum	116	DT	NA	30	Non-proportional threshold
Ge et al.2024	PD-non-Apathy	AAL	AAL	Cerebellum-excluded	90	DT	NA	30	Non-proportional threshold
Ge et al.2024	PD-Apathy	AAL	AAL	Cerebellum-excluded	90	DT	NA	30	Non-proportional threshold
Guan et al. 2019	Non-subgroup	AAL	AAL	Cerebellum-excluded	90	DT	FA	32	Proportional threshold
Hu et al. 2020	PD-non-Depression	AAL	AAL	Cerebellum-excluded	90	DT	NA	64	Non-proportional threshold
Hu et al. 2020	PD-Depression	AAL	AAL	Cerebellum-excluded	90	DT	NA	64	Non-proportional threshold
Inguanzo et al. 2021	PD-NC	Desikan–Killiany	Non-AAL	Cerebellum-excluded	86	PT	NOS	30	Non-proportional threshold
Inguanzo et al. 2021	PD-MCI	Desikan–Killiany	Non-AAL	Cerebellum-excluded	86	PT	NOS	30	Non-proportional threshold
Jin et al. 2022	PD-NFOG	AAL	AAL	Cerebellum-excluded	90	DT	NA	99	Non-proportional threshold
Jin et al. 2022	PD-FOG	AAL	AAL	Cerebellum-excluded	90	DT	NA	99	Non-proportional threshold
Kamagata et al. 2018	Non-subgroup	Desikan–Killiany	Non-AAL	Cerebellum-excluded	84	PT	NOS	32	Proportional threshold
Koirala et al. 2019	Non-subgroup	AAL	AAL	Contain cerebellum	116	PT	NOS	32	Non-proportional threshold
Kok et al. 2020	Data NL	Desikan–Killiany	Non-AAL	Cerebellum-excluded	85	PT	FA	60	Non-proportional threshold
Kok et al. 2020	Data CA	Desikan–Killiany	Non-AAL	Cerebellum-excluded	85	PT	FA	32	Non-proportional threshold
Li et al. 2017	Non-subgroup	AAL	AAL	Cerebellum-excluded	90	DT	FA	25	Non-proportional threshold
Li et al. 2024	PD-NPIGD	AAL	AAL	Contain cerebellum	116	DT	NOS	30	Non-proportional threshold
Li et al. 2024	PD-PIGD	AAL	AAL	Contain cerebellum	116	DT	NOS	30	Non-proportional threshold
Nigro et al. 2016	Non-subgroup	AAL	AAL	Cerebellum-excluded	90	DT	NA	27	Non-proportional threshold
Ren et al. 2024	Non-subgroup	AAL	AAL	Cerebellum-excluded	90	PT	NA	32	Non-proportional threshold
Shang et al. 2023b	Non-subgroup	AAL	AAL	Cerebellum-excluded	90	DT	NA	30	Proportional threshold
Vriend et al. 2018	Non-subgroup	BNA and FSL FIRST	Non-AAL	Cerebellum-excluded	224	PT	NOS	30	Proportional threshold
Wang et al. 2019	PD-non-dyskinetic	AAL	AAL	Cerebellum-excluded	90	DT	NOS	30	Non-proportional threshold
Wang et al. 2019	PD-dyskinetic	AAL	AAL	Cerebellum-excluded	90	DT	NOS	30	Non-proportional threshold
Wang et al. 2020	PD-NC	AAL	AAL	Cerebellum-excluded	90	DT	NOS	25	Non-proportional threshold
Wang et al. 2020	PD-MCI	AAL	AAL	Cerebellum-excluded	90	DT	NOS	25	Non-proportional threshold
Wang et al. 2023a	PD-nFOG	AAL	AAL	Cerebellum-excluded	116	DT	NOS	30	Non-proportional threshold
Wang et al. 2023a	PD-FOG	AAL	AAL	Cerebellum-excluded	116	DT	NOS	30	Non-proportional threshold
Wen et al. 2022	PD-non-Apathy	Destrieux	Non-AAL	Cerebellum-excluded	168	DT	NA	102	Non-proportional threshold
Wen et al. 2022	PD-Apathy	Destrieux	Non-AAL	Cerebellum-excluded	168	DT	NA	102	Non-proportional threshold
Zarkali et al. 2020	Non-subgroup	Glasser	Non-AAL	Cerebellum-excluded	379	PT	NA	17/8/64	Non-proportional threshold
Zhang et al. 2022	PD-L	AAL	AAL	Cerebellum-excluded	90	DT	FA	64	Proportional threshold
Zhang et al. 2022	PD-R	AAL	AAL	Cerebellum-excluded	90	DT	FA	64	Proportional threshold

Abbreviations: PD, Parkinson's disease; PDD-H, PD with dementia high-risk group; PDD-L, PD with dementia low-risk group; PD-Well, cognitively well PD; PD-NC, PD with normal cognition; PD-MCI, PD with mild cognitive impairment; PD-ICD, PD with impulse control disorders; PD-NICD, PD without impulse control disorders; PD-FOG, PD with freezing of gait; PD-NFOG, PD without freezing of gait; Data NL, Dutch dataset; Data CA, Canadian dataset; PD-PIGD, PD with postural instability/gait difficulty; PD-NPIGD, PD with without postural instability/gait difficulty; PD-L, left-onset PD; PD-R, right-onset PD; AAL, Automated Anatomical Labeling; BNA, Brainnetome Atlas; FSL, functional MRI of the brain (FMRIB) software library; DT, deterministic tractography; PT, probabilistic tractography; FA, fractional anisotropy; NOS, number of streamline; dMRI, diffusion MRI; NA, not available.

Table S11. Overview of graph theory methods in fMRI studies in case-control meta-analysis

Study	Subgroup	Scanning	Parcellation	Template	Nodes	Network framework	Threshold
Albano et al. 2022	PD-Candidates for DBS	1.5T	Desikan–Killiany	Macroanatomy	83	Weighted	Non-proportional threshold
Albano et al. 2022	PD-Non-candidates	1.5T	Desikan–Killiany	Macroanatomy	83	Weighted	Non-proportional threshold
Berman et al. 2016	Non-subgroup	3T	Power	Function	226	Binary	Proportional threshold
Chen et al. 2023	Non-subgroup	3T	AAL	Macroanatomy	116	Binary	Proportional threshold
Dan et al. 2024	PD with probable RBD	3T	Dosenbach	Function	160	Weighted	Proportional threshold
Dan et al. 2024	PD without probable RBD	3T	Dosenbach	Function	160	Weighted	Proportional threshold
De Micco et al. 2021	PD-all	3T	AAL-based (K-means)	NA	220	Weighted	Non-proportional threshold
Devignes et al. 2022	PD-FS	3T	Group-level parcellation (ICA)	NA	590	Weighted	Proportional threshold
Devignes et al. 2022	PD-MS	3T	Group-level parcellation (ICA)	NA	590	Weighted	Proportional threshold
Devignes et al. 2022	PD-NC	3T	Group-level parcellation (ICA)	NA	590	Weighted	Proportional threshold
Devignes et al. 2022	PD-PC	3T	Group-level parcellation (ICA)	NA	590	Weighted	Proportional threshold
Engels et al. 2018	Non-subgroup	3T	Power	Function	264	Weighted	Non-proportional threshold
Fang et al. 2017	Non-subgroup	3T	Shen	Function	278	Binary	Proportional threshold
Filippi et al. 2021	Moderate to severe-PD	1.5T	Desikan–Killiany	Macroanatomy	83	Weighted	Non-proportional threshold
Filippi et al. 2021	Mild-PD	1.5T	Desikan–Killiany	Macroanatomy	83	Weighted	Non-proportional threshold
Guan et al. 2019	Non-subgroup	3T	AAL	Macroanatomy	90	Weighted	Proportional threshold
Holtbernd et al. 2024	Non-subgroup	3T	AAL3v1 (Modification)	Macroanatomy	142	Weighted	Non-proportional threshold
Hou et al. 2020	PD-NC	3T	Dosenbach	Function	160	Binary	Proportional threshold
Hou et al. 2020	PD-MCI	3T	Dosenbach	Function	160	Binary	Proportional threshold
Hou et al. 2023	PD-GBA	3T	Dosenbach	Function	160	Binary	Proportional threshold
Hou et al. 2023	PD- noncarriers	3T	Dosenbach	Function	160	Binary	Proportional threshold
Klobušiaková et al. 2019	PD-NC	3T	AAL	Macroanatomy	78	Weighted	Non-proportional threshold
Klobušiaková et al. 2019	PD-MCI	3T	AAL	Macroanatomy	78	Weighted	Non-proportional threshold
Li et al. 2022	Non-subgroup	3T	AAL	Macroanatomy	116	Binary	Proportional threshold
Li et al. 2024	PD-Dementia	3T	ICA	NA	22	Weighted	Proportional threshold
Li et al. 2024	PD-NC	3T	ICA	NA	22	Weighted	Proportional threshold
Li et al. 2024	PD-MCI	3T	ICA	NA	22	Weighted	Proportional threshold
Lopes et al. 2017	Group 2	3T	Destrieux	Macroanatomy	164	Binary	Proportional threshold
Lopes et al. 2017	Group 4	3T	Destrieux	Macroanatomy	164	Binary	Proportional threshold
Lopes et al. 2017	Group 3	3T	Destrieux	Macroanatomy	164	Binary	Proportional threshold
Lopes et al. 2017	Group 1	3T	Destrieux	Macroanatomy	164	Binary	Proportional threshold
Ma et al. 2017	Non-subgroup	3T	Zalesky's random	NA	1024	Weighted	Non-proportional threshold
Qiu et al. 2021	PD-Depression	3T	AAL	Macroanatomy	90	Binary	Proportional threshold
Qiu et al. 2021	PD-non-Depression	3T	AAL	Macroanatomy	90	Binary	Proportional threshold
Sako et al. 2019	Non-subgroup	3T	AAL	Macroanatomy	132	Binary	Non-proportional threshold
Sarasso et al. 2022	PD-FOG	1.5T	Desikan–Killiany	Macroanatomy	83	Weighted	Non-proportional threshold
Sarasso et al. 2022	PD- FOG- converters	1.5T	Desikan–Killiany	Macroanatomy	83	Weighted	Non-proportional threshold
Sarasso et al. 2022	PD- non converters	1.5T	Desikan–Killiany	Macroanatomy	83	Weighted	Non-proportional threshold
Schill et al. 2023	Non-subgroup	3T	Eickhoff-Zilles cytoarchitectonic probabilistic atlas	NA	212	Weighted	Non-proportional threshold
Shang et al. 2023a	Non-subgroup	3T	AAL	Macroanatomy	90	Binary	Proportional threshold
Shang et al. 2023b	Non-subgroup	3T	AAL	Macroanatomy	90	Binary	Proportional threshold

Siva et al. 2024	PD-no/mild hyposmia	3T	Dosenbach	Function	160	Binary	Proportional threshold
Siva et al. 2024	PD-severe hyposmia	3T	Dosenbach	Function	160	Binary	Proportional threshold
Skidmore et al. 2011	Non-subgroup	3T	AAL	Macroanatomy	116	Weighted	Non-proportional threshold
Sreenivasan et al. 2023	PD-FOG	3T	Brainnetome	NA	242	Weighted	Proportional threshold
Sreenivasan et al. 2023	PD-nFOG	3T	Brainnetome	NA	242	Weighted	Proportional threshold
Suo et al. 2017	Non-subgroup	3T	AAL	Macroanatomy	90	Binary	Proportional threshold
Suo et al. 2022	PD-MCI	3T	AAL	Macroanatomy	116	Weighted	Proportional threshold
Suo et al. 2022	PD-NC	3T	AAL	Macroanatomy	116	Weighted	Proportional threshold
Tang et al. 2017	PD-Familial	3T	Brainnetome	NA	246	Weighted	Non-proportional threshold
Tang et al. 2017	PD-Sporadic	3T	Brainnetome	NA	246	Weighted	Non-proportional threshold
Tuovinen et al. 2018	Non-subgroup	3T	AAL	Macroanatomy	116	Weighted	Non-proportional threshold
Vancea et al. 2019	Non-subgroup	3T	Eickhoff-Zilles cytoarchitectonic probabilistic atlas	NA	206	Weighted	Proportional threshold
Wang et al. 2023a	PD-FOG	3T	AAL	Macroanatomy	116	Weighted	Proportional threshold
Wang et al. 2023a	PD-nFOG	3T	AAL	Macroanatomy	116	Weighted	Proportional threshold
Wang et al. 2023b	PD-Depression	3T	Brainnetome	NA	246	Binary	Proportional threshold
Wang et al. 2023b	PD-non-Depression	3T	Brainnetome	NA	246	Binary	Proportional threshold
Wright et al. 2020	PD-NC	3T	AAL&pons	Macroanatomy	118	Binary	Proportional threshold
Zhang et al. 2014	PD-non-tremor-dominant	1.5T	Zalesky's random	NA	1024	Weighted	Non-proportional threshold
Zhang et al. 2014	PD-tremor-dominant	1.5T	Zalesky's random	NA	1024	Weighted	Non-proportional threshold
Zhang et al. 2022	PD-R	3T	AAL	Macroanatomy	90	NA	Proportional threshold
Zhang et al. 2022	PD-L	3T	AAL	Macroanatomy	90	NA	Proportional threshold
Baggio et al. 2014	PD-NC	3T	AAL	Macroanatomy	90	Weighted	Proportional threshold
Baggio et al. 2014	PD-MCI	3T	AAL	Macroanatomy	90	Weighted	Proportional threshold
Gottlich et al. 2013	Non-subgroup	1.5T	AAL (further parcellated)	NA	343	Binary	Proportional threshold
Hou et al. 2018	PD-AR	3T	AAL	Macroanatomy	90	Binary	Proportional threshold
Prajapati et al. 2020	Non-subgroup	3T	Dosenbach	Function	160	Binary	Proportional threshold
Sang et al. 2015	Non-subgroup	3T	AAL	Macroanatomy	90	Binary	Proportional threshold

Abbreviations: PD, Parkinson's disease; DBS, deep brain stimulation; RBD, REM sleep behavior disorder; PD-FS, PD with frontostriatal cognitive subtype; PD-MS, PD with mixed cognitive subtype; PD-NC, PD with normal cognition; PD-PC, PD with posterior cortical cognitive subtype; PD-MCI, PD with mild cognitive impairment; PD-GBA, PD with glucocerebrosidase mutation; Group 1/2/3/4, PD with intact cognition(G1), only slight mental slowing (G2), mild to moderate deficits mainly in executive functions (G3), severe deficits in all cognitive domains (G4); PD-FOG, PD with freezing of gait; PD-nFOG, PD without freezing of gait; PD-L, left-onset PD; PD-R, right-onset PD; PD-AR, rigidity-dominant PD; AAL, Automated Anatomical Labeling; ICA, Independent Component Analysis; fMRI, functional MRI; NA, not available.

Table S12. Overview of graph theory methods in EEG studies in case-control meta-analysis

Study	Subgroup	Parcellation	Nodes	Edge definition	Network framework	Threshold
Bosch et al. 2022	Non-subgroup	Electrode positioning	59	Phase locking value	Weighted	Proportional threshold
Fogelson et al. 2013	Non-subgroup	Electrode positioning	64	Synchronization likelihood	Binary	Proportional threshold
Formaggio et al. 2021	Non-subgroup	Brodmann	8	Granger coefficients	Weighted	Non-proportional threshold
Mehraram et al. 2020	Non-subgroup	Electrode positioning	NA	Weighted phase lag index	Weighted	Proportional threshold
Peláez Suárez et al. 2021	PD-NC	Electrode positioning	45	Synchronization likelihood	NA	Non-proportional threshold
Peláez Suárez et al. 2021	PD-MCI	Electrode positioning	45	Synchronization likelihood	NA	Non-proportional threshold
Rajagopal et al. 2025	Non-subgroup	Electrode positioning	59	Phase locking value	Weighted	Non-proportional threshold
Vecchio et al. 2021	Non-subgroup	Brodmann	84	Lagged Linear Connectivity values	Weighted	Non-proportional threshold
Wang et al. 2024	Non-subgroup	AAL	90	Weighted phase lag index	NA	Non-proportional threshold
Yin et al. 2023	PD-NFOG	Electrode positioning	30	Transfer entropy	Binary	Non-proportional threshold
Yin et al. 2023	PD-FOG	Electrode positioning	30	Transfer entropy	Binary	Non-proportional threshold
Zhang et al. 2022	Non-subgroup	Electrode positioning	19	Phase lag index	Weighted	Proportional threshold

Abbreviations: PD, Parkinson's disease; PD-NC, PD with normal cognition; PD-MCI, PD with mild cognitive impairment; PD-FOG, PD with freezing of gait; PD-nFOG, PD without freezing of gait; AAL, Automated Anatomical Labeling; EEG, electroencephalography; NA, not available.

Figure S1. Forest plot for clustering coefficient in dMRI studies in case-control meta-analysis

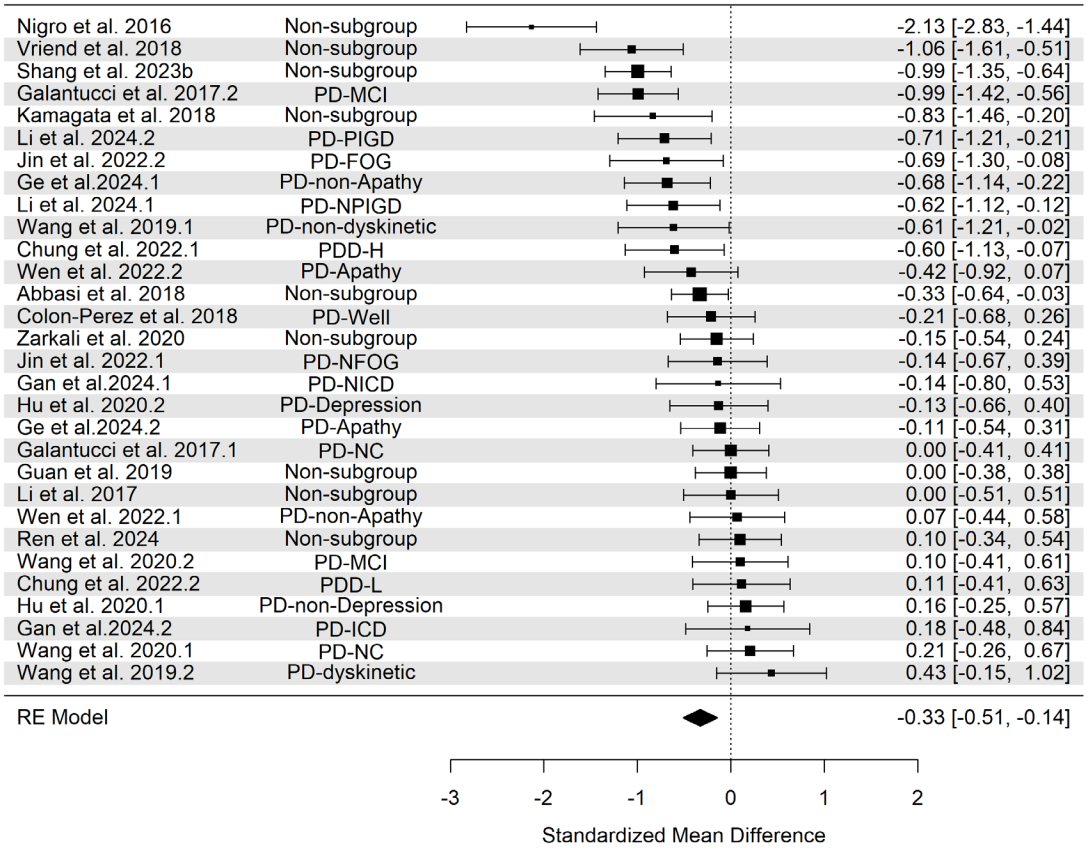

Effect sizes comparing Parkinson's disease with healthy controls are displayed for each dataset. Black squares denote dataset-specific effect sizes, with their size proportional to the corresponding study weight. Horizontal lines represent 95% confidence intervals, and the diamond indicates the pooled effect size from the multilevel random-effects model. Abbreviations: PD, Parkinson's disease; PD-MCI, PD with mild cognitive impairment; PD-PIGD, PD with postural instability/gait difficulty; PD-FOG, PD with freezing of gait; PD-NPIGD, PD with without postural instability/gait difficulty; PDD-H, PD with dementia high-risk group; PD-Well, cognitively well PD; PD-NFOG, PD without freezing of gait; PD-NICD, PD without impulse control disorders; PD; PD-NC, PD with normal cognition; PDD-L, PD with dementia low-risk group; PD-ICD, PD with impulse control disorders.

Figure S2. Forest plot for clustering coefficient in EEG studies in case-control meta-analysis

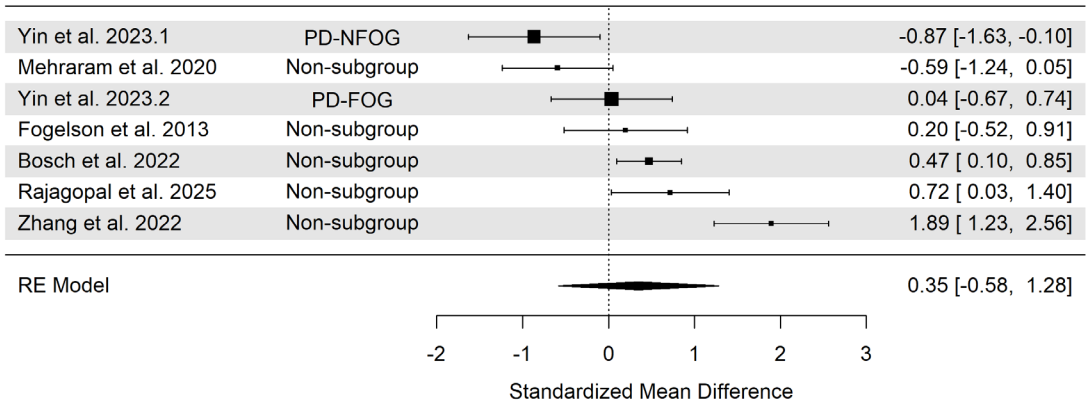

Effect sizes comparing Parkinson's disease with healthy controls are displayed for each dataset. Black squares denote dataset-specific effect sizes, with their size proportional to the corresponding study weight. Horizontal lines represent 95% confidence intervals, and the diamond indicates the pooled effect size from the multilevel random-effects model. Abbreviations: PD, Parkinson's disease; PD-FOG, PD with freezing of gait; PD-NFOG, PD without freezing of gait.

Figure S3. Forest plot for clustering coefficient in fMRI studies in case-control meta-analysis

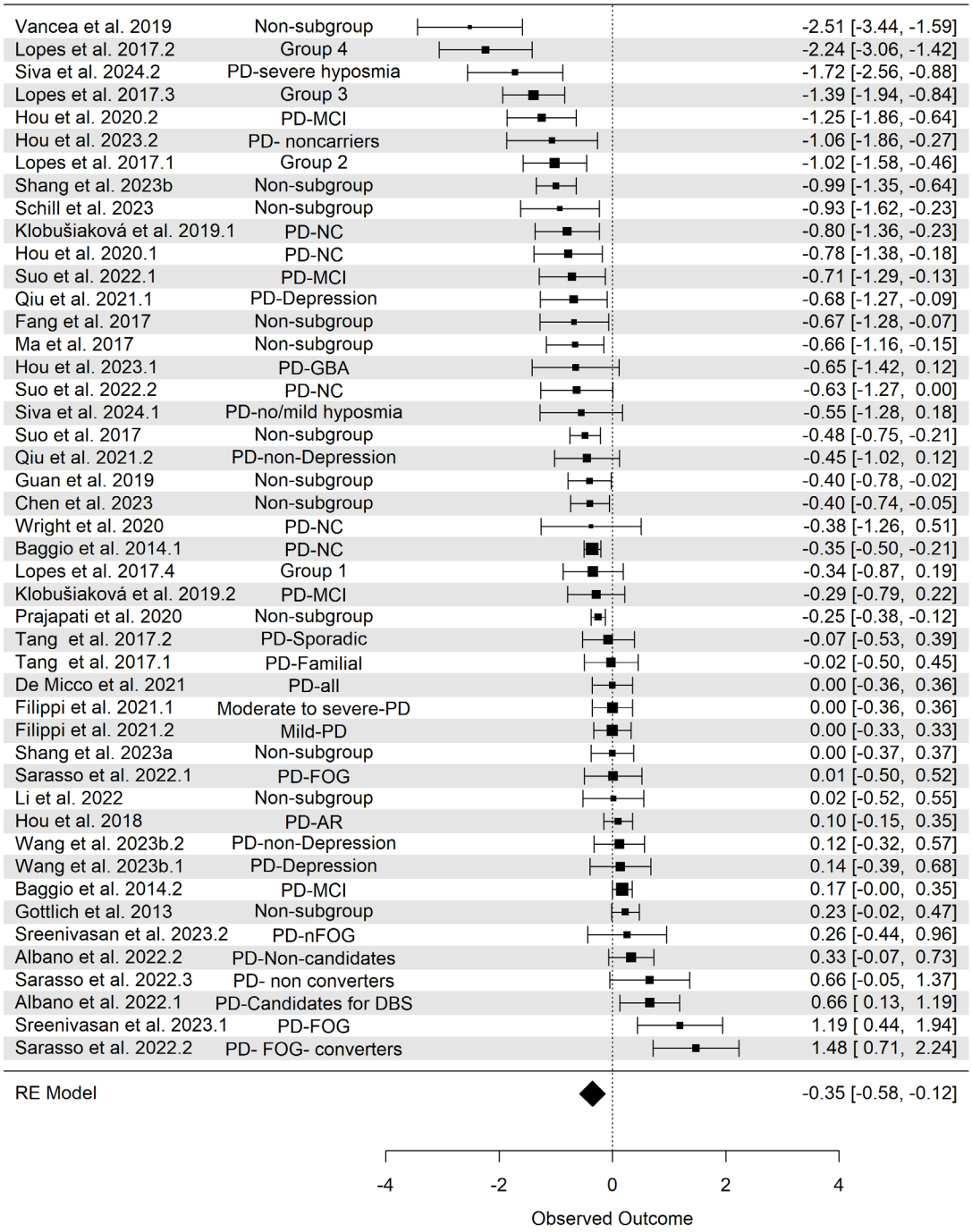

Effect sizes comparing Parkinson's disease with healthy controls are displayed for each dataset. Black squares denote dataset-specific effect sizes, with their size proportional to the corresponding study weight. Horizontal lines represent 95% confidence intervals, and the diamond indicates the pooled effect size from the multilevel random-effects model. Abbreviations: PD, Parkinson's disease; Group 1/2/3/4, PD with intact cognition (G1), only slight mental slowing (G2), mild to moderate deficits mainly in executive functions (G3), severe deficits in all cognitive domains (G4); PD-MCI, PD with mild cognitive impairment; PD-NC, PD with normal cognition; PD-GBA, PD with glucocerebrosidase mutation; PD-FOG, PD with freezing of gait; PD-nFOG, PD without freezing of gait; PD-AR, rigidity-dominant PD; DBS, deep brain stimulation.

Figure S4. Forest plot for local efficiency in dMRI studies in case-control meta-analysis

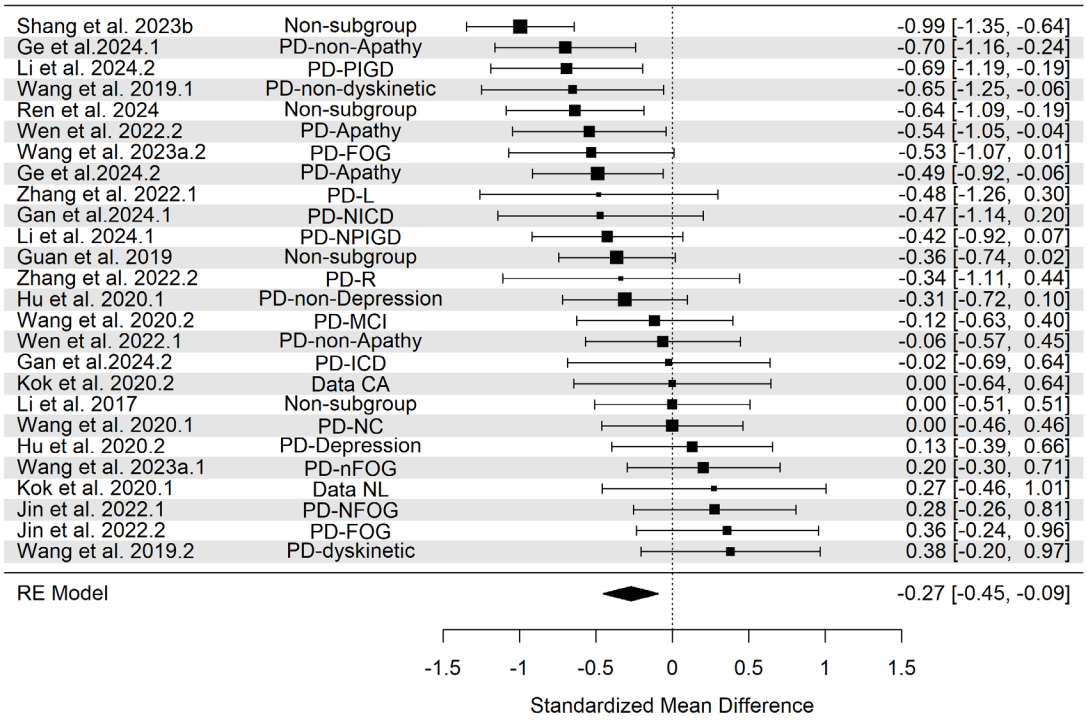

Effect sizes comparing Parkinson's disease with healthy controls are displayed for each dataset. Black squares denote dataset-specific effect sizes, with their size proportional to the corresponding study weight. Horizontal lines represent 95% confidence intervals, and the diamond indicates the pooled effect size from the multilevel random-effects model. Abbreviations: PD, Parkinson's disease; PD-PIGD, PD with postural instability/gait difficulty; PD-FOG, PD with freezing of gait; PD-L, left-onset PD; PD-NICD, PD without impulse control disorders; PD-NPIGD, PD with without postural instability/gait difficulty; PD-R, right-onset PD; PD-MCI, PD with mild cognitive impairment; PD-ICD, PD with impulse control disorders; Data CA, Canadian dataset; PD-NC, PD with normal cognition; PD-nFOG, PD without freezing of gait; Data NL, Dutch dataset.

Figure S5. Forest plot for local efficiency in fMRI studies in case-control meta-analysis

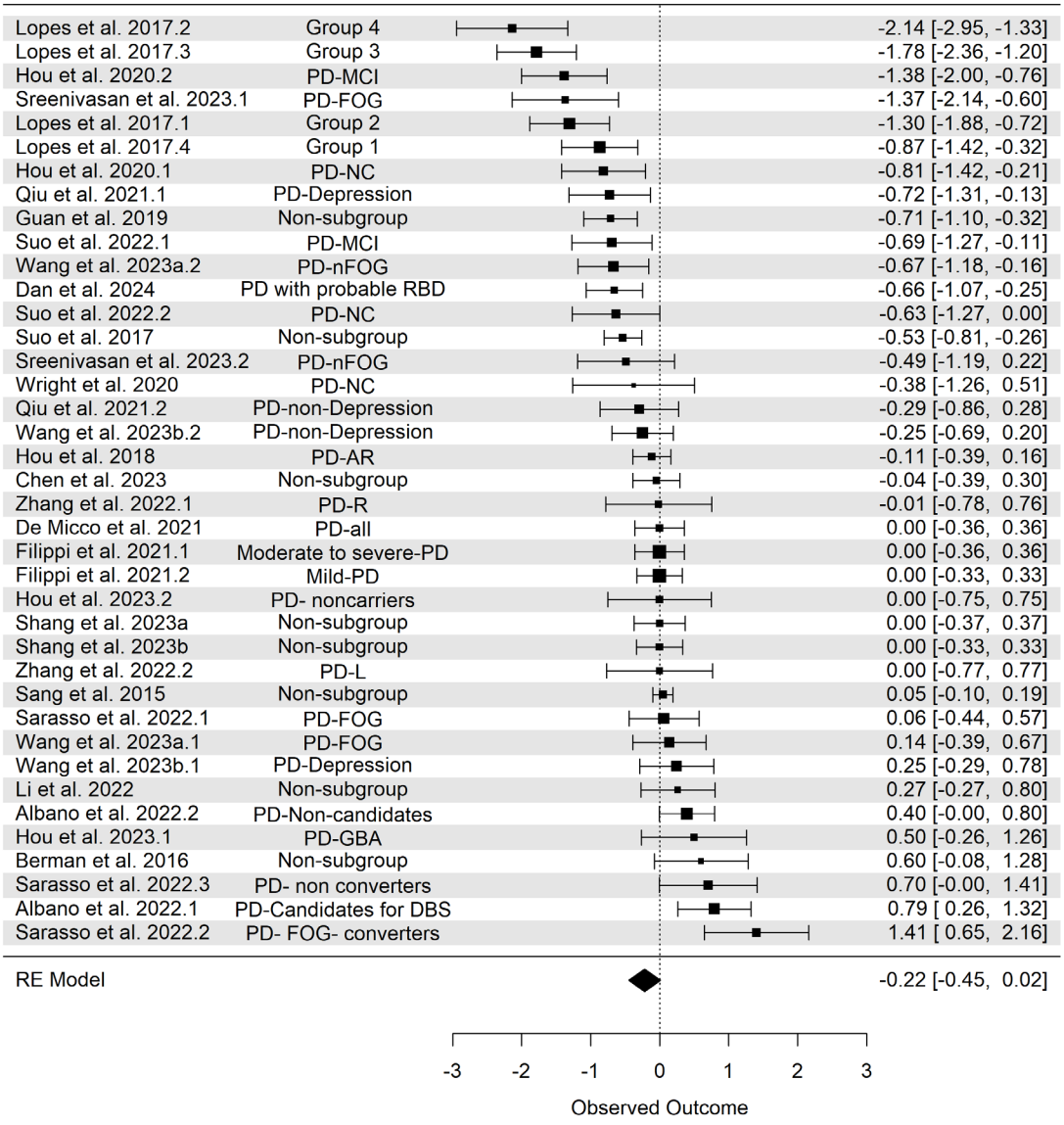

Effect sizes comparing Parkinson's disease with healthy controls are displayed for each dataset. Black squares denote dataset-specific effect sizes, with their size proportional to the corresponding study weight. Horizontal lines represent 95% confidence intervals, and the diamond indicates the pooled effect size from the multilevel random-effects model. Abbreviations: PD, Parkinson's disease; Group 1/2/3/4, PD with intact cognition (G1), only slight mental slowing (G2), mild to moderate deficits mainly in executive functions (G3), severe deficits in all cognitive domains (G4); PD-MCI, PD with mild cognitive impairment; PD-FOG, PD with freezing of gait; PD-NC, PD with normal cognition; PD-nFOG, PD without freezing of gait; PD-AR, rigidity-dominant PD; PD-R, right-onset PD; PD-L, left-onset PD PD-GBA, PD with glucocerebrosidase mutation; DBS, deep brain stimulation.

Figure S6. Forest plot for characteristic path length in dMRI studies in case-control meta-analysis

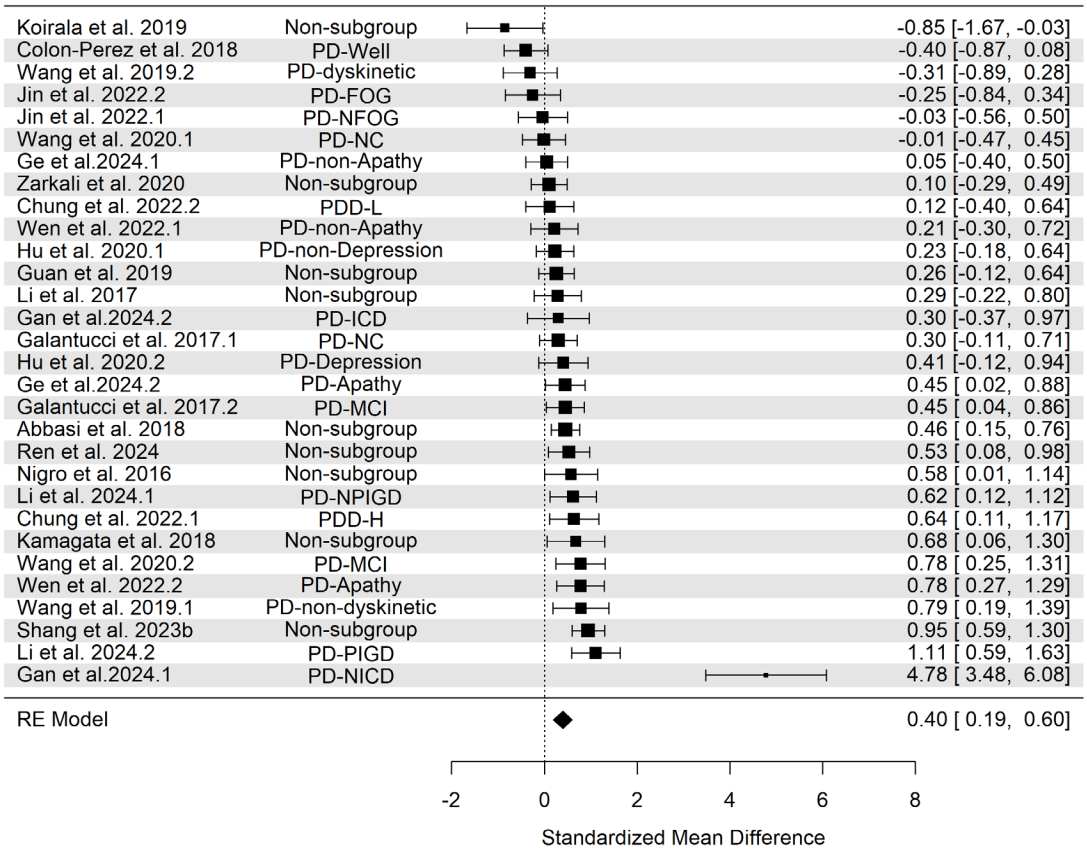

Effect sizes comparing Parkinson's disease with healthy controls are displayed for each dataset. Black squares denote dataset-specific effect sizes, with their size proportional to the corresponding study weight. Horizontal lines represent 95% confidence intervals, and the diamond indicates the pooled effect size from the multilevel random-effects model. Abbreviations: PD, Parkinson's disease; PD-Well, cognitively well PD; PD-FOG, PD with freezing of gait; PD-NFOG, PD without freezing of gait; PD-NC, PD with normal cognition; PDD-L, PD with dementia low-risk group; PD-ICD, PD with impulse control disorders; PD-MCI, PD with mild cognitive impairment; PD-NPIGD, PD with without postural instability/gait difficulty; PDD-H, PD with dementia high-risk group; PD-PIGD, PD with postural instability/gait difficulty; PD-NICD, PD without impulse control disorders; PD.

Figure S7. Forest plot for characteristic path length in EEG studies in case-control meta-analysis

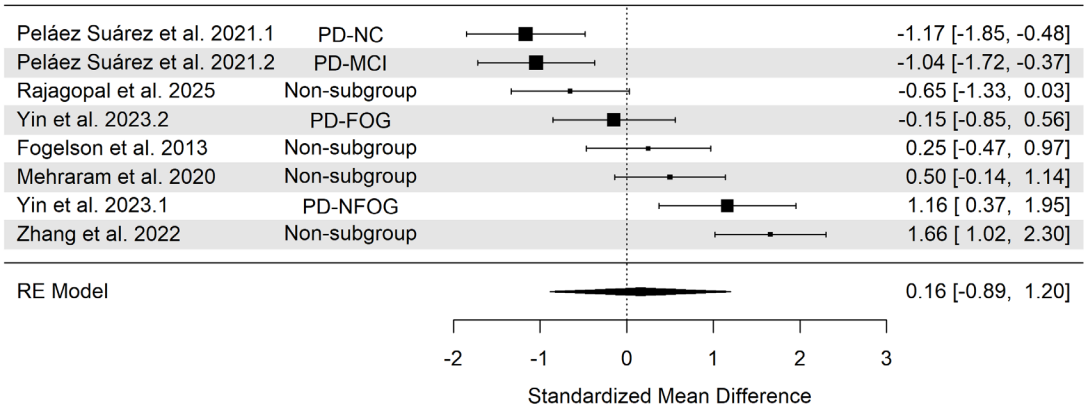

Effect sizes comparing Parkinson's disease with healthy controls are displayed for each dataset. Black squares denote dataset-specific effect sizes, with their size proportional to the corresponding study weight. Horizontal lines represent 95% confidence intervals, and the diamond indicates the pooled effect size from the multilevel random-effects model. Abbreviations: PD, Parkinson's disease; PD-NC, PD with normal cognition; PD-MCI, PD with mild cognitive impairment; PD-FOG, PD with freezing of gait; PD-NFOG, PD without freezing of gait.

Figure S8. Forest plot for characteristic path length in fMRI studies in case-control meta-analysis

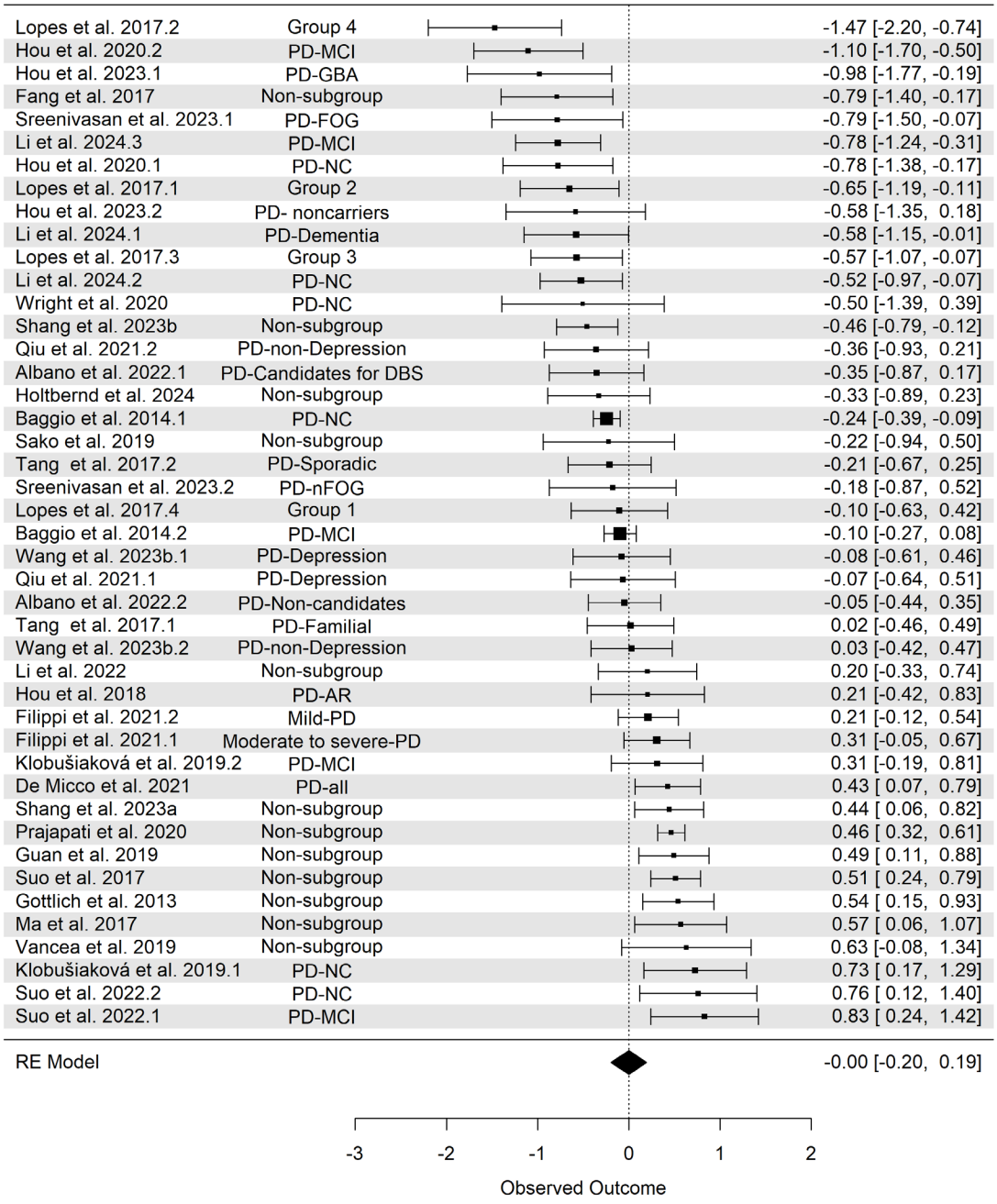

Effect sizes comparing Parkinson's disease with healthy controls are displayed for each dataset. Black squares denote dataset-specific effect sizes, with their size proportional to the corresponding study weight. Horizontal lines represent 95% confidence intervals, and the diamond indicates the pooled effect size from the multilevel random-effects model. Abbreviations: PD, Parkinson's disease; Group 1/2/3/4, PD with intact cognition (G1), only slight mental slowing (G2), mild to moderate deficits mainly in executive functions (G3), severe deficits in all cognitive domains (G4); PD-MCI, PD with mild cognitive impairment; PD-GBA, PD with glucocerebrosidase mutation; PD-FOG, PD with freezing of gait; PD-NC, PD with normal cognition; DBS, deep brain stimulation; PD-nFOG, PD without freezing of gait; PD-AR, rigidity-dominant PD.

Figure S9. Forest plot for global efficiency in dMRI studies in case-control meta-analysis

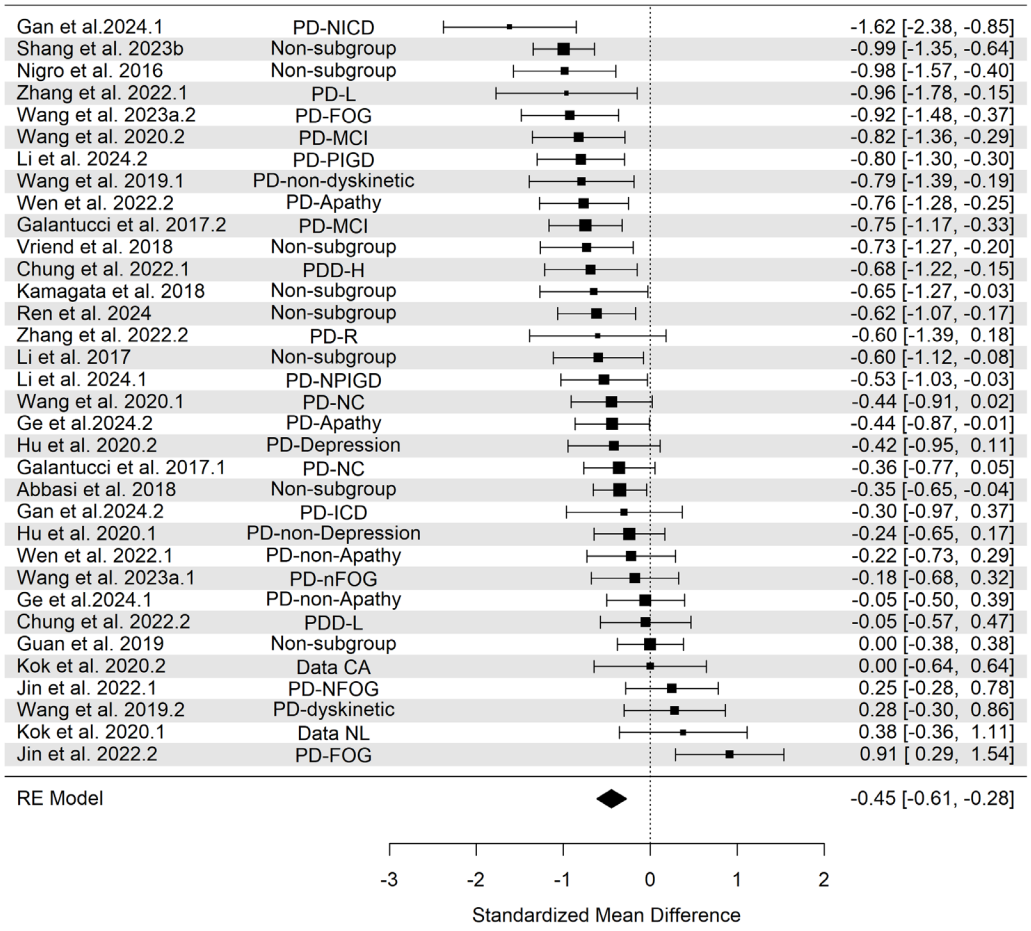

Effect sizes comparing Parkinson's disease with healthy controls are displayed for each dataset. Black squares denote dataset-specific effect sizes, with their size proportional to the corresponding study weight. Horizontal lines represent 95% confidence intervals, and the diamond indicates the pooled effect size from the multilevel random-effects model. Abbreviations: PD, Parkinson's disease; PD-NICD, PD without impulse control disorders; PD-L, left-onset PD; PD-FOG, PD with freezing of gait; PD-MCI, PD with mild cognitive impairment; PD-PIGD, PD with postural instability/gait difficulty; PDD-H, PD with dementia high-risk group; PD-R, right-onset PD; PD-NPIGD, PD with without postural instability/gait difficulty; PD; PD-NC, PD with normal cognition; PD-ICD, PD with impulse control disorders; PD-nFOG, PD without freezing of gait; PDD-L, PD with dementia low-risk group; Data CA, Canadian dataset; Data NL, Dutch dataset.

Figure S10. Forest plot for global efficiency in EEG studies in case-control meta-analysis

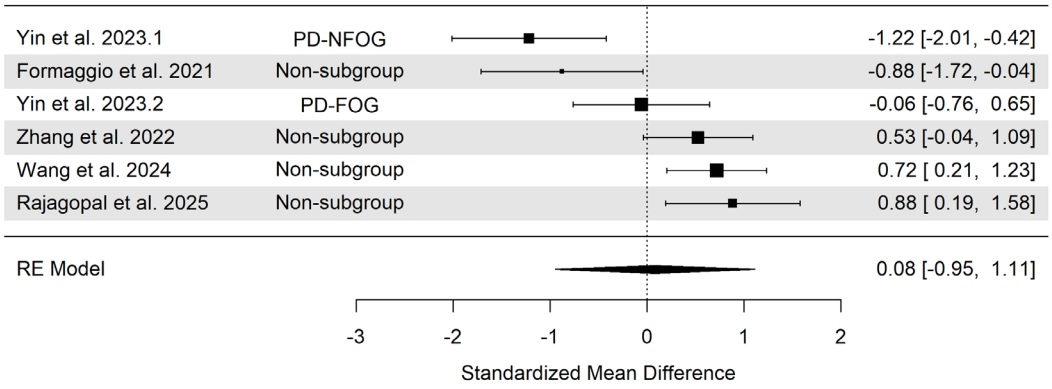

Effect sizes comparing Parkinson's disease with healthy controls are displayed for each dataset. Black squares denote dataset-specific effect sizes, with their size proportional to the corresponding study weight. Horizontal lines represent 95% confidence intervals, and the diamond indicates the pooled effect size from the multilevel random-effects model. Abbreviations: PD, Parkinson's disease; PD-NFOG, PD without freezing of gait; PD-FOG, PD with freezing of gait.

Figure S11. Forest plot for global efficiency in fMRI studies in case-control meta-analysis

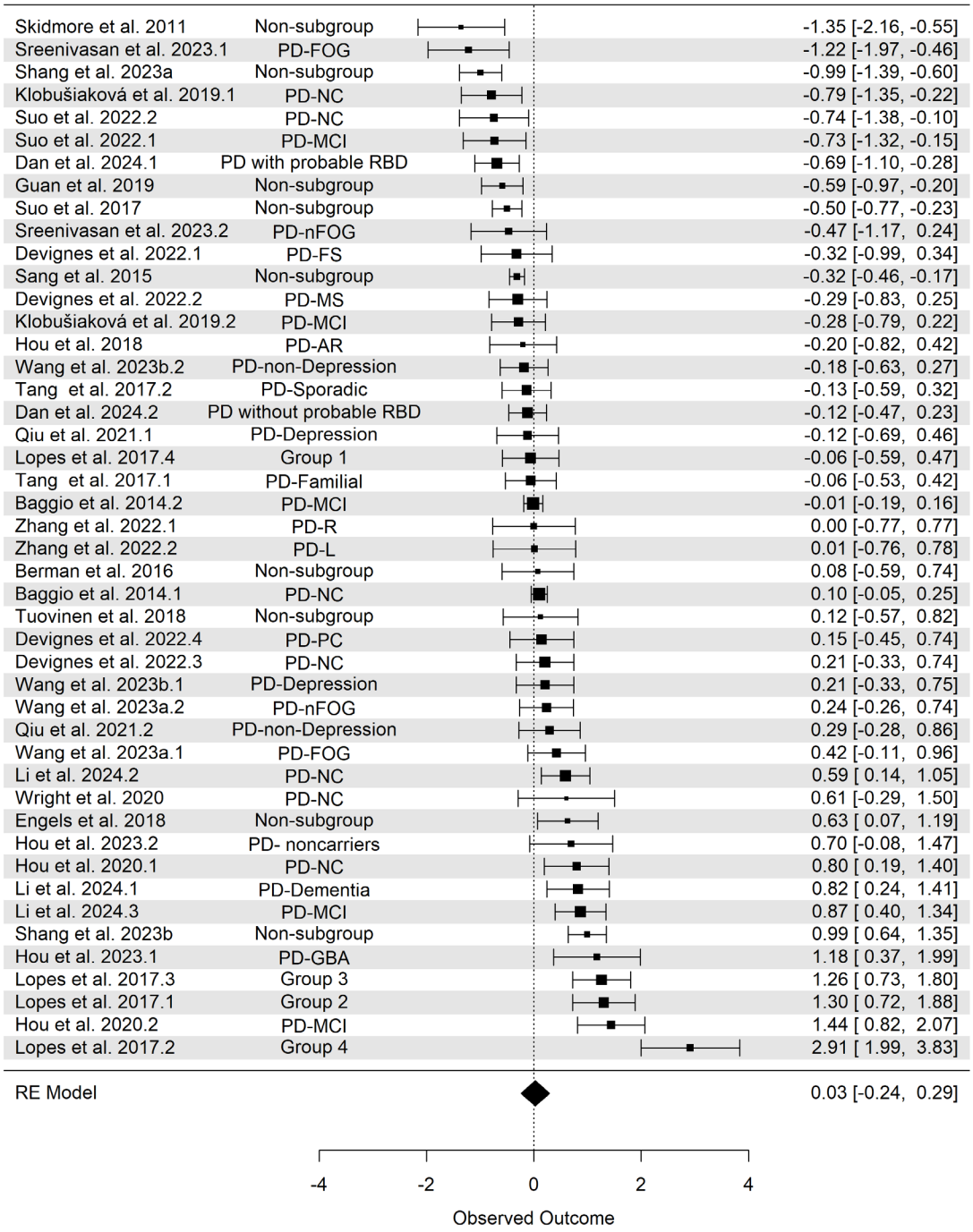

Effect sizes comparing Parkinson's disease with healthy controls are displayed for each dataset. Black squares denote dataset-specific effect sizes, with their size proportional to the corresponding study weight. Horizontal lines represent 95% confidence intervals, and the diamond indicates the pooled effect size from the multilevel random-effects model. Abbreviations: PD, Parkinson's disease; PD-FOG, PD with freezing of gait; PD-NC, PD with normal cognition; PD-MCI, PD with mild cognitive impairment; RBD, REM sleep behavior disorder; PD-nFOG, PD without freezing of gait; PD-FS, PD with frontostriatal cognitive subtype; PD-MS, PD with mixed cognitive subtype; PD-AR, rigidity-dominant PD; Group 1/2/3/4, PD with intact cognition (G1), only slight mental slowing (G2), mild to moderate deficits

mainly in executive functions (G3), severe deficits in all cognitive domains (G4); PD-R, right-onset PD; PD-L, left-onset PD; PD-PC, PD with posterior cortical cognitive subtype; PD-GBA, PD with glucocerebrosidase mutation.

Figure S12. Forest plot for normalized clustering coefficient in dMRI studies in case-control meta-analysis

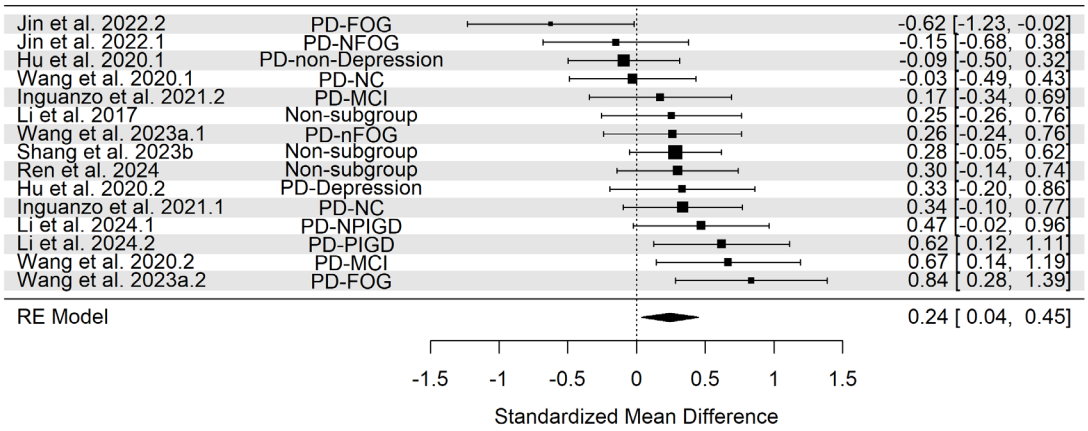

Effect sizes comparing Parkinson's disease with healthy controls are displayed for each dataset. Black squares denote dataset-specific effect sizes, with their size proportional to the corresponding study weight. Horizontal lines represent 95% confidence intervals, and the diamond indicates the pooled effect size from the multilevel random-effects model. Abbreviations: PD, Parkinson's disease; PD-FOG, PD with freezing of gait; PD-NFOG, PD without freezing of gait; PD-NC, PD with normal cognition; PD-MCI, PD with mild cognitive impairment; PD-NPIGD, PD with without postural instability/gait difficulty; PD-PIGD, PD with postural instability/gait difficulty.

Figure S13. Forest plot for normalized clustering coefficient in fMRI studies in case-control meta-analysis

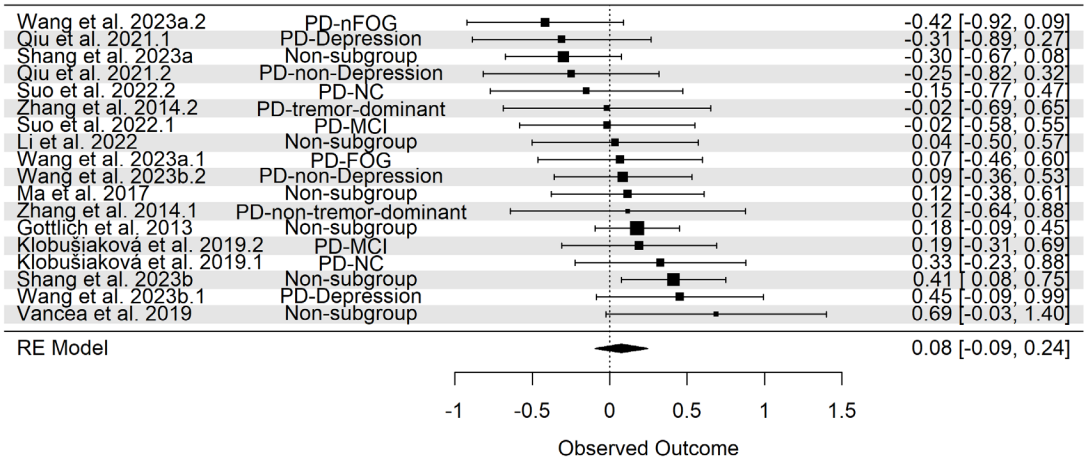

Effect sizes comparing Parkinson's disease with healthy controls are displayed for each dataset. Black squares denote dataset-specific effect sizes, with their size proportional to the corresponding study weight. Horizontal lines represent 95% confidence intervals, and the diamond indicates the pooled effect size from the multilevel random-effects model. Abbreviations: PD, Parkinson's disease; PD-nFOG, PD without freezing of gait; PD-NC, PD with normal cognition; PD-MCI, PD with mild cognitive impairment; PD-FOG, PD with freezing of gait.

Figure S14. Forest plot for small-worldness in dMRI studies in case-control meta-analysis

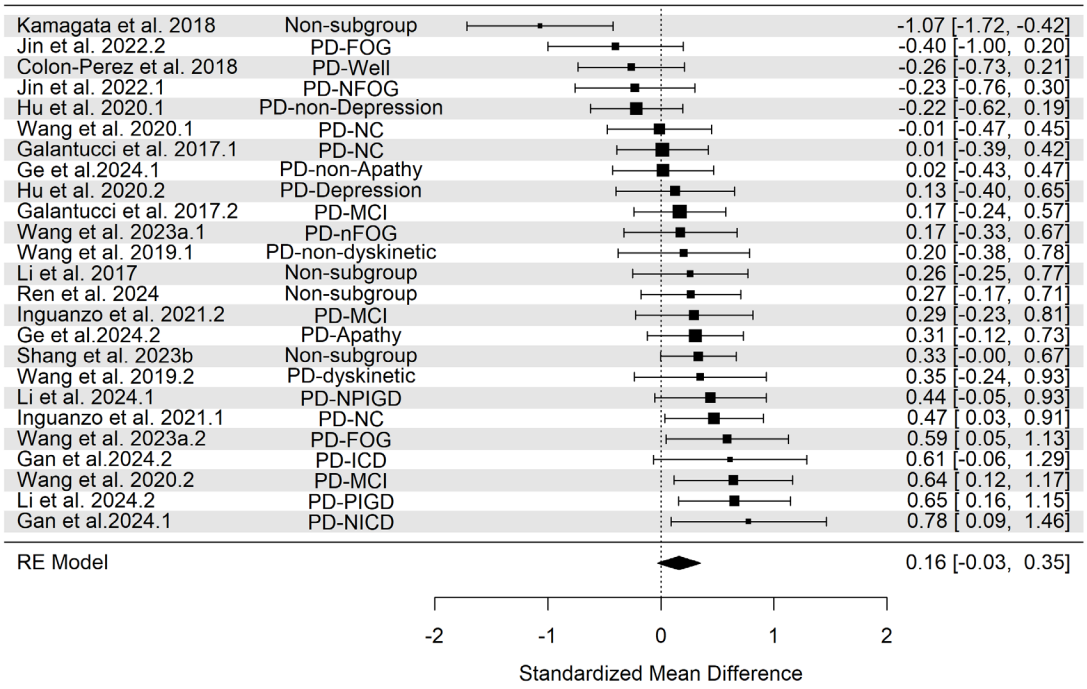

Effect sizes comparing Parkinson's disease with healthy controls are displayed for each dataset. Black squares denote dataset-specific effect sizes, with their size proportional to the corresponding study weight. Horizontal lines represent 95% confidence intervals, and the diamond indicates the pooled effect size from the multilevel random-effects model. Abbreviations: PD, Parkinson's disease; PD-FOG, PD with freezing of gait; PD-Well, cognitively well PD; PD-NFOG, PD without freezing of gait; PD-NC, PD with normal cognition; PD-MCI, PD with mild cognitive impairment; PD-NPIGD, PD with without postural instability/gait difficulty; PD-ICD, PD with impulse control disorders; PD-PIGD, PD with postural instability/gait difficulty; PD-NICD, PD without impulse control disorders.

Figure S15. Forest plot for small-worldness in fMRI studies in case-control meta-analysis

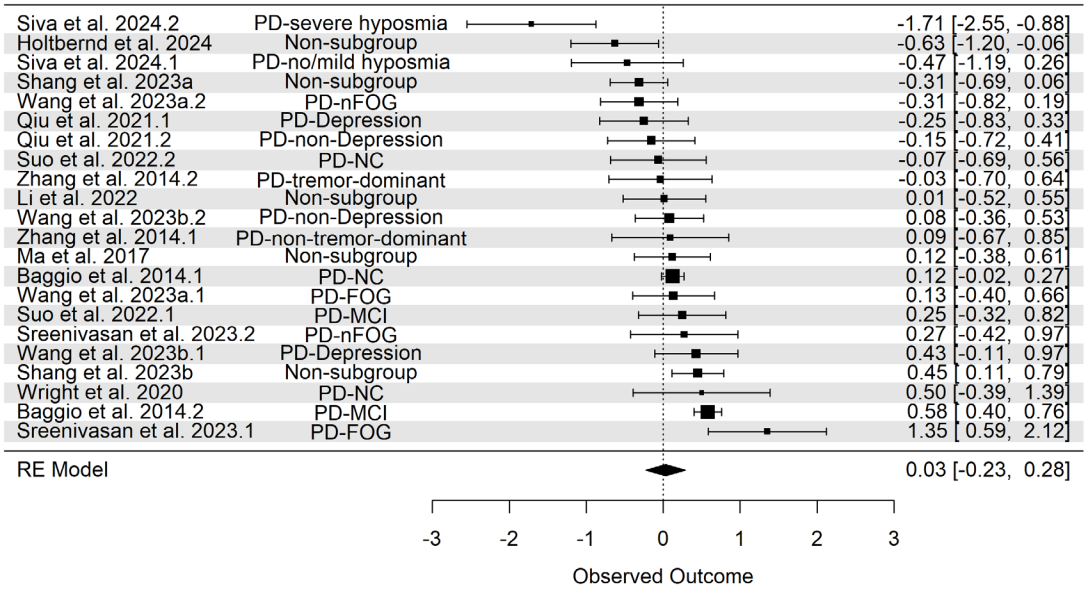

Effect sizes comparing Parkinson's disease with healthy controls are displayed for each dataset. Black squares denote dataset-specific effect sizes, with their size proportional to the corresponding study weight. Horizontal lines represent 95% confidence intervals, and the diamond indicates the pooled effect size from the multilevel random-effects model. Abbreviations: PD, Parkinson's disease; PD-nFOG, PD without freezing of gait; PD-NC, PD with normal cognition; PD-FOG, PD with freezing of gait; PD-MCI, PD with mild cognitive impairment.

Table S13. Other main results in case-control meta-analysis

Modalities	Metrics	No. of studies	No. of effect sizes	g	95% CI	SE	t	Pt	Q	PQ	I² %	Tau
dMRI	Transitivity	1	1	-0.340	-0.732 to 0.051	0.200	-1.705	0.088				
dMRI	BC	1	2	0.456	-1.429 to 2.341	0.148	3.076	0.200	0.178	0.673	< 0.001	< 0.001
dMRI	Eccentricity	1	1	-1.369	-2.240 to -0.497	0.445	-3.078	0.002				
fMRI	Transitivity	1	1	-0.133	-0.852 to 0.586	0.367	-0.362	0.717				
fMRI	BC	1	1	-0.122	-0.248 to 0.003	0.064	-1.912	0.056				
fMRI	Degree	1	1	-0.346	-1.069 to 0.377	0.369	-0.938	0.348				
fMRI	PC	1	2	-0.106	-3.395 to 3.184	0.259	-0.408	0.753	0.451	0.502	< 0.001	< 0.001
EEG	Transitivity	1	2	-0.431	-6.077 to 5.215	0.444	-0.970	0.510	2.801	0.094	64.302	0.504
EEG	Modularity	2	2	0.043	-8.617 to 8.702	0.682	0.063	0.960	10.448	0.001	90.429	0.917
EEG	Strength	1	1	0.719	0.338 to 1.101	0.195	3.693	< 0.001				
EEG	Degree	2	2	0.240	-6.180 to 6.660	0.505	0.475	0.718	5.908	0.015	83.074	0.652
MEG	Gamma	1	1	-0.748	-1.546 to 0.049	0.407	-1.839	0.066				
MEG	Lambda	1	1	-0.316	-1.092 to 0.459	0.396	-0.799	0.424				
PET	Cp	1	1	0.189	-0.208 to 0.585	0.202	0.931	0.352				
PET	Lp	1	1	0.340	-0.059 to 0.738	0.203	1.669	0.095				
PET	Gamma	1	1	0.322	-0.076 to 0.721	0.203	1.584	0.113				
PET	Lambda	1	1	0.645	0.239 to 1.051	0.207	3.112	0.002				
PET	Sigma	1	1	-0.072	-0.468 to 0.324	0.202	-0.356	0.722				
PET	Eloc	1	1	0.119	-0.277 to 0.515	0.202	0.589	0.556				
PET	Eglob	1	1	-0.560	-0.964 to -0.157	0.206	-2.720	0.007				
PET	Modularity	1	1	0.398	-0.002 to 0.798	0.204	1.952	0.051				
PET	Assortativity	1	1	0.347	-0.052 to 0.746	0.204	1.706	0.088				
PET	Hierarchy	1	1	0.075	-0.321 to 0.471	0.202	0.373	0.709				
PET	Synchronization	1	1	-0.770	-1.180 to -0.359	0.209	-3.677	< 0.001				
Rs-fMRI (WM)	Gamma	1	1	0.465	0.084 to 0.846	0.194	2.393	0.017				
Rs-fMRI (WM)	Lambda	1	1	-0.179	-0.556 to 0.198	0.192	-0.932	0.351				
Rs-fMRI (WM)	Sigma	1	1	-0.581	-0.965 to -0.198	0.196	-2.970	0.003				
Rs-fMRI (WM)	Eloc	1	1	< 0.001	-0.376 to 0.376	0.192	< 0.001	1.000				
Rs-fMRI (WM)	Eglob	1	1	-0.099	-0.475 to 0.277	0.192	-0.517	0.605				
Rs-fMRI (WM)	Strength	1	1	-0.192	-0.568 to 0.185	0.192	-0.997	0.319				

Abbreviations: dMRI, diffusion MRI; fMRI, functional MRI; EEG, electroencephalography; MEG, magnetic encephalography; PET, positron emission tomography; Rs-fMRI, resting-state fMRI; BC, betweenness centrality; PC, participation coefficient; Cp, clustering coefficient; Lp, characteristic path length; Eloc, local efficiency; Eglob, global efficiency; K, number of studies-number of samples; WM, white matter

Table S14. Quality assessment in case-control meta-analysis

Study	1	2	3	4	5	6	7	8	Total
dMRI									
Abbasi et al. 2018	1	1	1	1	2	1	1	1	9
Chung et al. 2022	1	0	1	1	2	1	1	1	8
Colon-Perez et al. 2018	1	0	0	0	1	1	1	0	4
Galantucci et al. 2017	1	0	1	1	1	1	1	1	7
Gan et al.2024	1	0	1	1	2	1	0	1	7
Ge et al.2024	1	0	1	0	2	1	0	0	5
Guan et al. 2019	1	0	1	1	1	1	1	1	7
Hu et al. 2020	1	0	1	1	2	1	1	0	7
Inguanzo et al. 2021	1	0	1	1	2	1	1	0	7
Jin et al. 2022	1	1	1	1	2	1	0	0	7
Kamagata et al. 2018	1	0	1	1	1	1	1	1	7
Koirala et al. 2019	0	1	1	1	1	1	1	0	6
Kok et al. 2020	1	0	1	0	1	1	1	1	6
Li et al. 2017	1	0	1	1	1	1	1	1	7
Li et al. 2024	1	0	1	1	1	1	1	1	7
Nigro et al. 2016	1	0	1	1	2	1	1	1	8
Ren et al. 2024	1	0	1	1	2	0	0	1	6
Shang et al. 2023b	1	1	1	0	1	1	1	1	7
Vriend et al. 2018	1	0	1	1	2	1	1	0	7
Wang et al. 2019	1	0	1	1	2	1	1	1	8
Wang et al. 2020	1	0	1	1	2	1	0	0	6
Wang et al. 2023a	1	0	1	1	2	1	1	1	8
Wen et al. 2022	1	0	1	1	2	1	1	1	8
Zarkali et al. 2020	1	0	1	1	1	1	0	1	6
Zhang et al. 2022	1	0	1	1	2	1	1	0	7
fMRI									
Albano et al. 2022	1	0	1	1	1	1	1	1	7
Berman et al. 2016	1	1	1	0	2	1	1	1	8
Chen et al. 2023	1	0	1	0	1	1	1	0	5
Dan et al. 2024	1	1	1	1	1	1	1	0	7
De Micco et al. 2021	1	0	1	0	1	1	1	1	6
Devignes et al. 2022	1	1	1	1	0	1	1	1	7
Engels et al. 2018	1	0	1	1	1	1	1	1	7
Fang et al. 2017	1	1	1	1	1	1	1	0	7
Filippi et al. 2021	0	0	1	1	1	1	1	1	6
Guan et al. 2019	1	0	1	1	1	1	1	1	7
Holtbernd et al. 2024	1	0	1	1	2	1	1	1	8
Hou et al. 2020	1	1	1	1	1	1	1	0	7
Hou et al. 2023	1	0	1	1	1	1	1	1	7
Klobušiaková et al. 2019	1	0	1	0	1	1	1	0	5
Li et al. 2022	1	0	1	1	2	1	1	0	7
Li et al. 2024	1	0	1	1	0	1	1	0	5
Lopes et al. 2017	1	0	1	0	0	1	1	0	4
Ma et al. 2017	1	0	1	1	1	1	1	1	7
Prajapati et al. 2020	1	1	1	1	1	1	1	0	7
Qiu et al. 2021	1	0	1	1	2	1	1	1	8
Sako et al. 2019	1	0	1	1	1	1	1	0	6
Sarasso et al. 2022	1	0	1	1	2	1	1	0	7
Shang et al. 2023a	1	1	1	1	2	1	1	1	9
Shang et al. 2023b	1	1	1	1	1	1	1	1	8
Siva et al. 2024	1	0	1	1	0	1	0	0	4
Skidmore et al. 2011	0	0	1	0	1	1	1	1	5
Sreenivasan et al. 2023	1	1	1	1	2	1	1	0	8
Suo et al. 2017	1	0	1	1	1	1	1	1	7
Suo et al. 2022	1	0	1	1	2	1	1	1	8
Tang et al. 2017	1	0	1	0	1	1	1	0	5
Tuovinen et al. 2018	1	0	1	1	1	1	1	1	7
Vancea et al. 2019	1	0	1	1	1	1	0	1	6
Wang et al. 2023a	1	0	1	1	2	1	1	1	8

Wang et al. 2023b	1	0	1	0	1	1	0	1	5
Wright et al. 2020	1	1	1	1	0	1	0	1	6
Zhang et al. 2014	1	0	1	1	2	1	1	0	7
Zhang et al. 2022	1	0	1	1	2	1	1	0	7
Baggio et al. 2014	1	0	1	1	2	1	1	1	8
Gottlich et al. 2013	0	0	1	1	1	1	1	0	5
Hou et al. 2018	1	0	1	1	2	1	1	0	7
Prajapati et al. 2020	1	1	0	1	1	1	1	0	6
Sang et al. 2015	1	0	1	1	2	1	1	0	7
sMRI									
Suo et al. 2021a	1	0	1	1	2	1	1	1	8
Suo et al. 2021b	1	0	1	1	2	1	1	1	8
Xu et al. 2017	1	0	1	1	1	1	1	0	6
Yan et al. 2024	1	1	1	1	2	1	1	0	8
EEG									
Bosch et al. 2022	0	0	1	0	1	1	0	1	4
Fogelson et al. 2013	0	0	1	0	2	1	1	1	6
Formaggio et al. 2021	0	0	1	0	0	1	1	0	3
Mehraram et al. 2020	1	0	1	1	1	1	1	0	6
Peláez Suárez et al. 2021	1	0	1	1	1	1	0	0	5
Rajagopal et al. 2025	1	0	0	1	1	1	1	0	5
Vecchio et al. 2021	0	0	0	1	1	1	1	1	5
Wang et al. 2024	1	0	1	0	1	1	1	0	5
Yin et al. 2023	0	1	1	0	2	1	1	0	6
Zhang et al. 2022	0	0	1	1	1	1	1	0	5
MEG									
Olde Dubbelink et al. 2014	1	0	1	1	2	1	1	1	8
PET									
Li et al. 2023	1	0	1	1	2	1	1	1	8
White matter fMRI									
Ji et al. 2019	1	1	1	1	2	1	1	1	9

The modified Newcastle-Ottawa Scale included: item 1= adequacy of case definition (PD); item 2 = adequacy of control definition (HC), with controls selected from communities (score of 1 if HC came from open datasets); item 3 = depth of sample characterization (PD), including age, gender, education level, cognition assessment (such as MMSE or MoCA), illness duration, medication status, UPDRS-Ⅲ score, and H&Y stage; item 4 = depth of sample characterization (HC), including age, gender, education level, MMSE score, and controls have no current or history of neurological or psychiatric conditions; item 5 = groups matched on age and gender (1 point); additional point if also matched on education and/or MMSE/MoCA (when the study did not primarily focus on cognition); item 6 = data acquisition and preprocessing procedures for MRI, EEG, MEG, or PET described in sufficient detail to allow replication; item 7 = graph theory analyses clearly described and reproducible; item 8 = availability of numerical data for effect size calculation (score of 0 if only figures were provided or data were converted from medians).

Table S15. Publication bias by Egger's regression in case-control meta-analysis

Modality & group	Metrics	No. of studies	No. of effect sizes	intercept	B	SE	t	Pt
dMRI	Cp	20	30	0.330	-2.670	2.933	-0.910	0.388
dMRI	Eloc	15	26	-1.005	2.770	1.783	1.554	0.178
dMRI	Lp	20	30	-0.717	4.322	4.907	0.881	0.448
dMRI	Eglob	21	34	-0.303	-0.543	1.703	-0.319	0.759
dMRI	Gamma	9	15	0.189	0.230	3.749	0.061	0.954
dMRI	Lambda	9	15	-0.080	1.053	2.301	0.458	0.674
dMRI	Sigma	15	25	0.142	0.068	2.810	0.024	0.981
dMRI	Modularity	3	4	-0.284	1.791	5.232	0.342	0.765
dMRI	Strength	4	5	1.212	-5.946	1.387	-4.287	0.062
dMRI	Degree	2	4	-0.809	1.935	3.670	0.527	0.670
dMRI	Density	3	4	-1.147	4.606	8.759	0.526	0.691
fMRI	Cp	29	46	0.199	-2.191	1.507	-1.454	0.168
fMRI	Eloc	24	39	-0.159	-0.232	1.583	-0.146	0.886
fMRI	Lp	28	44	0.595	-2.417	1.082	-2.233	0.046
fMRI	Eglob	26	46	-0.626	2.397	2.061	1.163	0.272
fMRI	Gamma	12	18	0.096	-0.086	1.213	-0.071	0.947
fMRI	Lambda	12	18	-0.140	0.579	2.209	0.262	0.805
fMRI	Sigma	14	22	0.271	-0.896	1.699	-0.528	0.627
fMRI	Modularity	6	9	0.164	0.313	0.877	0.357	0.747
fMRI	Assortativity	4	6	1.082	-4.261	4.292	-0.993	0.426
fMRI	Strength	6	10	0.498	-3.611	1.118	-3.231	0.042
sMRI	Cp	4	5	0.051	-0.115	7.373	-0.016	0.989
sMRI	Eloc	4	5	-0.724	3.457	7.019	0.493	0.683
sMRI	Lp	3	4	0.343	-2.982	1.086	-2.745	0.222
sMRI	Eglob	3	4	-0.340	2.793	5.871	0.476	0.717
sMRI	Gamma	2	3	-0.353	3.206	1.683	1.905	0.308
sMRI	Lambda	3	4	0.294	-2.887	1.355	-2.130	0.277
sMRI	Sigma	2	3	-0.432	3.688	1.279	2.883	0.213
EEG	Cp	6	7	1.342	-3.033	6.292	-0.482	0.695
EEG	Eloc	3	4	5.859	-19.518	5.510	-3.542	0.175
EEG	Lp	6	8	-7.310	21.459	16.254	1.320	0.383
EEG	Eglob	5	6	3.707	-10.563	2.772	-3.811	0.047
Cognitive normal	Cp	4	4	1.012	-5.542	6.563	-0.844	0.506
Cognitive normal	Eloc	3	3	-2.252	4.857	2.373	2.046	0.289
Cognitive normal	Lp	5	5	-2.340	8.288	6.715	1.234	0.360
Cognitive normal	Eglob	6	6	2.460	-8.696	7.158	-1.215	0.354
Cognitive impairment	Cp	4	6	1.708	-9.057	2.093	-4.328	0.129
Cognitive impairment	Eloc	3	5	0.580	-6.027	3.021	-1.995	0.292
Cognitive impairment	Lp	5	8	1.159	-5.190	4.900	-1.059	0.467
Cognitive impairment	Eglob	6	11	-1.486	6.629	3.740	1.772	0.271
Cognitive impairment *vs* normal	Cp	5	7	1.069	-4.827	2.180	-2.214	0.200
Cognitive impairment *vs* normal	Eloc	3	5	0.381	-3.105	2.803	-1.108	0.447
Cognitive impairment *vs* normal	Lp	6	9	0.391	-2.512	1.141	-2.201	0.128
Cognitive impairment *vs* normal	Eglob	7	12	-0.666	3.601	2.397	1.503	0.235

Abbreviations: dMRI, diffusion MRI; fMRI, functional MRI; sMRI, structural MRI; EEG, electroencephalography; Cp, clustering coefficient; Eloc, local efficiency; Lp, characteristic path length; Eglob, global efficiency; K, number of studies-number of samples.

Figure S16. Publication bias of clustering coefficient in case-control meta-analysis

A: Publication bias of clustering coefficient in dMRI studies

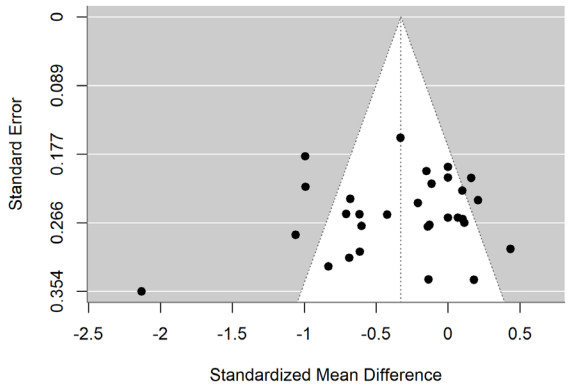

B: Publication bias of clustering coefficient in fMRI studies

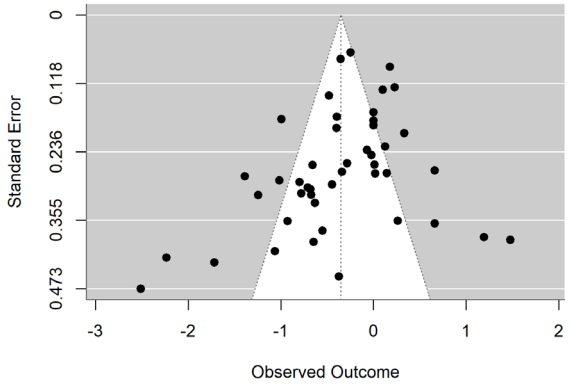

C: Publication bias of clustering coefficient in EEG studies

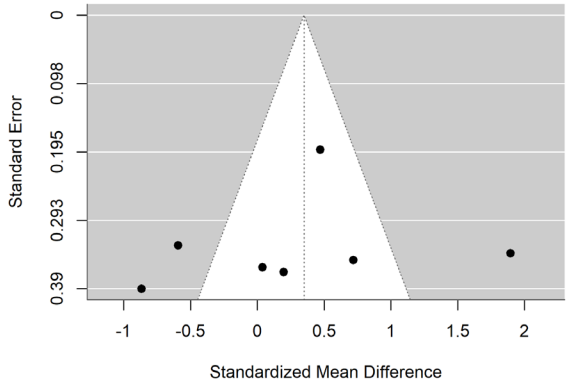

The plot depicts individual effect sizes plotted against their standard errors. The white inverted triangle denotes the region within which studies would be expected to fall in the absence of publication bias.

Figure S17. Publication bias of local efficiency in case-control meta-analysis

A: Publication bias of local efficiency in dMRI studies

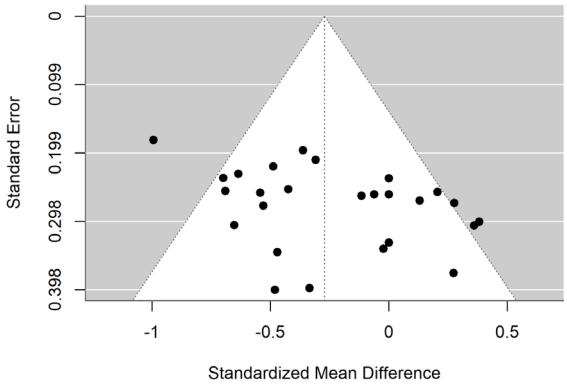

B: Publication bias of local efficiency in fMRI studies

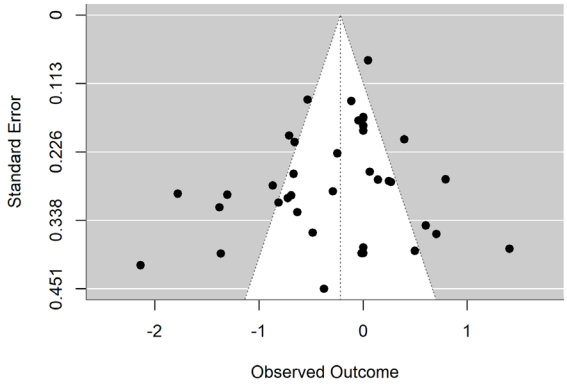

The plot depicts individual effect sizes plotted against their standard errors. The white inverted triangle denotes the region within which studies would be expected to fall in the absence of publication bias.

Figure S18. Publication bias of characteristic path length in case-control meta-analysis

A: Publication bias of characteristic path length in dMRI studies.

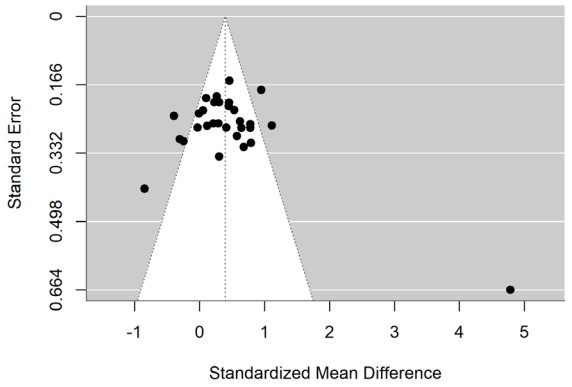

B: Publication bias of characteristic path length in fMRI studies

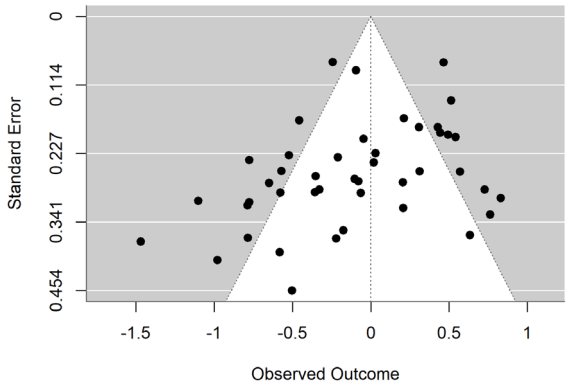

C: Publication bias of characteristic path length in EEG studies

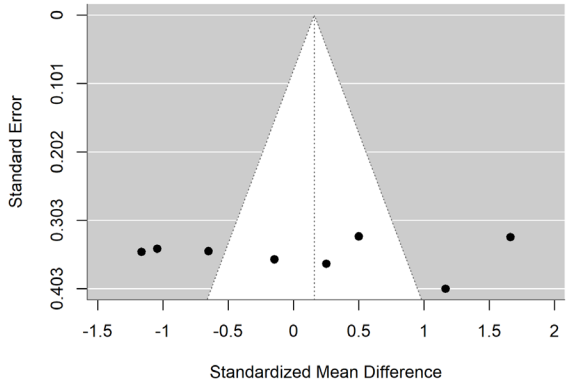

The plot depicts individual effect sizes plotted against their standard errors. The white inverted triangle denotes the region within which studies would be expected to fall in the absence of publication bias.

Figure S19. Publication bias of global efficiency in case-control meta-analysis

A: Publication bias of global efficiency in dMRI studies

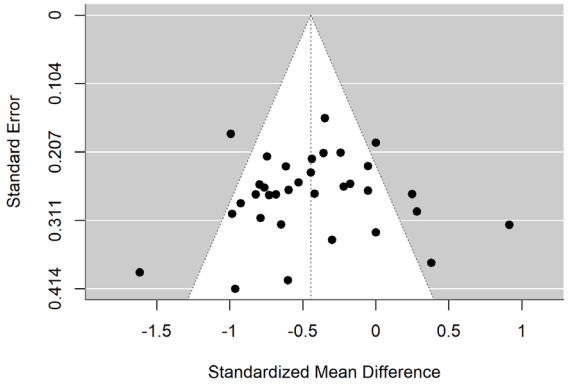

B: Publication bias of global efficiency in fMRI studies

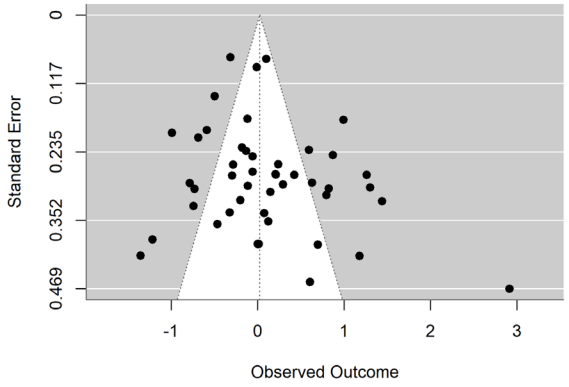

C: Publication bias of global efficiency in EEG studies

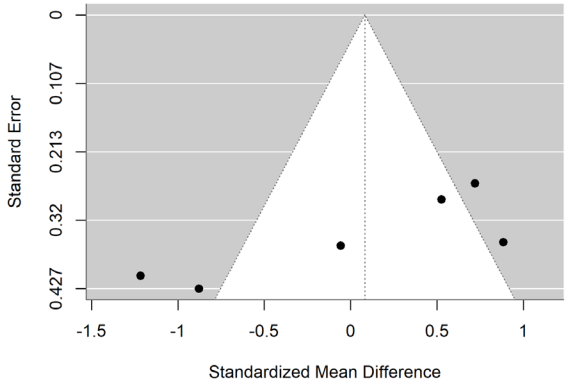

The plot depicts individual effect sizes plotted against their standard errors. The white inverted triangle denotes the region within which studies would be expected to fall in the absence of publication bias.

Figure S20. Publication bias of normalized clustering coefficient in case-control meta-analysis

A: Publication bias of normalized clustering coefficient in dMRI studies

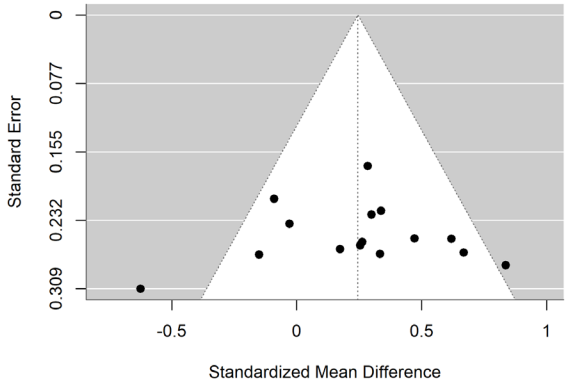

B: Publication bias of normalized clustering coefficient in fMRI studies

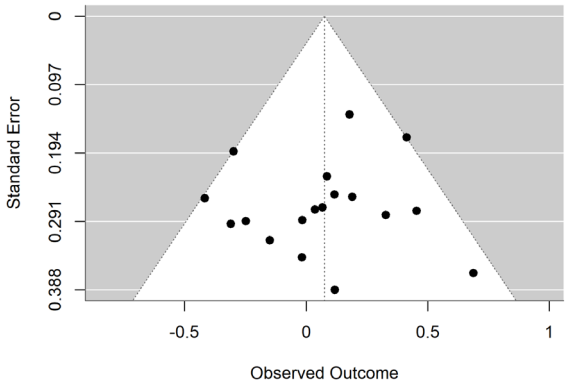

The plot depicts individual effect sizes plotted against their standard errors. The white inverted triangle denotes the region within which studies would be expected to fall in the absence of publication bias.

Figure S21. Publication bias of normalized characteristic path length in case-control meta-analysis

A: Publication bias of normalized characteristic path length in dMRI studies

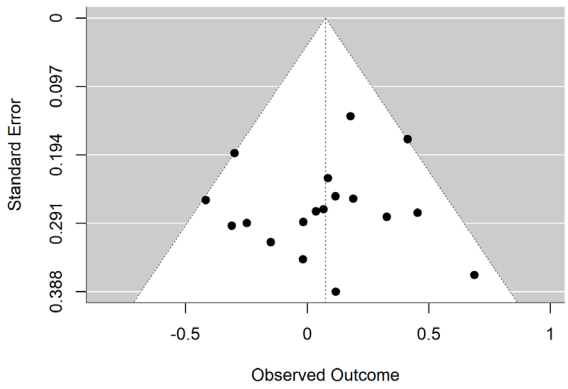

B: Publication bias of normalized characteristic path length in fMRI studies

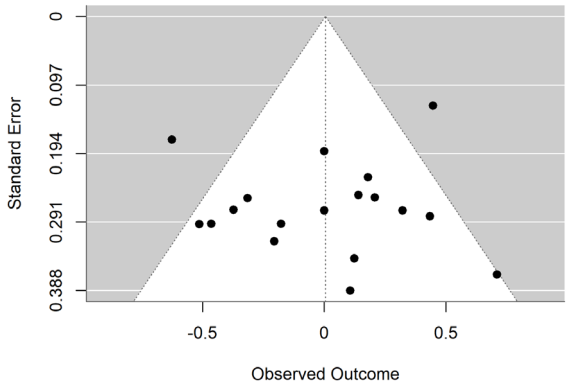

The plot depicts individual effect sizes plotted against their standard errors. The white inverted triangle denotes the region within which studies would be expected to fall in the absence of publication bias.

Figure S22. Publication bias of small-worldness in case-control meta-analysis

A: Publication bias of small-worldness in dMRI studies

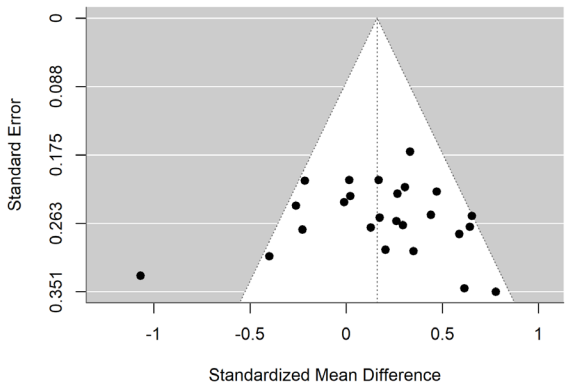

B: Publication bias of small-worldness in fMRI studies

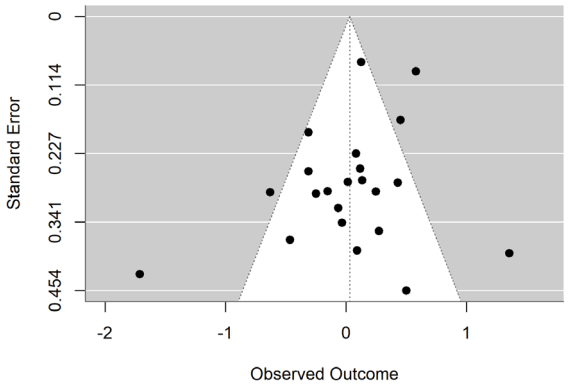

The plot depicts individual effect sizes plotted against their standard errors. The white inverted triangle denotes the region within which studies would be expected to fall in the absence of publication bias.

Table S16. Sensitivity analyses: removing outliers/influential effect sizes in case-control meta-analysis

Modality & group	Metric	No. of studies	No. of effect sizes	g	95% CI	SE	t	Pt	Q	PQ	I² %	Tau	Removing effect size
dMRI	Cp	19	29	-0.278	-0.434 to -0.123	0.073	-3.792	0.002	81.499	< 0.001	65.429	0.331	Nigro et al. 2016
dMRI	Lp	20	29	0.338	0.191 to 0.484	0.069	4.860	< 0.001	68.128	< 0.001	59.088	0.291	Gan et al.2024 PD-NICD
dMRI	Modularity	2	3	0.030	-0.340 to 0.399	0.029	1.024	0.492	0.671	0.715	< 0.001	< 0.001	Vriend et al. 2018
fMRI	Eglob	26	45	0.030	-0.248 to 0.307	0.135	0.220	0.828	311.641	< 0.001	90.413	0.646	Lopes et al. 2017 Group 4
fMRI	Lambda	11	17	0.070	-0.155 to 0.295	0.100	0.697	0.502	28.765	0.026	49.971	0.253	Shang et al. 2023b
fMRI	Sigma	14	21	0.089	-0.114 to 0.293	0.093	0.963	0.356	58.962	< 0.001	66.289	0.294	Siva et al. 2024 PD-ODP
fMRI	Modularity	6	8	0.104	-0.141 to 0.349	0.088	1.178	0.304	11.113	0.134	56.016	0.157	Baggio et al. 2014 PD-MCI
fMRI	Assortativity	4	5	0.102	-0.664 to 0.868	0.225	0.452	0.685	12.049	0.017	64.724	0.361	Sreenivasan et al. 2023 PD-FOG
sMRI	Cp	3	4	0.229	-0.734 to 1.192	0.223	1.029	0.412	7.792	0.051	64.297	0.335	Yan et al. 2024
sMRI	Eloc	3	4	0.357	-0.426 to 1.141	0.174	2.049	0.183	6.760	0.080	56.015	0.283	Yan et al. 2024
sMRI	Eglob	2	3	0.532	-1.224 to 2.288	0.138	3.849	0.162	2.312	0.315	6.679	0.074	Suo et al. 2021a
sMRI	Lambda	2	3	-0.465	-1.078 to 0.148	0.048	-9.635	0.066	1.042	0.594	< 0.001	< 0.001	Suo et al. 2021a
EEG	Cp	5	6	0.037	-0.679 to 0.752	0.252	0.145	0.892	17.471	0.004	72.043	0.504	Zhang et al. 2022
EEG	Eloc	3	3	0.221	-1.331 to 1.773	0.360	0.613	0.602	8.642	0.013	78.449	0.555	Peláez Suárez et al. 2021 PD-NC
EEG	Eglob	5	5	0.282	-0.541 to 1.105	0.295	0.956	0.394	14.135	0.007	75.382	0.574	Yin et al. 2023PD-NFOG
Cognitive normal	Cp	3	3	-0.743	-0.959 to -0.528	0.050	-15.008	0.005	0.169	0.919	< 0.001	< 0.001	Lopes et al. 2017 Group 1
Cognitive impairment	Cp	4	5	-0.867	-1.615 to -0.119	0.233	-3.717	0.035	10.654	0.031	64.307	0.382	Lopes et al. 2017 Group 4
Cognitive impairment	Eloc	2	4	-1.594	-3.330 to 0.141	0.137	-11.612	0.054	3.549	0.314	6.350	0.084	Suo et al. 2022 PD-MCI
Cognitive impairment	Lp	4	7	-0.579	-1.486 to 0.328	0.283	-2.048	0.134	21.355	0.002	78.479	0.533	Suo et al. 2022 PD-MCI
Cognitive impairment ***vs*** normal	Eloc	3	4	-0.609	-1.375 to 0.157	0.149	-4.101	0.072	3.023	0.388	5.000	0.069	Lopes et al. 2017 Group 2
Cognitive impairment ***vs*** normal	Lp	6	8	-0.156	-0.531 to 0.219	0.140	-1.113	0.323	15.839	0.027	58.697	0.260	Lopes et al. 2017 Group 4

Abbreviations: dMRI, diffusion MRI; fMRI, functional MRI; sMRI, structural MRI; EEG, electroencephalography; Cp, clustering coefficient; Lp, characteristic path length; Eglob, global efficiency; Eloc, local efficiency; PD-NICD, PD without impulse control disorders; Group 1/2/4, PD with intact cognition (G1), only slight mental slowing (G2), severe deficits in all cognitive domains (G4); PD-ODP, PD with severe hyposmia; PD-MCI, PD with mild cognitive impairment; PD-FOG, PD with freezing of gait; PD-NC, PD with normal cognition; PD-NFOG; PD without freezing of gait; K, number of studies-number of samples.

Table S17. Sensitivity analyses: excluding task studies, multiple sparsity studies and different data extraction strategies in case-control meta-analysis

Sensitivity	Modality	Metric	No. of studies	No. of effect sizes	g	95% CI	SE	t	Pt	Q	PQ	I² %	Tau
Excluding task-based studies	fMRI	Cp	28	45	-0.335	-0.566 to -0.105	0.112	-2.985	0.006	258.535	< 0.001	90.077	0.579
Excluding task-based studies	fMRI	Strength	5	9	-0.321	-0.764 to 0.123	0.159	-2.022	0.115	20.685	0.008	63.247	0.302
Excluding task-based studies	EEG	Cp	4	5	0.313	-1.431 to 2.056	0.546	0.573	0.607	39.738	< 0.001	92.527	1.078
Excluding task-based studies	EEG	Lp	4	6	0.337	-1.502 to 2.176	0.576	0.585	0.600	55.738	< 0.001	91.447	1.143
Excluding task-based studies	EEG	Eglob	4	5	-0.116	-1.405 to 1.174	0.388	-0.298	0.787	23.732	< 0.001	84.152	0.775
Excluding multi-sparsity studies	fMRI	Cp	25	41	-0.414	-0.674 to -0.153	0.126	-3.284	0.003	213.792	< 0.001	84.941	0.608
Excluding multi-sparsity studies	fMRI	Eloc	22	37	-0.235	-0.491 to 0.021	0.123	-1.912	0.070	194.990	< 0.001	82.604	0.549
Excluding multi-sparsity studies	fMRI	Lp	24	39	-0.046	-0.266 to 0.174	0.106	-0.435	0.668	162.768	< 0.001	77.654	0.466
Excluding multi-sparsity studies	fMRI	Eglob	23	42	0.049	-0.253 to 0.351	0.145	0.339	0.738	289.241	< 0.001	86.934	0.690
Excluding multi-sparsity studies	fMRI	Gamma	11	17	0.061	-0.133 to 0.254	0.086	0.706	0.497	20.705	0.190	32.556	0.183
Excluding multi-sparsity studies	fMRI	Lambda	11	17	-0.051	-0.294 to 0.193	0.109	-0.464	0.653	30.453	0.016	53.708	0.285
Excluding multi-sparsity studies	fMRI	Sigma	13	20	-0.008	-0.278 to 0.262	0.123	-0.062	0.951	51.940	< 0.001	64.903	0.383
Excluding multi-sparsity studies	fMRI	Modularity	4	6	0.262	-0.117 to 0.641	0.117	2.243	0.113	4.089	0.537	12.843	0.100
Using binary data	dMRI	Cp	20	30	-0.328	-0.513 to -0.143	0.088	-3.735	0.002	108.310	< 0.001	75.109	0.421
Using binary data	dMRI	Lp	20	30	0.396	0.194 to 0.599	0.096	4.128	0.001	112.261	< 0.001	78.669	0.471
Using binary data	dMRI	Eloc	15	26	-0.229	-0.424 to -0.033	0.091	-2.518	0.025	65.504	< 0.001	60.331	0.322
Using binary data	dMRI	Eglob	21	34	-0.445	-0.615 to -0.276	0.081	-5.496	< 0.001	89.490	< 0.001	64.917	0.348
Using binary data	fMRI	Cp	29	46	-0.364	-0.592 to -0.135	0.112	-3.257	0.003	269.256	< 0.001	90.071	0.584
Using binary data	fMRI	Lp	28	44	-0.044	-0.241 to 0.154	0.096	-0.456	0.652	224.613	< 0.001	83.738	0.458
Using binary data	fMRI	Eloc	24	39	-0.198	-0.427 to 0.031	0.111	-1.792	0.087	199.528	< 0.001	84.022	0.512
Using binary data	fMRI	Eglob	26	46	0.066	-0.197 to 0.329	0.128	0.520	0.608	310.025	< 0.001	90.116	0.638
Using functional atlas	dMRI	Cp	20	30	-0.328	-0.513 to -0.143	0.088	-3.735	0.002	108.310	< 0.001	75.109	0.421
Using functional atlas	dMRI	Lp	20	30	0.400	0.194 to 0.607	0.098	4.089	0.001	115.391	< 0.001	79.441	0.483
Using functional atlas	dMRI	Eloc	15	26	-0.272	-0.454 to -0.090	0.085	-3.209	0.007	55.906	< 0.001	54.884	0.288
Using functional atlas	dMRI	Eglob	21	34	-0.445	-0.615 to -0.276	0.081	-5.496	< 0.001	89.490	< 0.001	64.917	0.348
Using functional atlas	dMRI	Gamma	9	15	0.279	0.050 to 0.508	0.099	2.821	0.023	28.001	0.014	50.343	0.245
Using functional atlas	dMRI	Lambda	9	15	0.249	-0.012 to 0.509	0.113	2.208	0.059	27.062	0.019	56.598	0.278
Using functional atlas	dMRI	Sigma	15	25	0.076	-0.165 to 0.317	0.112	0.679	0.508	70.115	< 0.001	70.512	0.384
Using functional atlas	fMRI	Cp	29	46	-0.351	-0.577 to -0.124	0.111	-3.175	0.004	262.520	< 0.001	89.880	0.577
Using functional atlas	fMRI	Lp	28	44	-0.013	-0.215 to 0.188	0.098	-0.136	0.893	231.959	< 0.001	84.360	0.469
Using functional atlas	fMRI	Eloc	24	39	-0.217	-0.450 to 0.016	0.113	-1.931	0.066	206.980	< 0.001	84.569	0.523
Using functional atlas	fMRI	Eglob	26	46	0.026	-0.240 to 0.291	0.129	0.198	0.844	311.667	< 0.001	90.273	0.643
Using functional atlas	fMRI	Gamma	12	18	0.099	-0.101 to 0.299	0.090	1.097	0.297	28.340	0.041	46.080	0.230
Using functional atlas	fMRI	Lambda	12	18	-0.024	-0.313 to 0.265	0.131	-0.184	0.857	62.291	< 0.001	72.272	0.397
Using functional atlas	fMRI	Sigma	14	22	0.045	-0.224 to 0.315	0.124	0.364	0.722	84.761	< 0.001	80.027	0.427

Abbreviations: fMRI, functional MRI; EEG, electroencephalography; dMRI, diffusion MRI; sMRI, structural MRI; Cp, clustering coefficient; Lp, characteristic path length; Eglob, global efficiency; Eloc, local efficiency; K, number of studies-number of samples.

Table S18. Findings for meta-regression with continuous variables in case-control meta-analysis

Modality	Metric	Variable	No. of studies	No. of effect sizes	B	95% CI	SE	t	Pt	Pt FDR corrected
dMRI	Cp	Age	20	30	-0.013	-0.091 to 0.064	0.030	-0.447	0.674	0.843
dMRI	Cp	Gender (Male%)	19	29	-0.012	-0.039 to 0.015	0.011	-1.127	0.309	0.843
dMRI	Cp	Education	16	26	-0.004	-0.044 to 0.036	0.016	-0.256	0.808	0.898
dMRI	Cp	Age at onset	19	29	0.007	-0.075 to 0.090	0.011	0.684	0.596	0.843
dMRI	Cp	Duration	19	29	0.067	-0.044 to 0.178	0.048	1.388	0.201	0.843
dMRI	Cp	UPDRS-III	20	30	0.011	-0.022 to 0.043	0.014	0.743	0.477	0.843
dMRI	Cp	Hoehn & Yahr	16	25	0.320	-0.709 to 1.348	0.430	0.742	0.483	0.843
dMRI	Cp	MMSE	14	21	0.039	-0.222 to 0.300	0.082	0.479	0.665	0.843
dMRI	Cp	LEDD	8	14	0.001	-0.002 to 0.004	0.001	0.722	0.512	0.843
dMRI	Cp	Number of Nodes	20	30	< 0.001	-0.008 to 0.008	0.001	-0.041	0.972	0.972
dMRI	Eloc	Age	15	26	-0.049	-0.117 to 0.019	0.029	-1.683	0.132	0.660
dMRI	Eloc	Gender (Male%)	15	26	-0.002	-0.024 to 0.021	0.007	-0.218	0.840	0.973
dMRI	Eloc	Education	12	21	0.003	-0.114 to 0.121	0.048	0.065	0.950	0.973
dMRI	Eloc	Age at onset	15	26	0.011	-0.071 to 0.092	0.010	1.072	0.448	0.896
dMRI	Eloc	Duration	15	26	0.041	-0.063 to 0.146	0.043	0.956	0.374	0.896
dMRI	Eloc	UPDRS-III	15	26	< 0.001	-0.029 to 0.028	0.011	-0.036	0.973	0.973
dMRI	Eloc	Hoehn & Yahr	14	24	0.305	-0.575 to 1.185	0.351	0.869	0.421	0.896
dMRI	Eloc	MMSE	12	20	0.048	-0.314 to 0.411	0.104	0.467	0.677	0.967
dMRI	Eloc	LEDD	7	13	0.002	0.000 to 0.003	0.001	3.143	**0.041**	0.410
dMRI	Eloc	Number of Nodes	15	26	-0.001	-0.012 to 0.010	0.002	-0.509	0.665	0.967
dMRI	Lp	Age	20	30	-0.021	-0.093 to 0.050	0.027	-0.775	0.475	0.766
dMRI	Lp	Gender (Male%)	19	29	0.015	-0.005 to 0.036	0.008	1.862	0.118	0.766
dMRI	Lp	Education	16	26	-0.042	-0.129 to 0.046	0.035	-1.203	0.280	0.766
dMRI	Lp	Age at onset	19	29	-0.006	-0.065 to 0.052	0.008	-0.817	0.536	0.766
dMRI	Lp	Duration	19	29	-0.058	-0.171 to 0.055	0.045	-1.275	0.252	0.766
dMRI	Lp	UPDRS-III	20	30	0.012	-0.024 to 0.049	0.016	0.743	0.476	0.766
dMRI	Lp	Hoehn & Yahr	16	25	-0.302	-1.162 to 0.557	0.308	-0.982	0.383	0.766
dMRI	Lp	MMSE	13	20	-0.017	-0.336 to 0.301	0.100	-0.175	0.873	0.992
dMRI	Lp	LEDD	9	15	< 0.001	-0.004 to 0.004	0.001	0.011	0.992	0.992
dMRI	Lp	Number of Nodes	20	30	< 0.001	-0.015 to 0.014	0.002	-0.134	0.911	0.992
dMRI	Eglob	Age	21	34	0.008	-0.043 to 0.059	0.020	0.433	0.684	0.760
dMRI	Eglob	Gender (Male%)	21	34	-0.004	-0.026 to 0.017	0.008	-0.545	0.611	0.760
dMRI	Eglob	Education	15	26	-0.018	-0.121 to 0.086	0.040	-0.449	0.673	0.760
dMRI	Eglob	Age at onset	20	33	0.008	-0.037 to 0.052	0.006	1.342	0.370	0.760
dMRI	Eglob	Duration	20	33	0.048	-0.021 to 0.117	0.030	1.577	0.151	0.723
dMRI	Eglob	UPDRS-III	21	34	-0.012	-0.032 to 0.008	0.009	-1.340	0.217	0.723
dMRI	Eglob	Hoehn & Yahr	18	29	0.235	-0.416 to 0.886	0.282	0.835	0.428	0.760
dMRI	Eglob	MMSE	15	24	-0.001	-0.390 to 0.388	0.118	-0.008	0.994	0.994
dMRI	Eglob	LEDD	8	15	< 0.001	-0.002 to 0.002	0.001	0.440	0.680	0.760
dMRI	Eglob	Number of Nodes	21	34	-0.003	-0.009 to 0.003	0.001	-1.866	0.202	0.723
dMRI	Gamma	Age	9	15	0.019	-0.079 to 0.118	0.032	0.608	0.584	0.876
dMRI	Gamma	Gender (Male%)	9	15	0.012	-0.007 to 0.031	0.005	2.609	0.116	0.522
dMRI	Gamma	Education	8	14	-0.018	-0.192 to 0.155	0.059	-0.315	0.771	0.911
dMRI	Gamma	Age at onset	9	15	< 0.001	-0.035 to 0.035	0.005	-0.011	0.993	0.993
dMRI	Gamma	Duration	9	15	-0.019	-0.080 to 0.043	0.023	-0.811	0.458	0.824
dMRI	Gamma	UPDRS-III	9	15	0.020	-0.042 to 0.083	0.019	1.081	0.364	0.824
dMRI	Gamma	Hoehn & Yahr	9	15	0.201	-0.387 to 0.789	0.210	0.957	0.394	0.824
dMRI	Gamma	MMSE	7	11	0.020	-0.280 to 0.321	0.075	0.272	0.810	0.911
dMRI	Gamma	Number of Nodes	9	15	0.014	-0.003 to 0.030	0.003	4.066	0.068	0.522
dMRI	Lambda	Age	9	15	-0.012	-0.064 to 0.040	0.017	-0.699	0.531	0.683
dMRI	Lambda	Gender (Male%)	9	15	-0.001	-0.026 to 0.024	0.005	-0.184	0.874	0.874
dMRI	Lambda	Education	8	14	-0.079	-0.183 to 0.025	0.035	-2.263	0.098	0.366
dMRI	Lambda	Age at onset	9	15	0.003	-0.012 to 0.019	0.002	1.595	0.311	0.560
dMRI	Lambda	Duration	9	15	-0.019	-0.140 to 0.103	0.047	-0.393	0.710	0.799
dMRI	Lambda	UPDRS-III	9	15	0.028	-0.032 to 0.087	0.018	1.532	0.228	0.513
dMRI	Lambda	Hoehn & Yahr	9	15	0.125	-0.314 to 0.564	0.166	0.751	0.489	0.683
dMRI	Lambda	MMSE	7	11	0.090	-0.039 to 0.219	0.031	2.869	0.098	0.366
dMRI	Lambda	Number of Nodes	9	15	0.013	-0.010 to 0.037	0.005	2.858	0.122	0.366

dMRI	Sigma	Age	15	25	-0.008	-0.083 to 0.067	0.031	-0.267	0.798	0.900
dMRI	Sigma	Gender (Male%)	14	24	0.010	-0.004 to 0.025	0.004	2.637	0.103	0.308
dMRI	Sigma	Education	13	23	-0.043	-0.161 to 0.076	0.040	-1.075	0.352	0.602
dMRI	Sigma	Age at onset	15	25	-0.003	-0.021 to 0.014	0.002	-1.376	0.361	0.602
dMRI	Sigma	Duration	15	25	0.004	-0.059 to 0.066	0.027	0.129	0.900	0.900
dMRI	Sigma	UPDRS-III	15	25	0.029	-0.010 to 0.068	0.016	1.773	0.123	0.308
dMRI	Sigma	Hoehn & Yahr	14	24	0.441	-0.073 to 0.954	0.218	2.017	0.082	0.308
dMRI	Sigma	MMSE	11	19	-0.009	-0.171 to 0.153	0.044	-0.214	0.848	0.900
dMRI	Sigma	LEDD	8	15	< 0.001	-0.001 to 0.001	< 0.001	0.743	0.502	0.717
dMRI	Sigma	Number of Nodes	15	25	0.017	0.002 to 0.032	0.005	3.464	**0.034**	0.308
fMRI	Cp	Age	29	46	-0.011	-0.072 to 0.050	0.028	-0.397	0.699	0.777
fMRI	Cp	Gender (Male%)	29	46	0.008	-0.010 to 0.026	0.008	0.971	0.349	0.749
fMRI	Cp	Education	22	37	0.002	-0.138 to 0.143	0.061	0.037	0.971	0.971
fMRI	Cp	Age at onset	27	43	-0.027	-0.095 to 0.042	0.031	-0.862	0.408	0.749
fMRI	Cp	Duration	27	43	0.030	-0.094 to 0.155	0.056	0.544	0.599	0.749
fMRI	Cp	UPDRS-III	27	43	0.020	-0.005 to 0.044	0.010	2.020	0.097	0.749
fMRI	Cp	Hoehn & Yahr	25	41	0.159	-0.494 to 0.812	0.232	0.686	0.532	0.749
fMRI	Cp	MMSE	17	27	0.107	-0.159 to 0.374	0.094	1.138	0.321	0.749
fMRI	Cp	LEDD	20	35	< 0.001	-0.001 to 0.002	0.001	0.873	0.402	0.749
fMRI	Cp	Number of Nodes	29	46	< 0.001	-0.002 to 0.002	< 0.001	-0.998	0.451	0.749
fMRI	Eloc	Age	24	39	-0.040	-0.106 to 0.026	0.028	-1.413	0.197	0.493
fMRI	Eloc	Gender (Male%)	24	39	-0.014	-0.029 to 0.001	0.007	-2.062	0.066	0.433
fMRI	Eloc	Education	20	34	0.042	-0.085 to 0.169	0.052	0.819	0.444	0.651
fMRI	Eloc	Age at onset	23	37	-0.049	-0.107 to 0.009	0.025	-1.944	0.088	0.433
fMRI	Eloc	Duration	23	37	-0.010	-0.139 to 0.120	0.053	-0.183	0.861	0.861
fMRI	Eloc	UPDRS-III	24	39	0.019	-0.009 to 0.048	0.010	1.883	0.130	0.433
fMRI	Eloc	Hoehn & Yahr	21	35	-0.100	-0.679 to 0.480	0.178	-0.562	0.615	0.704
fMRI	Eloc	MMSE	13	21	0.067	-0.407 to 0.541	0.122	0.547	0.634	0.704
fMRI	Eloc	LEDD	16	28	< 0.001	-0.002 to 0.001	0.001	-0.791	0.456	0.651
fMRI	Eloc	Number of Nodes	24	39	-0.002	-0.007 to 0.003	0.002	-0.905	0.395	0.651
fMRI	Lp	Age	28	44	-0.022	-0.063 to 0.019	0.019	-1.149	0.273	0.610
fMRI	Lp	Gender (Male%)	28	44	-0.003	-0.018 to 0.013	0.007	-0.377	0.713	0.792
fMRI	Lp	Education	20	35	0.055	-0.017 to 0.127	0.032	1.742	0.118	0.590
fMRI	Lp	Age at onset	26	41	-0.027	-0.077 to 0.024	0.023	-1.155	0.272	0.610
fMRI	Lp	Duration	26	41	0.001	-0.072 to 0.074	0.025	0.040	0.971	0.971
fMRI	Lp	UPDRS-III	25	40	0.002	-0.013 to 0.017	0.004	0.555	0.625	0.781
fMRI	Lp	Hoehn & Yahr	24	39	0.065	-0.379 to 0.509	0.102	0.635	0.591	0.781
fMRI	Lp	MMSE	16	25	0.121	-0.040 to 0.283	0.058	2.092	0.105	0.590
fMRI	Lp	LEDD	19	33	< 0.001	0.000 to 0.001	< 0.001	0.809	0.457	0.762
fMRI	Lp	Number of Nodes	28	44	0.001	-0.002 to 0.003	< 0.001	1.515	0.305	0.610
fMRI	Eglob	Age	26	46	0.027	-0.066 to 0.119	0.042	0.639	0.536	0.899
fMRI	Eglob	Gender (Male%)	26	46	-0.006	-0.024 to 0.012	0.007	-0.800	0.454	0.899
fMRI	Eglob	Education	19	37	-0.117	-0.204 to -0.030	0.038	-3.094	**0.015**	0.150
fMRI	Eglob	Age at onset	24	43	0.028	-0.063 to 0.119	0.040	0.701	0.501	0.899
fMRI	Eglob	Duration	24	43	0.041	-0.149 to 0.232	0.085	0.488	0.637	0.899
fMRI	Eglob	UPDRS-III	25	44	-0.001	-0.037 to 0.034	0.015	-0.092	0.929	0.929
fMRI	Eglob	Hoehn & Yahr	21	39	0.269	-0.803 to 1.341	0.475	0.565	0.585	0.899
fMRI	Eglob	MMSE	16	27	-0.250	-0.598 to 0.097	0.122	-2.057	0.114	0.570
fMRI	Eglob	LEDD	18	34	< 0.001	-0.002 to 0.001	0.001	-0.372	0.719	0.899
fMRI	Eglob	Number of Nodes	26	46	< 0.001	-0.003 to 0.003	0.001	0.107	0.924	0.929
fMRI	Gamma	Age	12	18	0.010	-0.022 to 0.042	0.012	0.821	0.455	0.650
fMRI	Gamma	Gender (Male%)	12	18	-0.010	-0.032 to 0.011	0.009	-1.206	0.277	0.612
fMRI	Gamma	Education	10	16	0.033	-0.070 to 0.136	0.031	1.070	0.367	0.612
fMRI	Gamma	Age at onset	11	16	< 0.001	-0.055 to 0.056	0.021	0.008	0.994	0.994
fMRI	Gamma	Duration	11	16	0.057	-0.057 to 0.171	0.040	1.447	0.227	0.612
fMRI	Gamma	UPDRS-III	11	16	-0.016	-0.044 to 0.013	0.010	-1.493	0.205	0.612
fMRI	Gamma	Hoehn & Yahr	10	15	-0.067	-1.214 to 1.080	0.392	-0.171	0.874	0.971
fMRI	Gamma	MMSE	11	17	-0.081	-0.173 to 0.010	0.018	-4.499	0.061	0.610
fMRI	Gamma	LEDD	7	11	< 0.001	-0.001 to 0.002	< 0.001	1.190	0.317	0.612
fMRI	Gamma	Number of Nodes	12	18	< 0.001	-0.001 to 0.001	< 0.001	0.548	0.646	0.808
fMRI	Lambda	Age	12	18	< 0.001	-0.059 to 0.059	0.021	-0.008	0.994	0.994
fMRI	Lambda	Gender (Male%)	12	18	0.006	-0.017 to 0.029	0.009	0.688	0.520	0.655
fMRI	Lambda	Education	10	16	0.067	-0.049 to 0.183	0.035	1.915	0.158	0.338
fMRI	Lambda	Age at onset	11	16	-0.019	-0.094 to 0.055	0.028	-0.690	0.524	0.655
fMRI	Lambda	Duration	11	16	0.084	-0.061 to 0.230	0.048	1.759	0.169	0.338
fMRI	Lambda	UPDRS-III	11	16	-0.031	-0.059 to -0.002	0.011	-2.774	**0.040**	0.338

fMRI	Lambda	Hoehn & Yahr	10	15	0.248	-1.062 to 1.559	0.455	0.546	0.617	0.686
fMRI	Lambda	MMSE	11	17	0.100	-0.098 to 0.299	0.043	2.317	0.155	0.338
fMRI	Lambda	LEDD	7	11	0.001	0.000 to 0.002	< 0.001	2.113	0.123	0.338
fMRI	Lambda	Number of Nodes	12	18	< 0.001	-0.001 to 0.001	< 0.001	1.642	0.261	0.435
fMRI	Sigma	Age	14	22	-0.003	-0.103 to 0.098	0.040	-0.066	0.950	0.950
fMRI	Sigma	Gender (Male%)	14	22	0.010	-0.019 to 0.039	0.012	0.831	0.433	0.619
fMRI	Sigma	Education	10	17	0.047	-0.273 to 0.367	0.080	0.587	0.612	0.680
fMRI	Sigma	Age at onset	13	20	-0.045	-0.173 to 0.084	0.048	-0.934	0.399	0.619
fMRI	Sigma	Duration	13	20	0.133	-0.022 to 0.287	0.032	4.082	0.065	0.357
fMRI	Sigma	UPDRS-III	13	20	0.016	-0.026 to 0.058	0.018	0.868	0.411	0.619
fMRI	Sigma	Hoehn & Yahr	12	19	0.866	-0.475 to 2.208	0.210	4.123	0.092	0.357
fMRI	Sigma	MMSE	12	19	-0.134	-0.338 to 0.069	0.049	-2.739	0.107	0.357
fMRI	Sigma	LEDD	10	16	0.001	-0.001 to 0.003	0.001	1.459	0.228	0.570
fMRI	Sigma	Number of Nodes	14	22	< 0.001	-0.001 to 0.001	< 0.001	0.633	0.611	0.680
fMRI	Strength	Age	6	10	0.006	-0.201 to 0.214	0.053	0.123	0.912	0.912
fMRI	Strength	Gender (Male%)	6	10	-0.043	-0.081 to -0.005	0.010	-4.282	**0.039**	0.248
fMRI	Strength	Education	6	10	-0.109	-0.228 to 0.009	0.042	-2.610	0.062	0.248
fMRI	Strength	Age at onset	6	10	0.007	-0.165 to 0.179	0.050	0.140	0.899	0.912
fMRI	Strength	Duration	6	10	0.008	-0.184 to 0.201	0.041	0.205	0.858	0.912
fMRI	Strength	UPDRS-III	6	10	0.023	-0.029 to 0.075	0.013	1.727	0.215	0.430
fMRI	Strength	Hoehn & Yahr	6	10	0.064	-1.793 to 1.921	0.275	0.234	0.845	0.912
fMRI	Strength	Number of Nodes	6	10	-0.004	-0.009 to 0.002	0.002	-1.957	0.132	0.352

Abbreviations: dMRI, diffusion MRI; fMRI, functional MRI; Cp, clustering coefficient; Eloc, local efficiency; Lp, characteristic path length; Eglob, global efficiency; UPDRS, Unified Parkinson's Disease Rating Scale; MMSE, Mini-mental state examination; LEDD, levodopa-equivalent daily dose; k, number of studies-number of samples.

Table S19. Findings for meta-regression with categorical variables in case-control meta-analysis

Modality	Metric	Variable	No. of studies	No. of effect sizes	B	95% CI	SE	t	Pt	g	Q	PQ	I² %	Tau	Pt FDR corrected
dMRI	Cp	Drug effect	19	28	0.292	-0.051 to 0.636	0.160	1.828	0.089						0.534
dMRI	Cp	Drug-naïve/off-state	11	16		-0.788 to -0.196	0.131	-3.759	0.005	-0.492	65.995	< 0.001	80.555	0.491	
dMRI	Cp	On-state	8	12		-0.427 to 0.041	0.096	-2.010	0.090	-0.193	25.860	0.007	57.194	0.284	
dMRI	Cp	Template effect	20	30	-0.147	-0.540 to 0.246	0.169	-0.870	0.411						0.788
dMRI	Cp	AAL	14	22		-0.570 to -0.040	0.122	-2.492	0.028	-0.305	83.166	< 0.001	77.981	0.459	
dMRI	Cp	Non-AAL	6	8		-0.774 to -0.090	0.126	-3.432	0.024	-0.432	23.811	0.001	70.803	0.375	
dMRI	Cp	Template effect	20	30	-0.018	-0.728 to 0.692	0.223	-0.080	0.942						0.942
dMRI	Cp	Contain cerebellum	3	6		-1.175 to 0.544	0.198	-1.594	0.253	-0.316	9.853	0.080	53.720	0.304	
dMRI	Cp	Cerebellum-excluded	17	24		-0.553 to -0.113	0.103	-3.244	0.006	-0.333	98.319	< 0.001	79.197	0.459	
dMRI	Cp	Tractography effect	20	30	-0.139	-0.949 to 0.671	0.290	-0.480	0.657						0.788
dMRI	Cp	Deterministic tractography	16	26		-0.511 to -0.108	0.094	-3.297	0.005	-0.309	94.561	< 0.001	75.299	0.423	
dMRI	Cp	Probabilistic tractography	4	4		-1.332 to 0.423	0.275	-1.657	0.197	-0.455	13.662	0.003	79.188	0.485	
dMRI	Cp	Edges effect	10	15	-0.121	-0.707 to 0.466	0.249	-0.485	0.642						0.788
dMRI	Cp	Fractional anisotropy	5	7		-0.548 to 0.027	0.099	-2.636	0.065	-0.261	19.317	0.004	70.467	0.333	
dMRI	Cp	Number of streamlines	5	8		-1.089 to 0.205	0.230	-1.921	0.129	-0.442	27.889	< 0.001	76.028	0.486	
dMRI	Cp	Threshold effect	20	30	-0.351	-0.926 to 0.223	0.232	-1.515	0.183						0.549
dMRI	Cp	Non-proportional threshold	15	25		-0.464 to -0.065	0.092	-2.869	0.013	-0.265	79.548	< 0.001	72.039	0.406	
dMRI	Cp	Proportional threshold	5	5		-1.212 to -0.022	0.213	-2.901	0.045	-0.617	20.223	< 0.001	79.820	0.416	
dMRI	Eloc	Drug effect	14	24	-0.018	-0.414 to 0.378	0.158	-0.111	0.915						0.933
dMRI	Eloc	Drug-naïve/off-state	10	17		-0.559 to -0.002	0.123	-2.283	0.049	-0.281	46.081	< 0.001	64.778	0.358	
dMRI	Eloc	On-state	4	7		-0.619 to 0.034	0.097	-3.011	0.064	-0.292	7.385	0.287	20.803	0.135	
dMRI	Eloc	Template effect	15	26	0.181	-1.495 to 1.857	0.233	0.777	0.551						0.933
dMRI	Eloc	AAL	13	22		-0.501 to -0.090	0.094	-3.140	0.009	-0.295	50.816	< 0.001	58.074	0.302	
dMRI	Eloc	Non-AAL	2	4		-2.800 to 2.552	0.211	-0.590	0.661	-0.124	3.954	0.266	36.002	0.223	
dMRI	Eloc	Template effect	15	26	0.172	-1.120 to 1.465	0.182	0.948	0.482						0.933
dMRI	Eloc	Contain cerebellum	2	4		-2.358 to 1.474	0.151	-2.930	0.209	-0.442	2.505	0.474	4.467	0.063	
dMRI	Eloc	Cerebellum-excluded	13	22		-0.448 to -0.039	0.094	-2.601	0.024	-0.243	52.242	< 0.001	58.998	0.309	
dMRI	Eloc	Tractography effect	15	26	0.040	-3.019 to 3.098	0.391	0.101	0.933						0.933
dMRI	Eloc	Deterministic tractography	13	23		-0.467 to -0.081	0.088	-3.105	0.009	-0.274	50.565	< 0.001	55.728	0.290	
dMRI	Eloc	Probabilistic tractography	2	3		-5.086 to 4.558	0.380	-0.695	0.613	-0.264	5.331	0.070	70.955	0.478	
dMRI	Eloc	Edges effect	8	14	-0.066	-0.522 to 0.390	0.183	-0.358	0.733						0.933
dMRI	Eloc	Fractional anisotropy	4	6		-0.612 to 0.260	0.132	-1.335	0.280	-0.176	3.859	0.570	10.957	0.106	
dMRI	Eloc	Number of streamlines	4	8		-0.606 to 0.151	0.119	-1.915	0.152	-0.227	15.252	0.033	54.220	0.288	
dMRI	Eloc	Threshold effect	15	26	-0.403	-1.170 to 0.363	0.234	-1.723	0.188						0.933

dMRI	Eloc	Non-proportional threshold	12	22		-0.390 to -0.020	0.084	-2.445	0.033	-0.205	38.833	0.010	46.080	0.246	
dMRI	Eloc	Proportional threshold	3	4		-1.579 to 0.360	0.221	-2.760	0.112	-0.610	6.669	0.083	58.873	0.308	
dMRI	Lp	Drug effect	19	28	0.035	-0.469 to 0.540	0.236	0.150	0.883						0.883
dMRI	Lp	Drug-naïve/off-state	10	15		0.155 to 0.645	0.108	3.718	0.005	0.400	37.030	0.001	63.153	0.311	
dMRI	Lp	On-state	9	13		-0.182 to 1.190	0.291	1.734	0.126	0.504	69.142	< 0.001	94.139	1.030	
dMRI	Lp	Template effect	20	30	-0.136	-0.600 to 0.328	0.188	-0.721	0.499						0.749
dMRI	Lp	AAL	15	23		0.147 to 0.739	0.137	3.243	0.007	0.443	95.705	< 0.001	85.576	0.608	
dMRI	Lp	Non-AAL	5	7		-0.207 to 0.715	0.163	1.562	0.197	0.254	14.674	0.023	63.501	0.311	
dMRI	Lp	Template effect	20	30	-0.382	-1.438 to 0.673	0.381	-1.003	0.372						0.749
dMRI	Lp	Contain cerebellum	4	7		-1.046 to 2.852	0.584	1.547	0.227	0.903	59.495	< 0.001	96.377	1.612	
dMRI	Lp	Cerebellum-excluded	16	23		0.181 to 0.464	0.066	4.895	< 0.001	0.322	48.528	0.001	54.585	0.255	
dMRI	Lp	Tractography effect	20	30	-0.259	-1.125 to 0.607	0.306	-0.844	0.448						0.749
dMRI	Lp	Deterministic tractography	16	26		0.205 to 0.654	0.104	4.115	0.001	0.430	100.316	< 0.001	79.767	0.484	
dMRI	Lp	Probabilistic tractography	4	4		-0.775 to 1.110	0.292	0.574	0.607	0.168	10.829	0.013	78.958	0.522	
dMRI	Lp	Edges effect	10	15	0.043	-0.424 to 0.511	0.197	0.221	0.832						0.883
dMRI	Lp	Fractional anisotropy	5	7		0.267 to 0.470	0.034	10.692	0.001	0.368	2.887	0.823	< 0.001	< 0.001	
dMRI	Lp	Number of streamlines	5	8		-0.231 to 0.995	0.207	1.848	0.150	0.382	29.788	< 0.001	78.681	0.550	
dMRI	Lp	Threshold effect	20	30	0.216	-0.309 to 0.740	0.190	1.138	0.318						0.749
dMRI	Lp	Non-proportional threshold	16	26		0.120 to 0.625	0.117	3.177	0.007	0.372	99.541	< 0.001	81.734	0.545	
dMRI	Lp	Proportional threshold	4	4		0.045 to 1.107	0.161	3.571	0.041	0.576	7.613	0.055	60.741	0.246	
dMRI	Eglob	Drug effect	20	32	-0.190	-0.513 to 0.133	0.143	-1.331	0.215						0.581
dMRI	Eglob	Drug-naïve/off-state	14	22		-0.635 to -0.128	0.117	-3.266	0.006	-0.382	70.610	< 0.001	72.412	0.416	
dMRI	Eglob	On-state	6	10		-0.741 to -0.335	0.074	-7.239	0.002	-0.538	14.546	0.104	26.180	0.152	
dMRI	Eglob	Template effect	21	34	0.021	-0.424 to 0.465	0.182	0.114	0.913						0.913
dMRI	Eglob	AAL	16	26		-0.661 to -0.241	0.098	-4.591	< 0.001	-0.451	76.863	< 0.001	69.653	0.383	
dMRI	Eglob	Non-AAL	5	8		-0.858 to -0.025	0.144	-3.058	0.043	-0.441	12.545	0.084	47.949	0.257	
dMRI	Eglob	Template effect	21	34	0.215	-0.368 to 0.797	0.175	1.230	0.313						0.581
dMRI	Eglob	Contain cerebellum	3	6		-1.283 to 0.030	0.150	-4.184	0.054	-0.627	12.599	0.027	61.855	0.366	
dMRI	Eglob	Cerebellum-excluded	18	28		-0.608 to -0.224	0.091	-4.585	< 0.001	-0.416	74.829	< 0.001	66.027	0.349	
dMRI	Eglob	Tractography effect	21	34	0.050	-0.684 to 0.783	0.264	0.189	0.859						0.913
dMRI	Eglob	Deterministic tractography	17	29		-0.639 to -0.265	0.088	-5.138	< 0.001	-0.452	80.747	< 0.001	67.335	0.360	
dMRI	Eglob	Probabilistic tractography	4	5		-1.143 to 0.250	0.218	-2.053	0.133	-0.447	8.741	0.068	56.994	0.341	
dMRI	Eglob	Edges effect	13	21	-0.203	-0.499 to 0.093	0.132	-1.538	0.157						0.581
dMRI	Eglob	Fractional anisotropy	7	11		-0.624 to -0.071	0.111	-3.123	0.022	-0.348	17.834	0.058	45.459	0.228	
dMRI	Eglob	Number of streamlines	6	10		-0.749 to -0.367	0.071	-7.817	0.001	-0.558	14.973	0.092	38.863	0.217	
dMRI	Eglob	Threshold effect	21	34	-0.168	-0.590 to 0.254	0.183	-0.916	0.387						0.581
dMRI	Eglob	Non-proportional threshold	15	27		-0.611 to -0.201	0.095	-4.262	0.001	-0.406	70.680	< 0.001	65.898	0.366	

dMRI	Eglob	Proportional threshold	6	7		-0.986 to -0.141	0.163	-3.468	0.019	-0.564	17.346	0.008	64.460	0.319	
dMRI	Gamma	Drug effect	8	13	-0.056	-0.538 to 0.426	0.180	-0.310	0.771						0.771
dMRI	Gamma	Drug-naïve/off-state	5	8		-0.202 to 0.715	0.165	1.560	0.195	0.257	17.367	0.015	60.407	0.307	
dMRI	Gamma	On-state	3	5		-0.169 to 0.557	0.078	2.493	0.141	0.194	2.797	0.592	< 0.001	< 0.001	
dMRI	Gamma	Tractography effect	9	15	0.045	-0.604 to 0.694	0.118	0.382	0.747						0.771
dMRI	Gamma	Deterministic tractography	7	12		-0.058 to 0.530	0.120	1.972	0.097	0.236	24.052	0.013	56.154	0.278	
dMRI	Gamma	Probabilistic tractography	2	3		0.077 to 0.484	0.016	17.497	0.036	0.280	0.235	0.889	< 0.001	< 0.001	
dMRI	Lambda	Drug effect	8	13	0.020	-0.667 to 0.707	0.256	0.078	0.941						0.941
dMRI	Lambda	Drug-naïve/off-state	5	8		-0.261 to 0.518	0.139	0.921	0.410	0.128	11.112	0.134	48.426	0.240	
dMRI	Lambda	On-state	3	5		-0.781 to 1.083	0.215	0.702	0.556	0.151	8.476	0.076	65.506	0.324	
dMRI	Lambda	Tractography effect	9	15	-0.115	-2.194 to 1.965	0.381	-0.301	0.797						0.941
dMRI	Lambda	Deterministic tractography	7	12		-0.055 to 0.459	0.105	1.934	0.102	0.202	14.139	0.225	40.637	0.202	
dMRI	Lambda	Probabilistic tractography	2	3		-4.563 to 4.779	0.368	0.294	0.818	0.108	7.127	0.028	80.729	0.484	
dMRI	Sigma	Drug effect	14	23	-0.185	-0.616 to 0.245	0.197	-0.939	0.367						0.612
dMRI	Sigma	Drug-naïve/off-state	7	12		-0.002 to 0.485	0.099	2.441	0.052	0.241	13.800	0.244	33.745	0.178	
dMRI	Sigma	On-state	7	11		-0.422 to 0.493	0.187	0.192	0.854	0.036	27.185	0.002	76.511	0.448	
dMRI	Sigma	Template effect	15	25	-0.336	-1.033 to 0.361	0.269	-1.248	0.269						0.612
dMRI	Sigma	AAL	11	19		0.065 to 0.420	0.079	3.052	0.013	0.242	25.696	0.107	33.096	0.177	
dMRI	Sigma	Non-AAL	4	6		-1.101 to 0.775	0.293	-0.556	0.618	-0.163	17.925	0.003	84.092	0.548	
dMRI	Sigma	Template effect	15	25	-0.506	-1.321 to 0.310	0.110	-4.593	0.092						0.460
dMRI	Sigma	Contain cerebellum	2	4		-0.300 to 1.493	0.071	8.458	0.075	0.597	0.704	0.872	< 0.001	< 0.001	
dMRI	Sigma	Cerebellum-excluded	13	21		-0.083 to 0.283	0.084	1.196	0.256	0.100	36.768	0.012	47.858	0.232	
dMRI	Sigma	Tractography effect	15	25	-0.199	-1.502 to 1.104	0.393	-0.507	0.650						0.813
dMRI	Sigma	Deterministic tractography	12	21		0.018 to 0.367	0.079	2.437	0.034	0.193	30.426	0.063	38.692	0.196	
dMRI	Sigma	Probabilistic tractography	3	4		-2.031 to 1.830	0.447	-0.225	0.843	-0.101	16.289	0.001	89.478	0.742	
dMRI	Sigma	Edges effect	8	14	0.028	-1.000 to 1.056	0.207	0.137	0.905						0.905
dMRI	Sigma	Fractional anisotropy	2	3		-0.790 to 1.054	0.073	1.821	0.320	0.132	0.596	0.742	< 0.001	< 0.001	
dMRI	Sigma	Number of streamlines	6	11		-0.312 to 0.691	0.194	0.977	0.374	0.190	24.898	0.006	73.864	0.444	
fMRI	Cp	Drug effect	29	46	0.099	-0.424 to 0.622	0.253	0.392	0.699						0.699
fMRI	Cp	Drug-naïve/off-state	17	23		-0.571 to -0.179	0.092	-4.066	0.001	-0.375	66.471	< 0.001	73.529	0.325	
fMRI	Cp	On-state	12	23		-0.875 to 0.226	0.249	-1.302	0.220	-0.325	186.357	< 0.001	94.899	0.884	
fMRI	Cp	Scanning effect	29	46	-0.803	-1.300 to -0.305	0.182	-4.398	**0.010**						**0.050**
fMRI	Cp	1.5T	4	8		-0.161 to 0.799	0.149	2.140	0.124	0.319	18.691	0.009	67.427	0.302	
fMRI	Cp	3T	25	38		-0.698 to -0.246	0.109	-4.321	< 0.001	-0.472	195.382	< 0.001	87.971	0.522	
fMRI	Cp	Template effect	21	35	0.501	-0.005 to 1.007	0.210	2.390	**0.052**						0.130
fMRI	Cp	Function	5	8		-1.249 to -0.334	0.162	-4.901	0.009	-0.792	27.749	< 0.001	66.386	0.371	
fMRI	Cp	Macroanatomy	16	27		-0.557 to 0.012	0.133	-2.049	0.059	-0.273	162.201	< 0.001	88.383	0.525	
fMRI	Cp	Network framework effect	29	46	0.269	-0.188 to 0.725	0.222	1.212	0.237						0.296

fMRI	Cp	Binary	16	24		-0.755 to -0.205	0.129	-3.732	0.002	-0.480	128.505	< 0.001	85.886	0.493	
fMRI	Cp	Weighted	13	22		-0.660 to 0.188	0.194	-1.214	0.248	-0.236	119.443	< 0.001	92.266	0.689	
fMRI	Cp	Threshold effect	29	46	-0.384	-0.868 to 0.100	0.224	-1.717	0.110						0.183
fMRI	Cp	Non-proportional threshold	8	14		-0.501 to 0.331	0.175	-0.485	0.643	-0.085	48.763	< 0.001	79.243	0.468	
fMRI	Cp	Proportional threshold	21	32		-0.739 to -0.189	0.132	-3.526	0.002	-0.464	199.346	< 0.001	91.260	0.589	
fMRI	Eloc	Drug effect	24	39	-0.038	-0.913 to 0.836	0.383	-0.100	0.922						0.922
fMRI	Eloc	Drug-naïve/off-state	18	25		-0.409 to -0.021	0.092	-2.342	0.032	-0.215	77.451	< 0.001	73.155	0.343	
fMRI	Eloc	On-state	6	14		-1.189 to 0.688	0.364	-0.689	0.522	-0.251	129.409	< 0.001	91.341	0.890	
fMRI	Eloc	Scanning effect	24	39	-0.708	-1.496 to 0.080	0.234	-3.029	0.064						0.160
fMRI	Eloc	1.5T	3	7		-0.513 to 1.297	0.210	1.868	0.203	0.392	19.645	0.003	73.369	0.392	
fMRI	Eloc	3T	21	32		-0.553 to -0.085	0.112	-2.849	0.010	-0.319	156.101	< 0.001	82.028	0.476	
fMRI	Eloc	Template effect	21	34	0.090	-1.012 to 1.192	0.410	0.221	0.835						0.922
fMRI	Eloc	Function	4	6		-1.495 to 0.982	0.388	-0.660	0.557	-0.256	27.573	< 0.001	84.769	0.736	
fMRI	Eloc	Macroanatomy	17	28		-0.470 to 0.090	0.132	-1.439	0.170	-0.190	160.669	< 0.001	85.832	0.517	
fMRI	Eloc	Network framework effect	23	37	0.049	-0.467 to 0.565	0.245	0.200	0.844						0.922
fMRI	Eloc	Binary	14	21		-0.572 to 0.089	0.153	-1.579	0.139	-0.241	126.533	< 0.001	86.690	0.535	
fMRI	Eloc	Weighted	9	16		-0.635 to 0.252	0.192	-0.999	0.347	-0.192	78.551	< 0.001	84.491	0.570	
fMRI	Eloc	Threshold effect	24	39	-0.640	-1.199 to -0.081	0.210	-3.054	**0.033**						0.160
fMRI	Eloc	Non-proportional threshold	4	8		-0.260 to 0.884	0.177	1.762	0.179	0.312	21.478	0.003	71.411	0.357	
fMRI	Eloc	Proportional threshold	20	31		-0.579 to -0.091	0.117	-2.876	0.010	-0.335	154.008	< 0.001	82.299	0.486	
fMRI	Lp	Drug effect	28	44	-0.144	-0.540 to 0.253	0.191	-0.753	0.460						0.460
fMRI	Lp	Drug-naïve/off-state	17	23		-0.216 to 0.325	0.128	0.429	0.674	0.055	108.297	< 0.001	82.913	0.476	
fMRI	Lp	On-state	11	21		-0.407 to 0.229	0.142	-0.628	0.545	-0.089	76.999	< 0.001	81.558	0.418	
fMRI	Lp	Scanning effect	28	44	-0.235	-1.029 to 0.560	0.226	-1.039	0.387						0.460
fMRI	Lp	1.5T	3	5		-0.642 to 1.045	0.195	1.037	0.409	0.202	9.099	0.059	68.909	0.296	
fMRI	Lp	3T	25	39		-0.244 to 0.187	0.104	-0.277	0.784	-0.029	206.054	< 0.001	84.185	0.469	
fMRI	Lp	Template effect	20	31	0.503	-0.555 to 1.562	0.398	1.264	0.268						0.460
fMRI	Lp	Function	4	6		-1.612 to 0.659	0.356	-1.339	0.274	-0.476	62.828	< 0.001	87.164	0.662	
fMRI	Lp	Macroanatomy	16	25		-0.172 to 0.298	0.110	0.574	0.575	0.063	101.985	< 0.001	79.277	0.382	
fMRI	Lp	Network framework effect	28	44	0.236	-0.153 to 0.626	0.189	1.251	0.223						0.460
fMRI	Lp	Binary	15	22		-0.425 to 0.174	0.139	-0.901	0.383	-0.125	130.675	< 0.001	82.641	0.488	
fMRI	Lp	Weighted	13	22		-0.158 to 0.399	0.127	0.945	0.364	0.121	84.307	< 0.001	81.878	0.412	

fMRI	Lp	Threshold effect	28	44	-0.186	-0.562 to 0.189	0.173	-1.075	0.302						0.460
fMRI	Lp	Non-proportional threshold	8	12		-0.137 to 0.424	0.117	1.225	0.263	0.143	21.299	0.030	55.546	0.257	
fMRI	Lp	Proportional threshold	20	32		-0.315 to 0.203	0.124	-0.453	0.656	-0.056	192.526	< 0.001	86.957	0.505	
fMRI	Eglob	Drug effect	26	46	0.203	-0.482 to 0.887	0.311	0.652	0.528						0.528
fMRI	Eglob	Drug-naïve/off-state	19	28		-0.349 to 0.267	0.147	-0.279	0.783	-0.041	165.531	< 0.001	87.613	0.597	
fMRI	Eglob	On-state	7	18		-0.518 to 0.884	0.284	0.644	0.544	0.183	123.115	< 0.001	93.609	0.806	
fMRI	Eglob	Template effect	21	33	-0.546	-1.410 to 0.318	0.360	-1.514	0.177						0.354
fMRI	Eglob	Function	5	8		-0.387 to 1.312	0.304	1.520	0.204	0.463	49.441	< 0.001	83.966	0.642	
fMRI	Eglob	Macroanatomy	16	25		-0.454 to 0.309	0.178	-0.408	0.690	-0.073	209.872	< 0.001	93.742	0.717	
fMRI	Eglob	Network framework effect	25	44	-0.446	-0.993 to 0.100	0.264	-1.693	0.104						0.354
fMRI	Eglob	Binary	12	19		-0.152 to 0.835	0.222	1.538	0.154	0.342	209.002	< 0.001	92.879	0.807	
fMRI	Eglob	Weighted	13	25		-0.511 to 0.161	0.154	-1.135	0.279	-0.175	102.370	< 0.001	85.595	0.512	
fMRI	Eglob	Threshold effect	26	46	0.303	-0.498 to 1.105	0.323	0.939	0.386						0.515
fMRI	Eglob	Non-proportional threshold	5	7		-1.056 to 0.629	0.302	-0.709	0.518	-0.214	21.678	0.001	82.615	0.618	
fMRI	Eglob	Proportional threshold	21	39		-0.219 to 0.383	0.144	0.569	0.576	0.082	287.183	< 0.001	91.259	0.659	
fMRI	Gamma	Drug effect	12	18	0.270	-0.168 to 0.707	0.132	2.047	0.140						0.560
fMRI	Gamma	Drug-naïve/off-state	9	14		-0.209 to 0.218	0.092	0.049	0.962	0.005	16.111	0.243	31.487	0.176	
fMRI	Gamma	On-state	3	4		-0.279 to 0.770	0.075	3.289	0.134	0.246	1.846	0.605	< 0.001	< 0.001	
fMRI	Gamma	Scanning effect	12	18	-0.068	-0.749 to 0.613	0.114	-0.600	0.626						0.835
fMRI	Gamma	1.5T	2	3		-0.582 to 0.876	0.057	2.556	0.237	0.147	0.289	0.866	< 0.001	< 0.001	
fMRI	Gamma	3T	10	15		-0.149 to 0.275	0.093	0.676	0.517	0.063	20.631	0.111	38.068	0.200	
fMRI	Gamma	Network framework effect	12	18	0.015	-0.338 to 0.367	0.156	0.094	0.927						0.927
fMRI	Gamma	Binary	6	8		-0.247 to 0.375	0.120	0.537	0.615	0.064	13.057	0.071	51.967	0.223	
fMRI	Gamma	Weighted	6	10		-0.200 to 0.340	0.101	0.698	0.520	0.070	8.186	0.516	8.293	0.088	
fMRI	Gamma	Threshold effect	12	18	-0.097	-0.464 to 0.270	0.118	-0.823	0.469						0.835
fMRI	Gamma	Non-proportional threshold	3	5		-0.171 to 0.492	0.071	2.256	0.163	0.160	0.678	0.954	< 0.001	< 0.001	
fMRI	Gamma	Proportional threshold	9	13		-0.174 to 0.281	0.097	0.550	0.599	0.053	20.149	0.064	43.759	0.209	
fMRI	Lambda	Drug effect	12	18	0.589	0.167 to 1.011	0.130	4.521	**0.022**						0.088
fMRI	Lambda	Drug-naïve/off-state	9	14		-0.392 to 0.098	0.106	-1.391	0.203	-0.147	19.725	0.102	44.699	0.233	
fMRI	Lambda	On-state	3	4		0.059 to 0.798	0.050	8.655	0.041	0.429	1.362	0.714	< 0.001	< 0.001	
fMRI	Lambda	Scanning effect	12	18	-0.380	-1.608 to 0.848	0.201	-1.894	0.241						0.321
fMRI	Lambda	1.5T	2	3		-1.523 to 2.236	0.148	2.409	0.250	0.356	1.351	0.509	15.641	0.119	
fMRI	Lambda	3T	10	15		-0.331 to 0.204	0.118	-0.538	0.604	-0.063	29.814	0.008	57.904	0.301	
fMRI	Lambda	Network framework effect	12	18	0.083	-0.432 to 0.598	0.230	0.361	0.726						0.726
fMRI	Lambda	Binary	6	8		-0.469 to 0.401	0.169	-0.203	0.847	-0.034	30.253	< 0.001	74.813	0.363	

fMRI	Lambda	Weighted	6	10		-0.358 to 0.446	0.155	0.284	0.788	0.044	14.204	0.115	49.928	0.294	
fMRI	Lambda	Threshold effect	12	18	-0.251	-0.716 to 0.214	0.154	-1.627	0.193						0.321
fMRI	Lambda	Non-proportional threshold	3	5		-0.130 to 0.558	0.074	2.898	0.111	0.214	0.844	0.932	< 0.001	< 0.001	
fMRI	Lambda	Proportional threshold	9	13		-0.374 to 0.269	0.139	-0.381	0.714	-0.053	41.141	< 0.001	70.266	0.358	
fMRI	Sigma	Drug effect	14	22	-0.026	-0.857 to 0.806	0.355	-0.073	0.944						0.944
fMRI	Sigma	Drug-naïve/off-state	9	14		-0.166 to 0.251	0.090	0.473	0.649	0.043	15.334	0.287	28.820	0.165	
fMRI	Sigma	On-state	5	8		-1.033 to 1.027	0.366	-0.008	0.994	-0.003	58.214	< 0.001	95.189	0.821	
fMRI	Sigma	Network framework effect	14	22	0.192	-0.334 to 0.717	0.240	0.800	0.440						0.708
fMRI	Sigma	Binary	7	10		-0.529 to 0.405	0.189	-0.328	0.755	-0.062	32.005	< 0.001	73.352	0.440	
fMRI	Sigma	Weighted	7	12		-0.205 to 0.475	0.136	0.994	0.362	0.135	40.098	< 0.001	75.588	0.344	
fMRI	Sigma	Threshold effect	14	22	0.212	-0.610 to 1.033	0.258	0.821	0.472						0.708
fMRI	Sigma	Non-proportional threshold	3	4		-1.105 to 0.817	0.222	-0.649	0.583	-0.144	4.315	0.229	45.424	0.284	
fMRI	Sigma	Proportional threshold	11	18		-0.243 to 0.380	0.139	0.492	0.634	0.068	70.286	< 0.001	81.955	0.432	
fMRI	Strength	Scanning effect	6	10	-0.604	-1.489 to 0.281	0.254	-2.376	0.111						0.111
fMRI	Strength	1.5T	2	4		-2.746 to 2.685	0.214	-0.142	0.910	-0.030	5.019	0.170	63.268	0.262	
fMRI	Strength	3T	4	6		-1.104 to -0.217	0.129	-5.119	0.019	-0.660	9.727	0.083	49.041	0.281	
EEG	Cp	Threshold effect	6	7	0.393	-2.621 to 3.407	0.755	0.521	0.651						0.651
EEG	Cp	Non-proportional threshold	2	3		-6.982 to 7.137	0.556	0.139	0.912	0.077	9.146	0.010	81.619	0.771	
EEG	Cp	Proportional threshold	4	4		-1.133 to 2.115	0.510	0.963	0.407	0.491	28.671	< 0.001	91.593	0.974	
EEG	Lp	Threshold effect	6	8	1.225	-0.650 to 3.100	0.672	1.824	0.143						0.143
EEG	Lp	Non-proportional threshold	3	5		-2.629 to 1.799	0.509	-0.815	0.501	-0.415	24.238	< 0.001	85.346	0.868	
EEG	Lp	Proportional threshold	3	3		-1.064 to 2.689	0.436	1.864	0.203	0.812	9.962	0.007	79.745	0.673	

Abbreviations: dMRI, diffusion MRI; fMRI, functional MRI; EEG, electroencephalography; Cp, clustering coefficient; Eloc, local efficiency; Lp, characteristic path length; Eglob, global efficiency; AAL, Automated Anatomical Labeling; k, number of studies-number of samples.

Table S20. Disease progression

Study	Sample characteristics	Features	Main findings
Abbasi et al. 2020[2]	Mild-motor predominant PD: 82 Intermediate PD: 48 Diffuse-malignant PD: 14	dMRI Predicting severity and progression	At baseline, *vs* Mild-motor predominant and intermediate PD, diffuse-malignant PD had significantly lower global efficiency and higher characteristic path length. Lower global efficiency and higher characteristic path length at baseline significantly correlated with increase in global composite outcome, increase in postural instability gait difficulty score and decline in Montreal cognitive assessment score after 4.5-years follow-up.
Bergamino et al. 2023[3]	PD: 86 HC: 75	dMRI Progression	At baseline, network density was lower in PD *vs* HC, but this difference was not statistically significant after correction for multiple comparisons. No significant differences between PD *vs* HC in global efficiency, strength, or assortativity. After 1.5-years of follow-up, PD still had lower density, but the difference did not survive correction. No significant differences in global efficiency, strength, or assortativity after follow-up.
Chung et al. 2022[6]	PD with high risk for developing dementia (5-year conversion from MCI): 38 PD with low risk for developing dementia: 37 HC: 23	dMRI Predicting dementia conversion in PD with MCI	PD with high risk for developing dementia had lower global efficiency, clustering coefficient and higher characteristic path length *vs* those with low risk for dementia and HC. No significant differences in global topological metrics between PD with low risk for developing dementia *vs* HC.
De Micco et al. 2021[51]	Combined PD: 147 early/mild PD: 77 early/severe PD: 70 HC: 38	Rs-fMRI Progression, PD subtype (mild and severe based data-drive k-means cluster)	Combined PD had lower strength and higher characteristic path length *vs* HC, but no significant differences in global network metrics among early/mild PD, early/severe PD and HC. In the combined PD group, cognitive COS changes negatively correlated with characteristic path length. For early/severe PD, cognitive COS changes positively correlated with strength, local efficiency, and clustering coefficient, but negatively correlated with characteristic path length. No correlations between cognitive COS changes and global metrics in early/mild PD.
Filippi et al. 2021[56]	Mild PD: 86 Moderate-to-severe PD: 60 Mild motor-predominant PD: 43 Mild-diffuse PD:43 HC: 60	Rs-fMRI Progression. PD subtypes including mild, moderate-to-severe, mild motor-predominant and mild-diffuse	No significant differences in strength, clustering coefficient, local efficiency or characteristic path length among mild PD, moderate-to-severe PD and HC, as well as among mild motor-predominant, mild-diffuse PD and HC. Moderate-to-severe PD had progressive changes with decreased strength, local efficiency and clustering coefficient, and increased characteristic path length *vs* mild PD, while mild PD, mild motor-predominant and mild-diffuse PD had no alterations in global metrics over time.
Klobušiaková et al. 2019[63]	PD without MCI: 17 PD with MCI: 22 HC: 51	Rs-fMRI MCI, progression	At baseline, PD without MCI had lower strength, clustering coefficient, and global efficiency, and higher characteristic path length than HC, whereas PD with MCI did not differ significantly from either HC or PD without MCI. No significant differences in normalized clustering coefficient, normalized characteristic path length or modularity among the three groups. After 1 year follow-up, although trends emerged in the overall PD group, no significant differences were detected in either PD or HC.
Li et al. 2022[66]	Combined PD: 40 PD with freezing of gait-transition (5-years follow-up): 20 PD without freezing of gait-transition: 20 HC: 20	Rs-fMRI Freezing of gait-transition	No significant differences in clustering coefficient, characteristic path length, normalized clustering coefficient, normalized characteristic path length, local efficiency global efficiency or small-worldness between combined PD and HC, or among PD with and without freezing of gait transition, and HC.
Sarasso et al. 2022[79]	PD with freezing of gait: 30 PD with freezing of gait converters: 11 PD with freezing of gait non-converters: 11 HC: 30	Rs-fMRI Freezing of gait, progression	PD with freezing of gait converters had higher clustering coefficient and local efficiency *vs* both HC and PD with freezing of gait. Lower local efficiency and clustering coefficient at baseline correlated with worsening of executive functions at 2-year follow-up.

Tuovinen et al. 2018[89]	PD: 16 HC: 16	Rs-fMRI Progression	At baseline, PD had higher global efficiency *vs* HC. At follow-up, PD global efficiency declined while HC remained unchanged.
Olde Dubbelink et al. 2014[135]	At baseline PD: 43, de novo PD: 12, HC: 14 After follow-up PD: 59, HC: 14	MEG Progression	In delta band, de novo PD had lower normalized clustering coefficient *vs* HC, with no significant difference in normalized characteristic path length. Normalized clustering coefficient (theta, alpha 1 and alpha 2 bands) and normalized characteristic path length (alpha 2 only) decreased over time in PD.

Abbreviations: PD, Parkinson's disease; HC, healthy controls; dMRI, diffusion MRI; MCI, mild cognitive impairment; Rs-fMRI, resting-state functional MRI.

Table S21. Treatment response

Study	Sample characteristics	Features	Main findings
Du et al. 2022[8]	PD with levodopa irresponsive group (UPDRS-III score improvement rate < 30%): 22 PD with levodopa responsive group (improvement rate ≥ 30%): 32	dMRI Levodopa responsiveness therapy	For the number of streamlines weighed network, responsive PD had higher global efficiency and local efficiency, and lower characteristic path length *vs* the irresponsive group. No significant differences in clustering coefficient, normalized clustering coefficient, normalized characteristic path length, or small-worldness between the two groups. For the fractional anisotropy weighted network, only higher local efficiency was found in the responsive PD.
Wang et al. 2019[31]	PD with levodopa-induced dyskinesias: 21 PD without levodopa-induced dyskinesias: 21 HC: 25	dMRI Levodopa-induced dyskinesias	PD without levodopa-induced dyskinesias had lower global efficiency and higher characteristic path length *vs* HC. No significant differences in global network metrics between PD with levodopa-induced dyskinesias *vs* HC. PD with levodopa-induced dyskinesias had higher local efficiency, global efficiency and clustering coefficient, and lower characteristic path length *vs* PD without levodopa-induced dyskinesias. No significant difference in small-worldness among the three groups. Negative correlation between characteristic path length and abnormal involuntary movement scale scores in PD with levodopa-induced dyskinesias.
Albano et al. 2022[42]	PD with candidates for DBS: 19 PD with non-candidates for DBS: 41 HC: 60	Rs-fMRI PD candidates for DBS	No significant differences in strength, characteristic path length, local efficiency or clustering coefficient between PD *vs* HC. Among PD, only DBS candidates had progressive changes in global network metrics over 4 years, while non-candidates did not.
Berman et al. 2016[45]	PD: 19 HC: 16	Rs-fMRI On-medication and off-medication	PD with on-medication had lower local efficiency and a trend toward reduced global efficiency *vs* PD with off-medication. No significant differences between either PD group and HC. Local and global efficiency did not correlate with duration or MDS-UPDRS.
Borchert et al. 2019[46]	PD: 30 HC: 75	Rs-fMRI Atomoxetine and citalopram drug	PD on placebo had lower clustering coefficient *vs* HC. No significant differences in characteristic path length and modularity between PD on placebo *vs* HC. No significant main effect of atomoxetine on global clustering coefficient, path length, or modularity, relative to placebo. Citalopram did not alter group-wise global metrics, decreasing clustering coefficient, characteristic path length and modularity in proportion to UPDRS-III scores.
Engels et al. 2018[54]	PD: 24 HC: 27	Rs-fMRI On-medication and off-medication	PD in on-state had higher global efficiency *vs* HC, while PD in off-state had a trend of higher global efficiency in whole brain; however, on-off differences did not reach significances.
van Balkom et al. 2022[90]	PD with cognition training: 37 PD with active control: 34	Rs-fMRI Eight-week multi-domain cognitive training	No significant differences in global efficiency, modularity and participation coefficient between PD with cognition training *vs* PD with active control after 8-week multi-domain cognitive training.
Wu et al. 2021[94]	PD: 18	Rs-fMRI Deep brain stimulation of the subthalamic nucleus	Deep brain stimulation of subthalamic nucleus was not correlated with global efficiency, assortativity, clustering coefficient, or betweenness centrality.
Yuan et al. 2024[95]	PD with end-of-dose wearing-off: 61 PD without end-of-dose wearing-off: 39	Rs-fMRI End-of-dose wearing-off	No significant differences in global efficiency and local efficiency between PD with and without end-of-dose wearing-off. Positive correlation between degree centrality and daily dopamine or dopamine agonist therapy in control group.
Diao et al. 2024[99]	PD: 138 HC: 40	sMRI Bilateral STN-DBS	No correlation between global network metrics and long-term DBS outcomes.

Xie et al. 2022[108]	PD with levodopa challenge test high improvement: 25 PD with levodopa challenge test low improvement: 13	sMRI Predicts levodopa responsiveness to identify candidates for DBS	No significant differences between the two groups in clustering coefficient, characteristic path length, normalized clustering coefficient, normalized characteristic path length, local efficiency, global efficiency, assortativity, modularity, synchronization, hierarchy and small-worldness.
Bočková et al. 2021[113]	PD with DBS optimal responders: 12 PD with DBS suboptimal responders: 6 PD with DBS non-responders: 14	Task-EEG Deep brain stimulation (DBS)	In 1-8 Hz, PD with DBS suboptimal responders in DBS on state had lower strength and higher clustering coefficient and characteristic path length *vs* patients in DBS off state with and target stimuli. In 55-80 Hz, different global network metrics significant differences between DBS on state *vs* off state in PD with DBS suboptimal responders and patients with DBS non-responders with and target, frequent and distractors stimuli, while no significant differences in PD *vs* DBS optimal responders. No significant differences in 8-20 Hz, 20-45 Hz.
Li et al. 2021[118]	PD after DBS: 20 HC: 21	Rs-EEG The effect of acute deep brain stimulation	In alpha, beta 1 and beta 2 frequency bands, both PD with DBS-OFF and DBS-ON conditions had lower local efficiency and clustering coefficient at sparsity 0.05. No significant differences in global metrics between PD with DBS-OFF and DBS-ON states.
Stylianou et al. 2022[123]	PD: 15 HC: 16	Rs-EEG Dopaminergic Treatment: on-medication and off-medication	PD on-medication had lower clustering coefficient and characteristic path length, and higher degree *vs* PD off-medication and HC in the network based on bivariate focus-based multifractal, with no significant differences in the network by generalized Hurst exponent. In the network by generalized Hurst exponent, the North American Adult Reading Test scores positive correlated with degree and clustering coefficient, and negative with characteristic path length.
Wang et al. 2022[136]	PD: 11 HC: 34	Rs-EEG After deep brain stimulation	PD in DBS-ON state had higher strength, global efficiency and clustering coefficient *vs* PD in DBS-OFF state and HC, and lower modularity *vs* patients in DBS-OFF state. Both PD in DBS-ON and DBS-OFF states had lower transitivity relative to HC.
Zhang et al. 2022[128]	PD: 15	Rs-EEG On-medication and off-medication	No significant differences in global efficiency and clustering coefficient between PD on-medication *vs* off-medication.

Abbreviations: PD, Parkinson's disease; HC, healthy controls; dMRI, diffusion MRI; UPDRS, Unified Parkinson's Disease Rating Scale; DBS, deep brain stimulation; Rs-fMRI, resting-state functional MRI; MDS, Movement Disorder Society; sMRI, structural MRI; EEG, electroencephalography.

Table S22. Contingency tables for diagnosis of PD vs HC

Study	Total	PD	HC	TP	FP	FN	TN	Accuracy	SE	SP	AUC	Method	Modality	Features set
Zhang et al. 2014[96]	45	25	20	25	4	0	16	0.890	1.000	0.800	NA	MLDA	rs-fMRI	Local efficiencies (with cerebellum, PD *vs* HC)
Zhang et al. 2014[96]	45	25	20	19	1	6	19	0.860	0.750	0.960	NA	MLDA	rs-fMRI	Local efficiencies (without cerebellum, PD *vs* HC)
Zhang et al. 2014[96]	35	15	20	14	0	1	20	0.970	0.950	1.000	NA	MLDA	rs-fMRI	Local efficiencies (with cerebellum, TPD *vs* HC)
Zhang et al. 2014[96]	35	15	20	12	3	3	17	0.820	0.800	0.860	NA	MLDA	rs-fMRI	Local efficiencies (without cerebellum, TPD *vs* HC)
Zhang et al. 2014[96]	30	10	20	9	0	1	20	0.900	0.850	1.000	NA	MLDA	rs-fMRI	Local efficiencies (with cerebellum, NTPD *vs* HC)
Zhang et al. 2014[96]	30	10	20	9	0	1	20	0.930	0.900	1.000	NA	MLDA	rs-fMRI	Local efficiencies (without cerebellum, NTPD *vs* HC)
Zhang et al. 2014[96]	45	25	20	21	6	4	14	0.770	0.850	0.720	NA	MLDA	rs-fMRI	Global efficiencies (with cerebellum, PD *vs* HC)
Zhang et al. 2014[96]	45	25	20	8	10	17	10	0.400	0.300	0.480	NA	MLDA	rs-fMRI	Global efficiencies (without cerebellum, PD *vs* HC)
Zhang et al. 2014[96]	35	15	20	13	1	2	19	0.880	0.850	0.930	NA	MLDA	rs-fMRI	Global efficiencies (with cerebellum, TPD *vs* HC)
Zhang et al. 2014[96]	35	15	20	11	3	4	17	0.800	0.750	0.860	NA	MLDA	rs-fMRI	Global efficiencies (without cerebellum, TPD *vs*. HC)
Zhang et al. 2014[96]	30	10	20	8	2	2	18	0.800	0.750	0.900	NA	MLDA	rs-fMRI	Global efficiencies (with cerebellum, NTPD *vs* HC)
Zhang et al. 2014[96]	30	10	20	5	8	5	12	0.530	0.500	0.600	NA	MLDA	rs-fMRI	Global efficiencies (without cerebellum, NTPD *vs* HC)
Kamagata et al. 2018[18]	42	21	21	7	9	14	12	0.600	0.333	0.571	0.669	SVM	dMRI	All global GTA metrics (deterministic SSST-CSD)
Kamagata et al. 2018[18]	42	21	21	11	11	10	10	0.567	0.524	0.476	0.419	SVM	dMRI	All global GTA metrics (probabilistic SSST-CSD)
Kamagata et al. 2018[18]	42	21	21	17	3	4	18	0.783	0.810	0.857	0.853	SVM	dMRI	All global GTA metrics (probabilistic MSMT-CSD)
Kamagata et al. 2018[18]	42	21	21	10	12	11	9	0.500	0.476	0.429	0.433	SVM	dMRI	Local clustering & local efficiency (deterministic SSST-CSD)
Kamagata et al. 2018[18]	42	21	21	10	14	11	7	0.458	0.476	0.333	0.533	SVM	dMRI	Local clustering & local efficiency

														(probabilistic SSST-CSD)
Kamagata et al. 2018[18]	42	21	21	11	12	10	9	0.617	0.524	0.429	0.681	SVM	dMRI	Local clustering & local efficiency (probabilistic MSMT-CSD)
Kamagata et al. 2018[18]	42	21	21	8	13	13	8	0.417	0.381	0.381	0.417	SVM	dMRI	All global GTA metrics, local clustering, local efficiency (deterministic SSST-CSD)
Kamagata et al. 2018[18]	42	21	21	10	7	11	14	0.575	0.476	0.667	0.717	SVM	dMRI	All global GTA metrics, local clustering, local efficiency (probabilistic SSST-CSD)
Kamagata et al. 2018[18]	42	21	21	16	4	5	17	0.767	0.762	0.810	0.814	SVM	dMRI	All global GTA metrics, local clustering, local efficiency (probabilistic MSMT-CSD)
Ma et al. 2017[71]	63	32	31	23	13	9	18	0.651	0.710	0.594	0.638	ROC	rs-fMRI	Intra-modular characteristic path length (mPFC)
Ma et al. 2017[71]	63	32	31	14	4	18	27	0.667	0.452	0.875	0.667	ROC	rs-fMRI	Intra-modular characteristic path length (SN)
Ma et al. 2017[71]	63	32	31	18	9	14	22	0.635	0.548	0.719	0.623	ROC	rs-fMRI	Intra-modular characteristic path length (FPN)
Ma et al. 2017[71]	63	32	31	15	6	17	25	0.651	0.484	0.813	0.653	ROC	rs-fMRI	Intra-modular characteristic path length (SMN)
Suo et al. 2021[104]	108	54	54	34	10	20	44	0.727	0.636	0.818	NA	SVM	sMRI	GTA metrics
Jin et al. 2021[137]	46	24	22	21	2	3	20	0.891	0.875	0.909	0.895	ROC	rs-fMRI	Degree Centrality (PD FOG+ *vs* HC, R_ITG)
Jin et al. 2021[137]	59	37	22	28	6	9	16	0.746	0.767	0.727	0.777	ROC	rs-fMRI	Degree Centrality (PD FOG– *vs* HC, R_ITG)
Jin et al. 2021[137]	46	24	22	16	7	8	15	0.674	0.667	0.682	0.697	ROC	rs-fMRI	Degree Centrality (PD FOG+ *vs* HC, L_MFG)
Jin et al. 2021[137]	59	37	22	32	10	5	12	0.746	0.865	0.545	0.695	ROC	rs-fMRI	Degree Centrality (PD FOG- *vs* HC, L_MFG)
Li et al. 2023[133]	98	49	49	31	16	18	33	0.653	0.633	0.674	0.724	SVM	PET	Global GTA metrics
Li et al. 2023[133]	98	49	49	40	14	9	35	0.765	0.816	0.714	0.835	SVM	PET	Nodal GTA metrics
Li et al. 2023[133]	98	49	49	44	7	5	42	0.878	0.898	0.857	0.917	SVM	PET	Global GTA metrics & Connection
Li et al. 2023[133]	98	49	49	46	6	3	43	0.908	0.939	0.878	0.957	SVM	PET	Nodal GTA metrics & Connection
Li et al. 2023[133]	98	49	49	38	7	11	42	0.816	0.776	0.857	0.888	SVM	PET	Nodal GTA metrics & Global metrics
Li et al. 2023[133]	98	49	49	46	5	3	44	0.918	0.939	0.899	0.957	SVM	PET	Nodal GTA metrics & Global GTA metrics & Connection
Jiji et al. 2023[138]	200	100	100	92	5	8	95	0.935	0.923	0.951	0.935	Adaboost	EEG/fMRI	EEG spatial & Bispectrum features & fMRI GTA metrics
Xiao et al. 2024[139]	35	18	17	16	2	2	15	0.863	0.863	0.864	0.926	SVM	rs-fMRI	Global & nodal GTA metrics (Testing set)
Xiao et al. 2024[139]	137	68	69	67	1	1	68	0.989	0.987	0.991	0.994	SVM	rs-fMRI	Global & nodal GTA metrics (Training set)
Lu et al. 2024[140]	53	34	19	32	3	2	16	0.868	0.947	0.853	0.916	SVM	PET	Nodal degree
Akguller et al. 2024[141]	3074	1537	1537	1298	132	239	1405	0.879	0.845	0.914	NA	CNN	rs-fMRI	Information-theoretic & GTA metrics (Using SMOTE)
Akguller et al. 2024[141]	3074	1537	1537	1271	173	266	1364	0.857	0.827	0.888	NA	RNN	rs-fMRI	Information-theoretic & GTA metrics (Using SMOTE)
Akguller et al. 2024[141]	3074	1537	1537	1083	218	454	1319	0.781	0.705	0.858	NA	LSTM	rs-fMRI	Information-theoretic & GTA metrics (Using SMOTE)

Note: The table summarizes 43 tables from 10 studies. Abbreviations: PD, Parkinson's Disease; HC, Healthy Controls; TP, true positive; TN, true negative; FP, false positive; FN, false negative; SE, sensitivity; SP, specificity; AUC, area under the receiver operating characteristic curve; rs-fMRI, resting-state functional magnetic resonance imaging; DKI, diffusion kurtosis imaging; dMRI, diffusion MRI; DTI, diffusion tensor imaging; sMRI, structural magnetic resonance imaging; PET, positron emission tomography; EEG, electroencephalography; MLDA, maximum uncertainty linear discriminate analysis; ROC, Receiver Operating Characteristic Curve analysis; SVM, support vector machine; CNN, convolutional neural networks; RNN, recurrent neural network; LSTM, long short-term memory; RF, random forest; TPD, tremor-dominant PD; NTPD, non-tremor-dominant PD; CSD, constrained spherical deconvolution; MSMT-CSD; multi-shell multi-tissue CSD; SSST-CSD; single-shell single-tissue CSD; mPFC, medial prefrontal cortex; SN, salience network; FPN, fronto-parietal network; SMN, somatomotor network; PD FOG+, PD with freezing of gait; PD FOG-, PD without freezing of gait; R_ITG: right inferior temporal gyrus; L_MFG, left middle frontal gyrus; SMOTE, synthetic minority over-sampling technique; GTA, graph theory analysis; *AUC is estimated as half the sum of SE and SP for studies without reported AUC; NA, not available.

Table S23. Moderator analysis results for DOR in diagnostic meta-analysis

Term	Estimate	SE	Z	P	95% CI
Algorithm (AI algorithm)	1.340	1.224	1.095	0.274	[-0.351, 3.873]
Imaging technique (Functional imaging)	1.934	0.997	1.940	0.052	[-0.020, 3.889]
Feature selection (GTA Plus)	1.997	0.768	4.700	0.009*	[0.492, 3.502]
Threshold (non-proportion)	0.307	1.070	0.286	0.775	[-1.791, 2.404]

Abbreviations: CI, confidence interval; GTA, graph theory analysis; AI, artificial intelligence; GTA Plus, both GTA metrics and other imaging metrics used as classification features; The reference groups for the four moderator analyses are: without AI algorithms, structural imaging, using only GTA metrics as input features, and proportion threshold; * $P < 0.05$.

Figure S23. Forest plot for diagnostic meta-analysis (10 studies with 43 contingency tables)

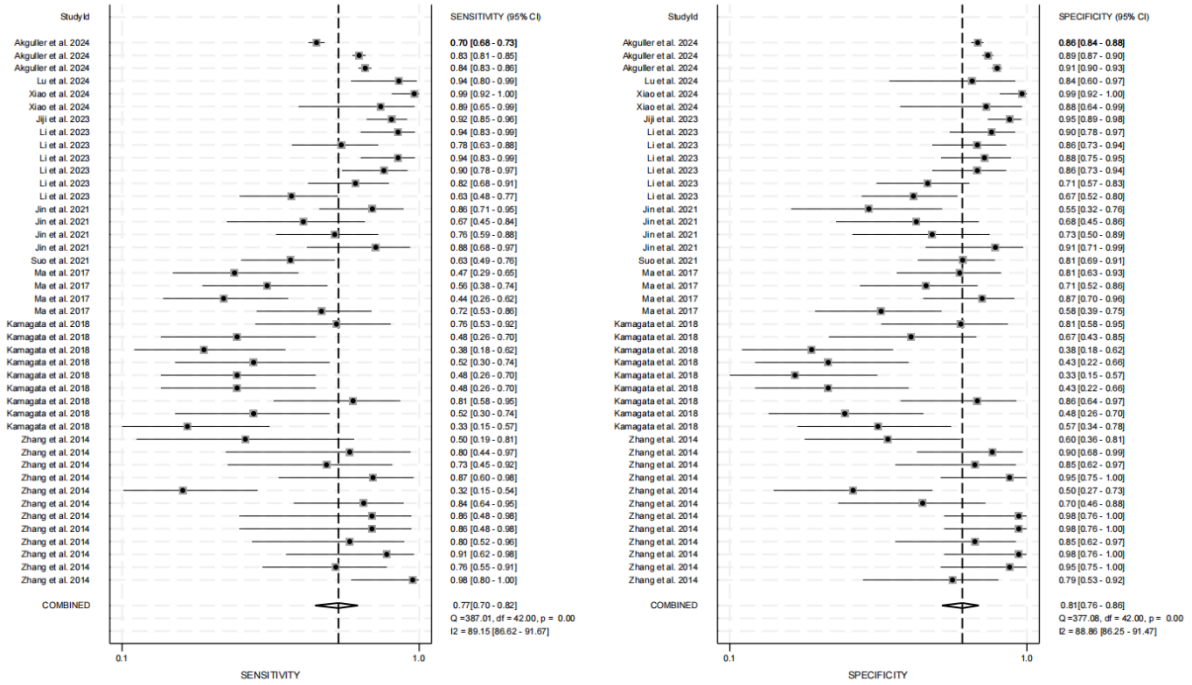

Forest plot presenting sensitivity and specificity results. Each study is represented by a square (point estimate) with a horizontal line indicating its 95% confidence interval. Individual study sensitivity (left panel) and specificity (right panel) are displayed. The diamond at the bottom represents the pooled sensitivity/specificity and its 95% confidence interval. Statistical measures, including combined sensitivity/specificity, Q-statistic, p-value, and I^2, are provided to assess heterogeneity.

Figure S24. Publication bias for diagnostic meta-analysis (10 studies with 43 contingency tables)

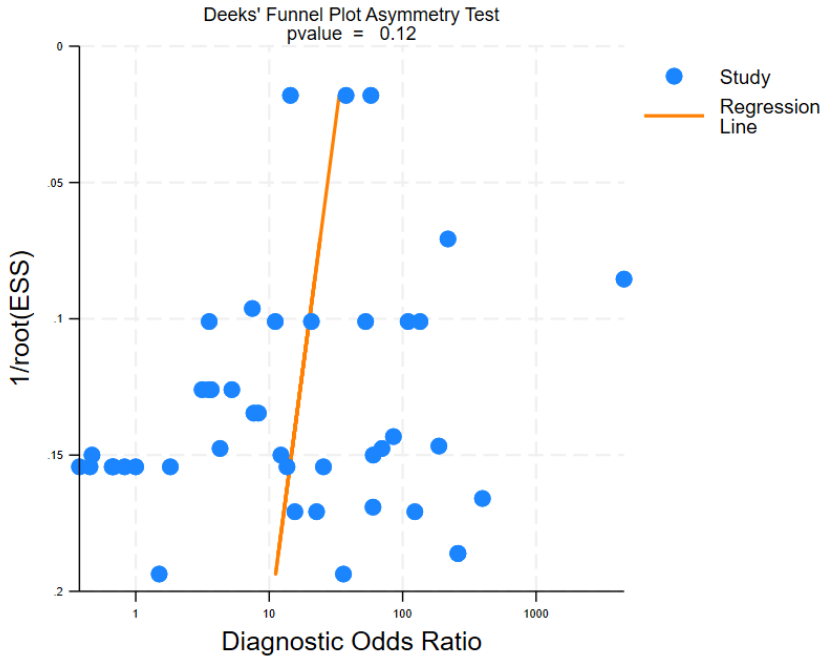

Funnel plot illustrating publication bias for diagnostic meta-analysis using Deeks' test. Each blue dot corresponds to an individual study included in the analysis. The orange regression line assesses asymmetry in the funnel plot.

Figure S25. Forest plot for subgroup analysis of algorithm

a. AI algorithm group (8 studies with 35 contingency tables)

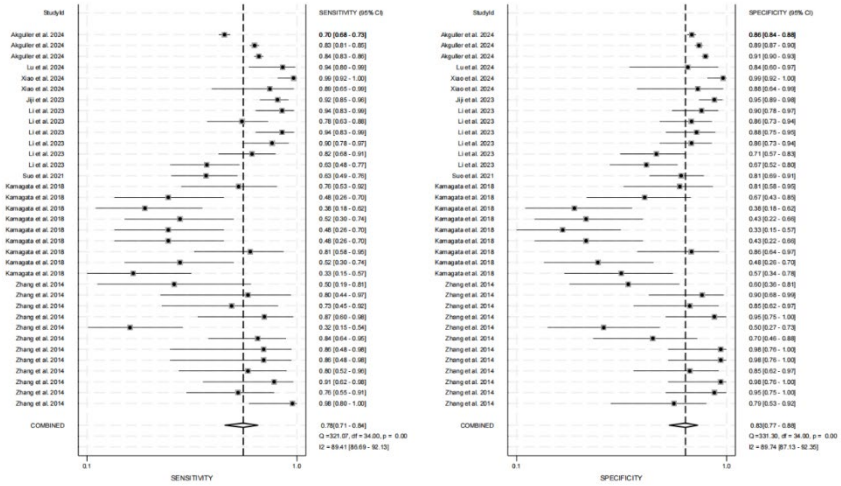

b. Without AI algorithm group (2 studies with 8 contingency tables)

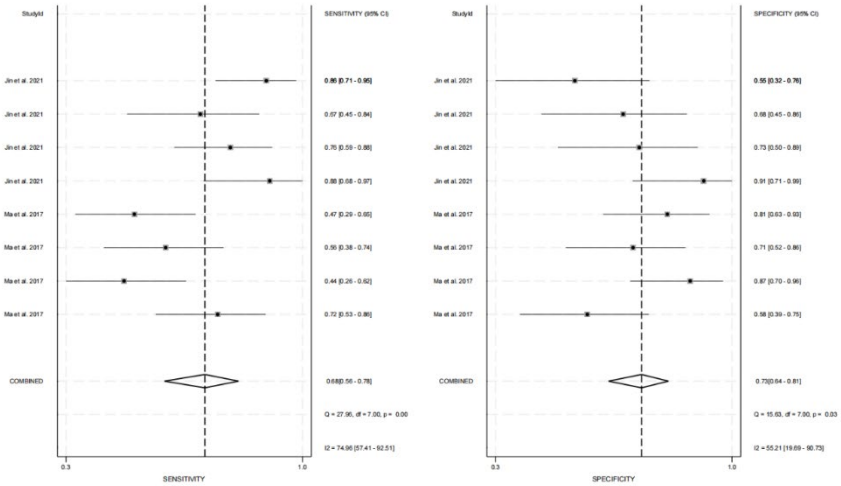

Forest plot presenting sensitivity and specificity results. Each study is represented by a square (point estimate) with a horizontal line indicating its 95% confidence interval. Individual study sensitivity (left panel) and specificity (right panel) are displayed. The diamond at the bottom represents the pooled sensitivity/specificity and its 95% confidence interval. Statistical measures, including combined sensitivity/specificity, Q-statistic, p-value, and I^2, are provided to assess heterogeneity.

Figure S26. Forest plot for subgroup analysis of imaging techniques

a. Functional imaging group (8 studies with 33 contingency tables)

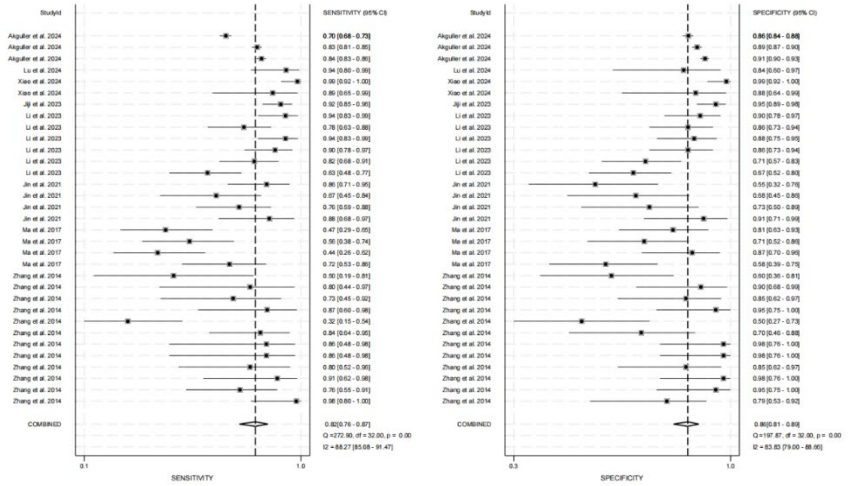

b. Structural imaging group (2 studies with 10 contingency tables)

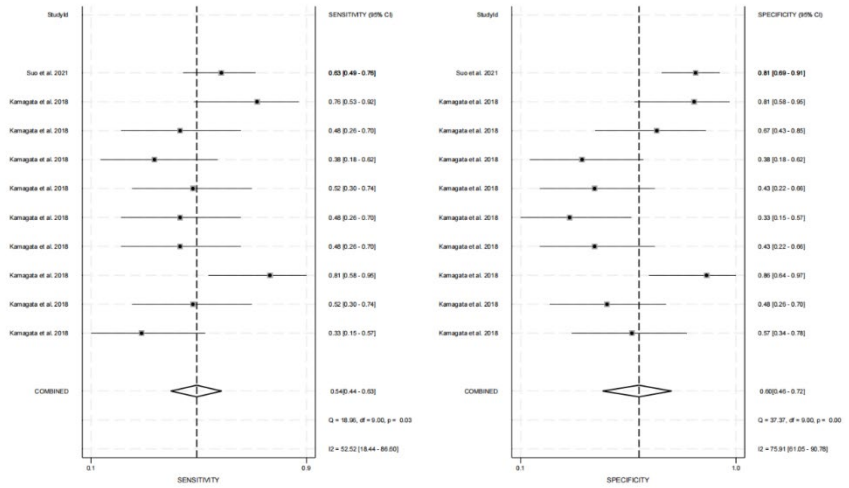

Forest plot presenting sensitivity and specificity results. Each study is represented by a square (point estimate) with a horizontal line indicating its 95% confidence interval. Individual study sensitivity (left panel) and specificity (right panel) are displayed. The diamond at the bottom represents the pooled sensitivity/specificity and its 95% confidence interval. Statistical measures, including combined sensitivity/specificity, Q-statistic, p-value, and I^2, are provided to assess heterogeneity.

Figure S27. Forest plot for subgroup analysis of feature selection

a. GTA Only group (8 studies with 36 contingency tables)

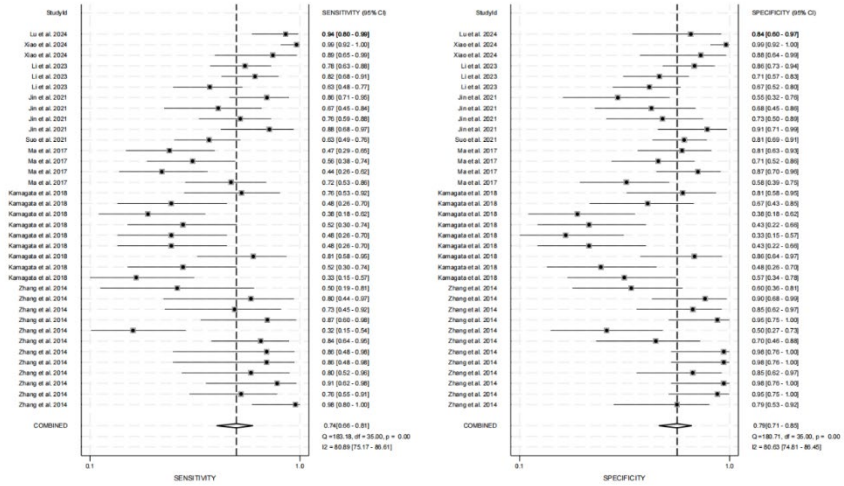

b. GTA Plus group (3 studies with 7 contingency tables)

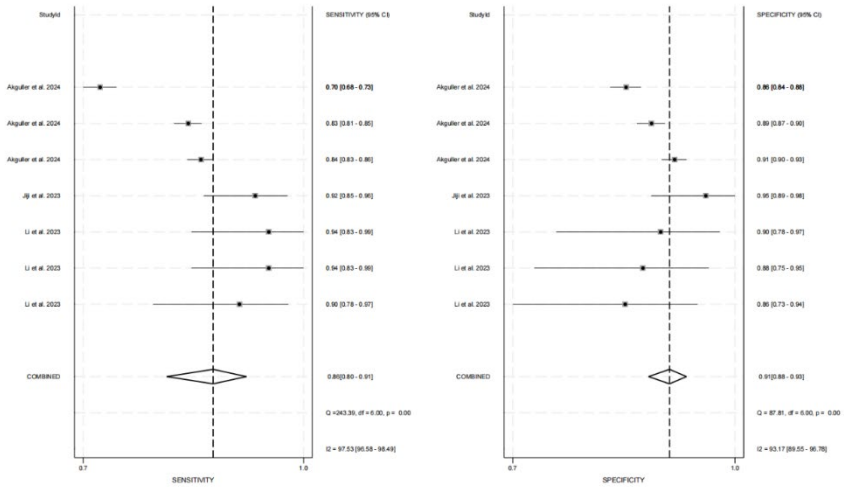

Forest plot presenting sensitivity and specificity results. Each study is represented by a square (point estimate) with a horizontal line indicating its 95% confidence interval. Individual study sensitivity (left panel) and specificity (right panel) are displayed. The diamond at the bottom represents the pooled sensitivity/specificity and its 95% confidence interval. Statistical measures, including combined sensitivity/specificity, Q-statistic, p-value, and I^2, are provided to assess heterogeneity.

Figure S28. Forest plot for subgroup analysis of threshold

a. Non-proportion group (4 studies with 20 contingency tables)

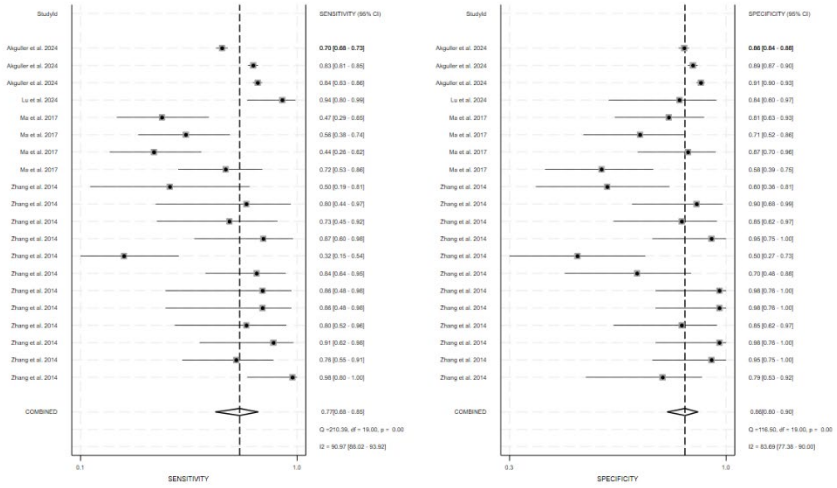

b. Proportion group (5 studies with 22 contingency tables)

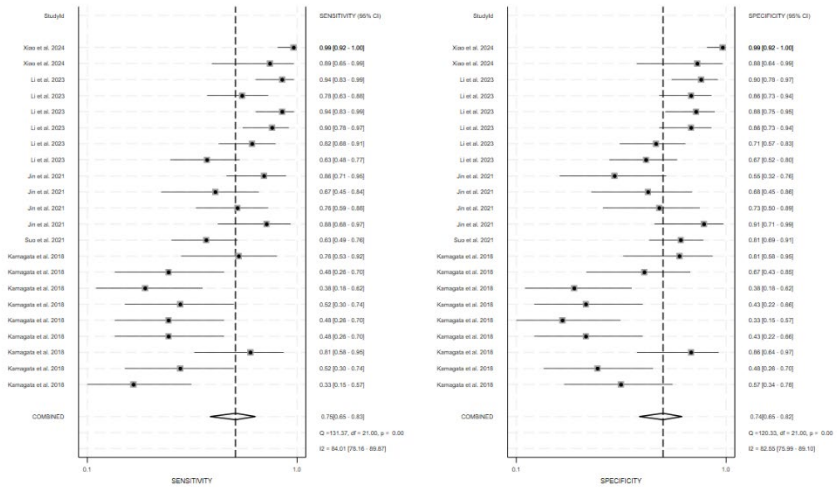

Forest plot presenting sensitivity and specificity results. Each study is represented by a square (point estimate) with a horizontal line indicating its 95% confidence interval. Individual study sensitivity (left panel) and specificity (right panel) are displayed. The diamond at the bottom represents the pooled sensitivity/specificity and its 95% confidence interval. Statistical measures, including combined sensitivity/specificity, Q-statistic, p-value, and I^2, are provided to assess heterogeneity.

Figure S29. SROC curves for subgroup analysis of algorithm

a. AI algorithm group (8 studies with 35 contingency tables)

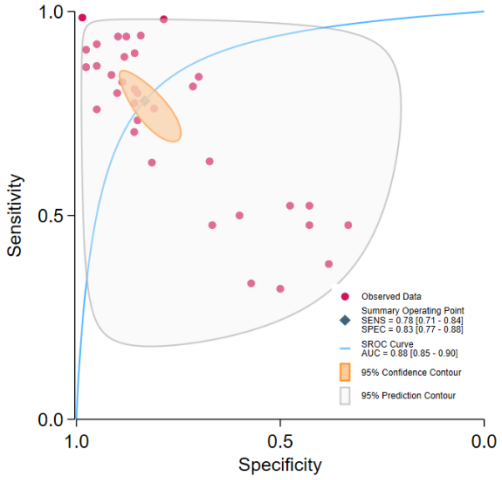

b. Without AI algorithm group (2 studies with 8 contingency tables)

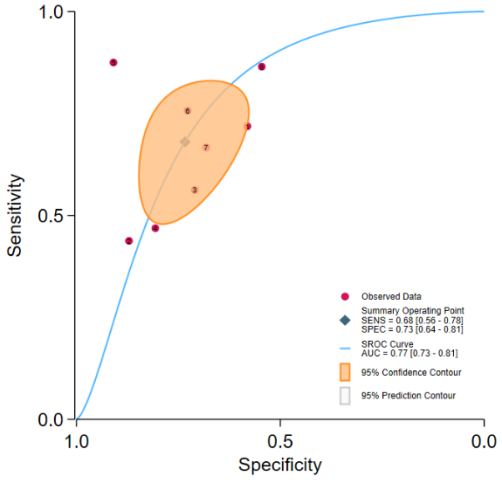

SROC curves. Red dots represent data points from contingency tables. The blue line shows the SROC curve, with the blue diamond marking the Summary Operating Point (pooled sensitivity and specificity). The gray area represents the 95% Prediction Contour, and the orange area represents the 95% Confidence Contour. Abbreviations: SROC, summary receiver operating characteristic; SENS, summary sensitivity; SPEC, summary specificity; AUC, area under the curve.

Figure S30. SROC curves for subgroup analysis of imaging techniques

a. Functional imaging group (8 studies with 33 contingency tables)

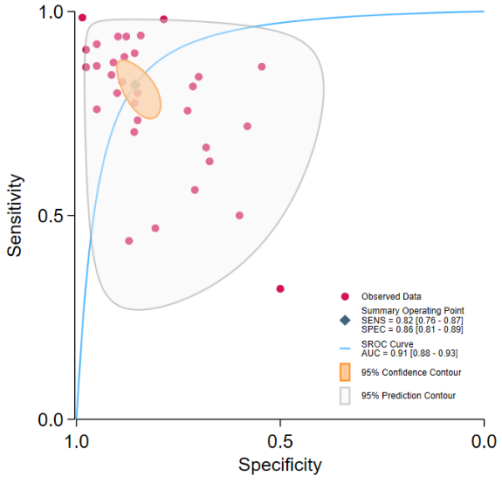

b. Structural imaging group (2 studies with 10 contingency tables)

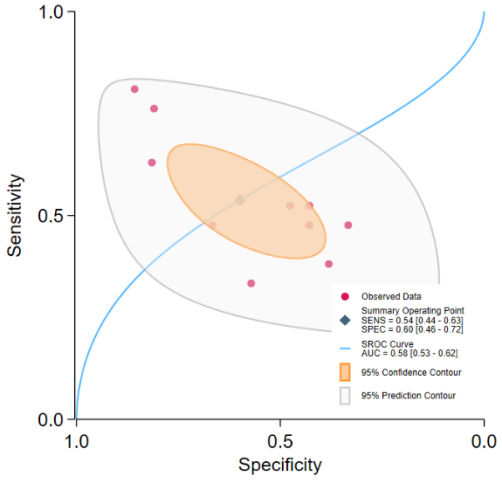

SROC curves. Red dots represent data points from contingency tables. The blue line shows the SROC curve, with the blue diamond marking the Summary Operating Point (pooled sensitivity and specificity). The gray area represents the 95% Prediction Contour, and the orange area represents the 95% Confidence Contour. Abbreviations: SROC, summary receiver operating characteristic; SENS, summary sensitivity; SPEC, summary specificity; AUC, area under the curve.

Figure S31. SROC curves for subgroup analysis of feature selection

a. GTA Only group (8 studies with 36 contingency tables)

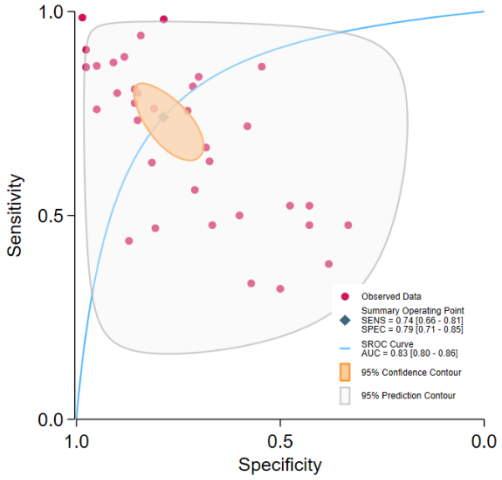

a. GTA Plus group (3 studies with 7 contingency tables)

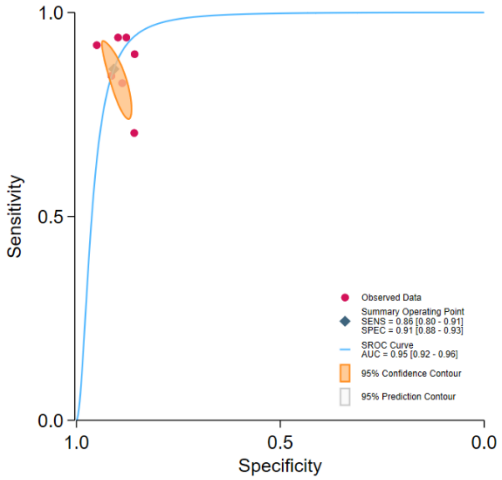

SROC curves. Red dots represent data points from contingency tables. The blue line shows the SROC curve, with the blue diamond marking the Summary Operating Point (pooled sensitivity and specificity). The gray area represents the 95% Prediction Contour, and the orange area represents the 95% Confidence Contour. Abbreviations: SROC, summary receiver operating characteristic; SENS, summary sensitivity; SPEC, summary specificity; AUC, area under the curve.

Figure S32. SROC curves for subgroup analysis of threshold

a. Non-proportion group (4 studies with 20 contingency tables)

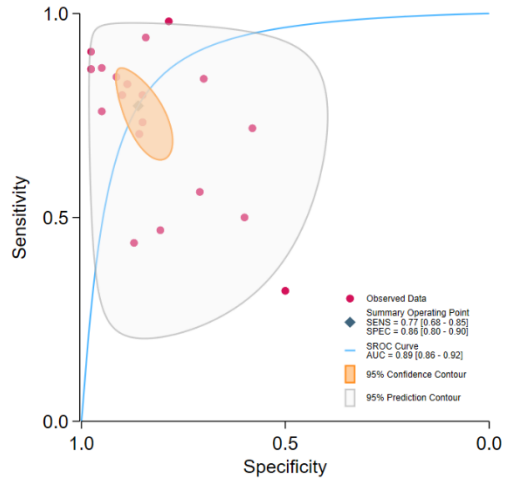

b. Proportion group (5 studies with 22 contingency tables)

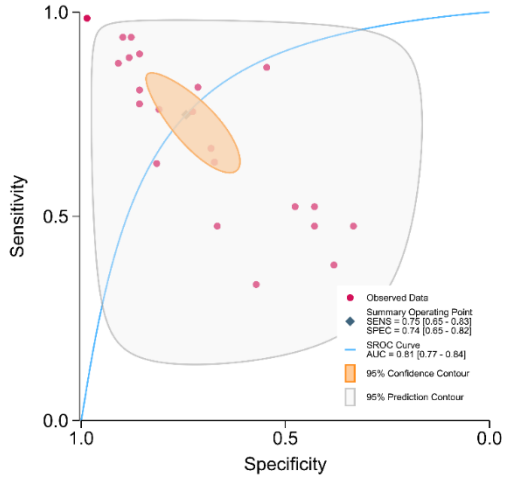

SROC curves. Red dots represent data points from contingency tables. The blue line shows the SROC curve, with the blue diamond marking the Summary Operating Point (pooled sensitivity and specificity). The gray area represents the 95% Prediction Contour, and the orange area represents the 95% Confidence Contour. Abbreviations: SROC, summary receiver operating characteristic; SENS, summary sensitivity; SPEC, summary specificity; AUC, area under the curve.

Figure S33. Publication bias for subgroup analysis

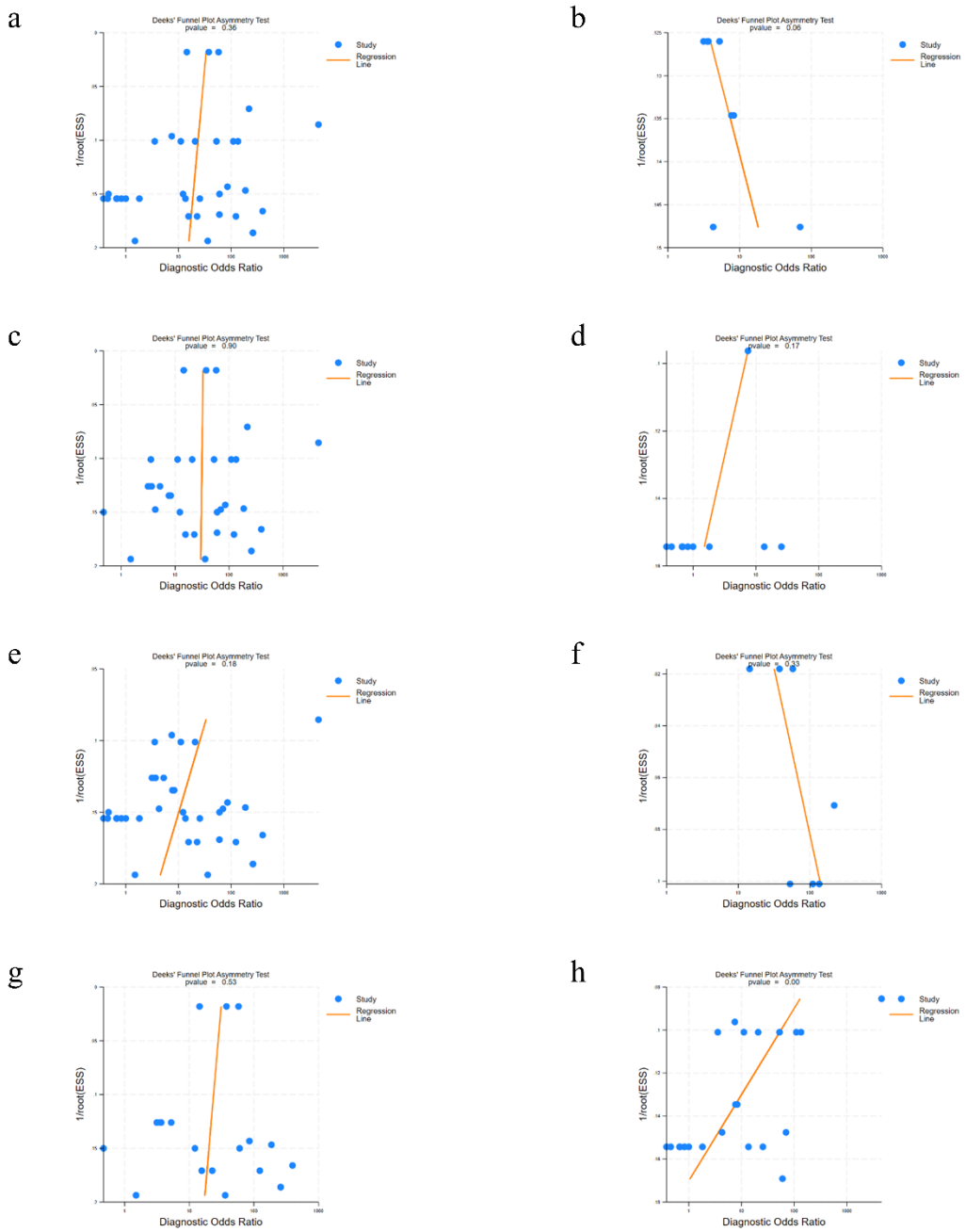

Funnel plot illustrating publication bias for subgroup diagnostic meta-analysis using Deeks' test. (a) AI algorithm subgroup, (b) without AI algorithm subgroup, (c) functional imaging subgroup, (d) structural imaging subgroup, (e) GTA Only subgroup, (f) GTA Plus subgroup, (g) non-proportion subgroup, (h) proportion subgroup. Each blue dot corresponds to an individual study included in the analysis. The orange regression line assesses asymmetry in the funnel plot.

Figure S34. Forest plot for exploratory analysis of diagnostic performance

a. Highest performing group (10 studies with 10 contingency tables)

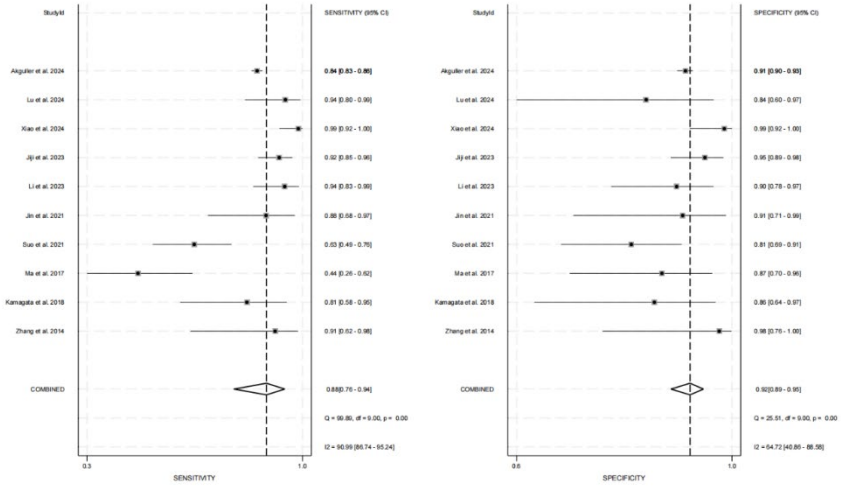

b. Lowest performing group (10 studies with 10 contingency tables)

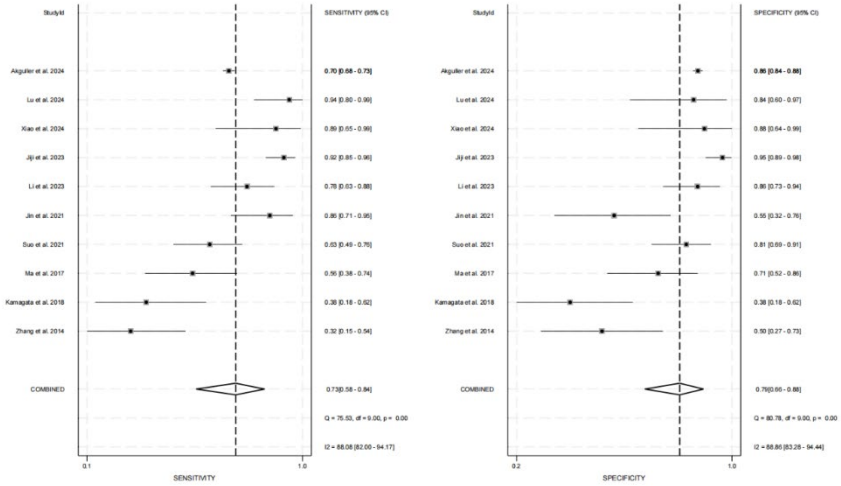

Forest plot presenting sensitivity and specificity results. Each study is represented by a square (point estimate) with a horizontal line indicating its 95% confidence interval. Individual study sensitivity (left panel) and specificity (right panel) are displayed. The diamond at the bottom represents the pooled sensitivity/specificity and its 95% confidence interval. Statistical measures, including combined sensitivity/specificity, Q-statistic, p-value, and I^2, are provided to assess heterogeneity.

Figure S35. SROC curves for exploratory analysis of diagnostic performance

a. Highest performing group (10 studies with 10 contingency tables)

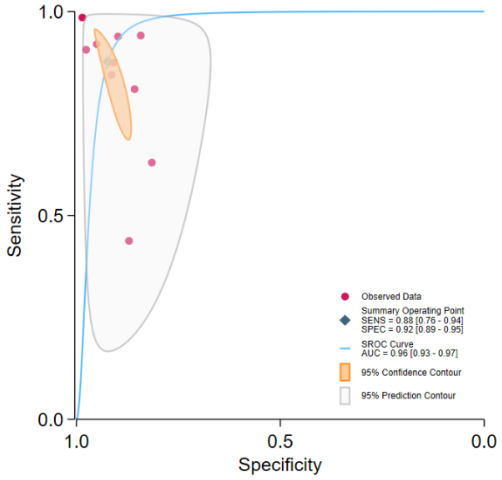

b. Lowest performing group (10 studies with 10 contingency tables)

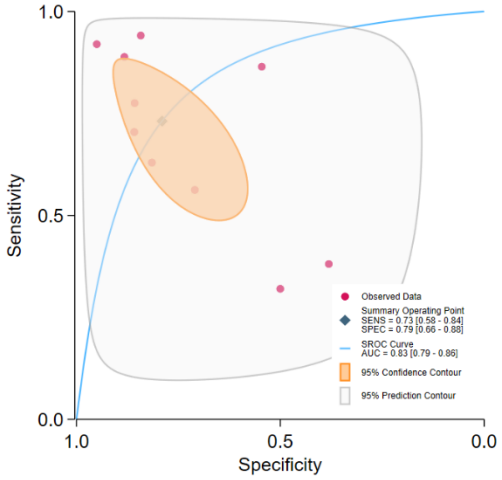

SROC curves. Red dots represent data points from contingency tables. The blue line shows the SROC curve, with the blue diamond marking the Summary Operating Point (pooled sensitivity and specificity). The gray area represents the 95% Prediction Contour, and the orange area represents the 95% Confidence Contour. Abbreviations: SROC, summary receiver operating characteristic; SENS, summary sensitivity; SPEC, summary specificity; AUC, area under the curve.

Figure S36. Publication bias for exploratory analysis

a. Highest performance (10 studies with 10 contingency tables)

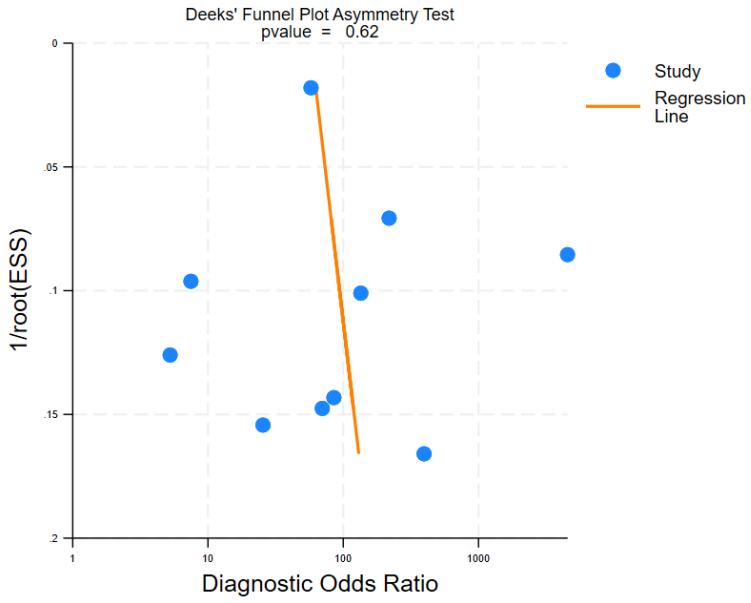

b. Lowest performance (10 studies with 10 contingency tables)

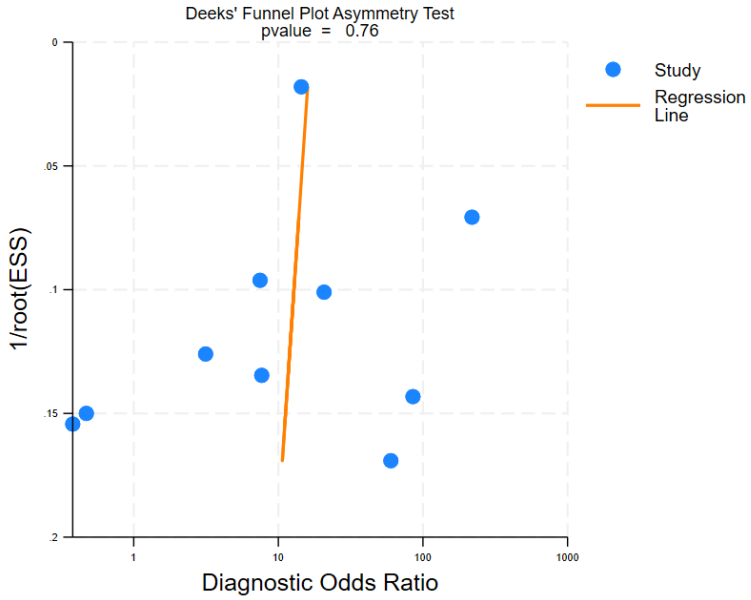

Funnel plot illustrating publication bias for exploratory diagnostic meta-analysis using Deeks' test. Each blue dot corresponds to an individual study included in the analysis. The orange regression line assesses asymmetry in the funnel plot.

Table S24. Tabular presentation of QUADAS-AI

Study	Subject selection						Index Test		Reference standard		Flow and Timing	
	Q1	Q2	Q3	Q4	Q5	Risk	Q6	Risk	Q7	Risk	Q8	Risk
Zhang et al. 2014[96]	YES	NO	YES	YES	YES	High	NO	High	YES	Low	YES	Low
Kamagata et al. 2018[18]	YES	NO	YES	YES	YES	High	NO	High	YES	Low	YES	Low
Ma et al. 2017[71]	YES	NO	YES	YES	YES	High	NO	High	YES	Low	YES	Low
Suo et al. 2021[104]	YES	NO	YES	YES	YES	High	NO	High	YES	Low	YES	Low
Jin et al. 2021[137]	YES	NO	YES	YES	YES	High	NO	High	YES	Low	YES	Low
Li et al. 2023[133]	YES	NO	YES	YES	YES	High	NO	High	YES	Low	YES	Low
Jiji et al. 2023[138]	NO	YES	NO	YES	NO	High	NO	High	NO	High	NO	High
Xiao et al. 2024[139]	YES	NO	YES	YES	YES	High	YES	Low	YES	Low	YES	Low
Lu et al. 2024[140]	YES	NO	YES	YES	YES	High	NO	High	YES	Low	YES	Low
Akguller et al. 2024[141]	YES	YES	YES	YES	YES	Low	NO	High	YES	Low	YES	Low

Table S25. Search strategy

PubMed		
1	"Parkinson Disease"[MeSH]	89,478
2	("parkinson's disease"[Title/Abstract] OR "parkinson"[Title/Abstract])	145,599
3	#1 OR #2	157,891
4	("graph theor*"[Title/Abstract] OR "graph metric*"[Title/Abstract] OR "graph analys*"[Title/Abstract] OR "brain network*"[Title/Abstract] OR "network analys*"[Title/Abstract] OR "connectom*"[Title/Abstract] OR "topolog*"[Title/Abstract] OR "segregation"[Title/Abstract] OR "integration"[Title/Abstract] OR "small worldness"[Title/Abstract] OR "clustering coefficient"[Title/Abstract] OR "characteristic path length"[Title/Abstract] OR "global path length"[Title/Abstract] OR "shortest path length"[Title/Abstract] OR "global efficienc*"[Title/Abstract] OR "local efficienc*"[Title/Abstract] OR "betweenness centrality"[Title/Abstract] OR "modularity"[Title/Abstract] OR "assortativity" [Title/Abstract])	486,428
5	#3 AND #4	3,029
Web of Science		
1	TI=("parkinson's disease" or "parkinson") and Preprint Citation Index (Exclude – Database)	151,009
2	AB=("parkinson's disease" or "parkinson") and Preprint Citation Index (Exclude – Database)	220,271
3	#1 OR #2 and Preprint Citation Index (Exclude – Database)	278,503
4	TI=("graph theor*" or "graph metric*" or "graph analys*" or "brain network*" or "network analys*" or "connectom*" or "topolog*" or "segregation" or "integration" or "small worldness" or "clustering coefficient" or "characteristic path length" or "global path length" or "shortest path length" or "global efficienc*" or "local efficienc*" or "betweenness centrality" or "modularity" or "assortativity") and Preprint Citation Index (Exclude – Database)	627,023
5	AB=("graph theor*" or "graph metric*" or "graph analys*" or "brain network*" or "network analys*" or "connectom*" or "topolog*" or "segregation" or "integration" or "small worldness" or "clustering coefficient" or "characteristic path length" or "global path length" or "shortest path length" or "global efficienc*" or "local efficienc*" or "betweenness centrality" or "modularity" or "assortativity") and Preprint Citation Index (Exclude – Database)	2,645,873
6	#4 OR #5 and Preprint Citation Index (Exclude – Database)	2,858,600
7	#3 AND #6 and Preprint Citation Index (Exclude – Database)	4,631
Embase		
1	exp Parkinson Disease/	211431
2	("parkinson's disease" or "parkinson").ab,ti.	193870
3	("graph theor*" or "graph metric*" or "graph analys*" or "brain network*" or "network analys*" or "connectom*" or "topolog*" or "segregation" or "integration" or "small worldness" or "clustering coefficient" or "characteristic path length" or "global path length" or "shortest path length" or "global efficienc*" or "local efficienc*" or "betweenness centrality" or "modularity" or "assortativity").ab,ti.	528231
4	1 or 2	244672
5	3 and 4	4598

Table S26. Description of quality assessment based on QUADAS-AI domains

Domain	Subject selection	Index text (AI)	Reference standard	Work-flow
Concern	Signaling question: Q1: Accurately characterize the source, size and quality of input data alongside clear patient eligibility criteria? Q2: Was it derived from open-source datasets? Q3: Present the rationale and breakdown of its training, validation and test sets? Q4: Whether to perform image preprocessing? Q5: Provide the scanner model information used to acquire imaging data?	Signaling question: Q6: Was External verification performed?	Signaling question: Q7: Was the reference standard likely to correctly classify the target condition?	Signaling question: Q8: Was the time between the index test and the reference standard reasonable?
Concerns regarding risk of bias	Risk of bias is judged as “low”, “high”, or “unclear”. If all signaling questions for a domain are answered “yes” then risk of bias can be judged “low”. If any signaling question is answered “no” this flags the potential for bias. Review authors then need to have in-depth discussions to judge risk of bias. The “unclear” category should be used only when insufficient data are reported to permit a judgment.			

References

1 Abbasi, N. *et al.* Relationship between cerebrospinal fluid biomarkers and structural brain network properties in Parkinson's disease. *Mov Disord* **33**, 431-439, doi:10.1002/mds.27284 (2018).

2 Abbasi, N. *et al.* Predicting severity and prognosis in Parkinson's disease from brain microstructure and connectivity. *Neuroimage Clin* **25**, 102111, doi:10.1016/j.nicl.2019.102111 (2020).

3 Bergamino, M. *et al.* Structural connectivity and brain network analyses in Parkinson's disease: A cross-sectional and longitudinal study. *Front Neurol* **14**, 1137780, doi:10.3389/fneur.2023.1137780 (2023).

4 Chen, A. *et al.* Disrupted Brain Structural Network Connection in de novo Parkinson's Disease With Rapid Eye Movement Sleep Behavior Disorder. *Front Hum Neurosci* **16**, 902614, doi:10.3389/fnhum.2022.902614 (2022).

5 Chen, Z. *et al.* Age and sex differentially shape brain networks in Parkinson's disease. *CNS Neurosci Ther* **29**, 1907-1922, doi:10.1111/cns.14149 (2023).

6 Chung, S. J. *et al.* Association Between White Matter Connectivity and Early Dementia in Patients With Parkinson Disease. *Neurology* **98**, e1846-e1856, doi:10.1212/wnl.0000000000200152 (2022).

7 Colon-Perez, L. M. *et al.* Cognition and connectomes in nondementia idiopathic Parkinson's disease. *Netw Neurosci* **2**, 106-124, doi:10.1162/NETN_a_00027 (2018).

8 Du, J. *et al.* Levodopa responsiveness and white matter alterations in Parkinson's disease: A DTI-based study and brain network analysis: A cross-sectional study. *Brain Behav* **12**, e2825, doi:10.1002/brb3.2825 (2022).

9 Frigerio, I. *et al.* Pathologic Substrates of Structural Brain Network Resilience and Topology in Parkinson Disease Decedents. *Neurology* **103**, e209678, doi:10.1212/wnl.0000000000209678 (2024).

10 Galantucci, S. *et al.* Structural Brain Connectome and Cognitive Impairment in Parkinson Disease. *Radiology* **283**, 515-525, doi:10.1148/radiol.2016160274 (2017).

11 Gan, C. *et al.* Aberrant brain topological organization and granger causality connectivity in Parkinson's disease with impulse control disorders. *Front Aging Neurosci* **16**, 1364402, doi:10.3389/fnagi.2024.1364402 (2024).

12 Ge, S. *et al.* Topological alteration of the brain structural network in Parkinson's disease with apathy. *Brain Res Bull* **208**, 110899, doi:10.1016/j.brainresbull.2024.110899 (2024).

13 Gou, L. *et al.* Structural Brain Network Alteration and its Correlation With Structural Impairments in Patients With Depression in de novo and Drug-Naïve Parkinson's Disease. *Front Neurol* **9**, 608, doi:10.3389/fneur.2018.00608 (2018).

14 Guan, X. *et al.* Iron-related nigral degeneration influences functional topology mediated by striatal dysfunction in Parkinson's disease. *Neurobiol Aging* **75**, 83-97, doi:10.1016/j.neurobiolaging.2018.11.013 (2019).

15 Hu, X. *et al.* Topological changes in white matter connectivity network in patients with Parkinson's disease and depression. *Brain Imaging Behav* **14**, 2559-2568, doi:10.1007/s11682-019-00208-2 (2020).

16 Inguanzo, A. *et al.* Impaired Structural Connectivity in Parkinson's Disease Patients with Mild Cognitive Impairment: A Study Based on Probabilistic Tractography. *Brain Connect* **11**, 380-392, doi:10.1089/brain.2020.0939 (2021).

17 Jin, C. *et al.* Structural Brain Network Abnormalities in Parkinson's Disease With Freezing of Gait. *Front Aging Neurosci* **14**, 944925, doi:10.3389/fnagi.2022.944925 (2022).

18 Kamagata, K. *et al.* Connectome analysis with diffusion MRI in idiopathic Parkinson's disease: Evaluation using multi-shell, multi-tissue, constrained spherical deconvolution. *Neuroimage Clin* **17**, 518-529, doi:10.1016/j.nicl.2017.11.007 (2018).

19 Koirala, N. *et al.* Alterations in White Matter Network and Microstructural Integrity Differentiate Parkinson's Disease Patients and Healthy Subjects. *Front Aging Neurosci* **11**, 191, doi:10.3389/fnagi.2019.00191 (2019).

20 Kok, J. G. *et al.* Structural Network Analysis Using Diffusion MRI Tractography in Parkinson's Disease and Correlations With Motor Impairment. *Front Neurol* **11**, 841, doi:10.3389/fneur.2020.00841 (2020).

21 Li, C. *et al.* Impaired topological architecture of brain structural networks in idiopathic Parkinson's disease: a DTI study. *Brain Imaging Behav* **11**, 113-128, doi:10.1007/s11682-015-9501-6 (2017).

22 Li, S. *et al.* Increased prevalence of vertebrobasilar dolichoectasia in Parkinson's disease and its effect on white matter microstructure and network. *Neuroreport* **35**, 627-637, doi:10.1097/wnr.0000000000002046 (2024).

23 Li, Z. *et al.* Reorganization of structural brain networks in Parkinson's disease with postural instability/gait difficulty. *Neurosci Lett* **827**, 137736, doi:10.1016/j.neulet.2024.137736 (2024).

24 Liu, H. *et al.* Corpus callosum and cerebellum participate in semantic dysfunction of Parkinson's disease: a diffusion tensor imaging-based cross-sectional study. *Neuroreport* **35**, 366-373, doi:10.1097/wnr.0000000000002015 (2024).

25 Mishra, V. R. *et al.* Unique white matter structural connectivity in early-stage drug-naive Parkinson disease. *Neurology* **94**, e774-e784, doi:10.1212/wnl.0000000000008867 (2020).

26 Nigro, S. *et al.* Characterizing structural neural networks in de novo Parkinson disease patients using diffusion tensor imaging. *Hum Brain Mapp* **37**, 4500-4510, doi:10.1002/hbm.23324 (2016).

27 Ren, Q. *et al.* Thalamic-limbic circuit dysfunction and white matter topological alteration in Parkinson's disease are correlated with gait disturbance. *Front Aging Neurosci* **16**, 1426754, doi:10.3389/fnagi.2024.1426754 (2024).

28 Shah, A. *et al.* Altered Brain Wiring in Parkinson's Disease: A Structural Connectome-Based Analysis. *Brain Connect* **7**, 347-356, doi:10.1089/brain.2017.0506 (2017).

29 Shang, S. *et al.* Optimization of structural connectomes and scaled patterns of structural-functional decoupling in Parkinson's disease. *Neuroimage* **284**, 120450, doi:10.1016/j.neuroimage.2023.120450 (2023).

30 Vriend, C., van den Heuvel, O. A., Berendse, H. W., van der Werf, Y. D. & Douw, L. Global and Subnetwork Changes of the Structural Connectome in de novo Parkinson's Disease. *Neuroscience* **386**, 295-308, doi:10.1016/j.neuroscience.2018.06.050 (2018).

31 Wang, L. *et al.* Altered brain structural topological properties in Parkinson's disease with levodopa-induced dyskinesias. *Parkinsonism Relat Disord* **67**, 36-41, doi:10.1016/j.parkreldis.2019.09.022 (2019).

32 Wang, W. *et al.* Changes of brain structural network connection in Parkinson's disease patients with mild cognitive dysfunction: a study based on diffusion tensor imaging. *J Neurol* **267**, 933-943, doi:10.1007/s00415-019-09645-x (2020).

33 Wang, L. *et al.* Impaired structural and reserved functional topological organizations of brain networks in Parkinson's disease with freezing of gait. *Quant Imaging Med Surg* **13**, 66-79, doi:10.21037/qims-22-351 (2023).

34 Wen, M. C. *et al.* Structural connectome alterations in prodromal and de novo Parkinson's disease patients. *Parkinsonism Relat Disord* **45**, 21-27, doi:10.1016/j.parkreldis.2017.09.019 (2017).

35 Wen, M. C. *et al.* Microstructural network alterations of olfactory dysfunction in newly diagnosed Parkinson's disease. *Sci Rep* **7**, 12559, doi:10.1038/s41598-017-12947-7 (2017).

36 Wen, M. C. *et al.* Differential White Matter Regional Alterations in Motor Subtypes of Early Drug-Naive Parkinson's Disease Patients. *Neurorehabil Neural Repair* **32**, 129-141, doi:10.1177/1545968317753075 (2018).

37 Wen, M. C. *et al.* Apathy is associated with white matter network disruption and specific cognitive deficits in Parkinson's disease. *Psychol Med* **52**, 264-273, doi:10.1017/s0033291720001907 (2022).

38 Zarkali, A. *et al.* Differences in network controllability and regional gene expression underlie hallucinations in Parkinson's disease. *Brain* **143**, 3435-3448, doi:10.1093/brain/awaa270 (2020).

39 Zhang, X. *et al.* Topological patterns of motor networks in Parkinson's disease with different sides of onset: A resting-state-informed structural connectome study. *Front Aging Neurosci* **14**, 1041744, doi:10.3389/fnagi.2022.1041744 (2022).

40 Zhong, Y. *et al.* Structural changes in early-stage Parkinson's disease with resting tremor at node, edge and network level. *Brain Res Bull* **220**, 111169, doi:10.1016/j.brainresbull.2024.111169 (2025).

41 Zhu, S. *et al.* Application of diffusional kurtosis imaging for insights into structurally aberrant topology in Parkinson's disease. *Acta Radiol* **65**, 233-240, doi:10.1177/02841851231216039 (2024).

42 Albano, L. *et al.* Functional connectivity in Parkinson's disease candidates for deep brain stimulation. *NPJ Parkinsons Dis* **8**, 4, doi:10.1038/s41531-021-00268-6 (2022).

43 Baagil, H. *et al.* Neural correlates of impulse control behaviors in Parkinson's disease: Analysis of multimodal imaging data. *Neuroimage Clin* **37**, 103315, doi:10.1016/j.nicl.2023.103315 (2023).

44 Baggio, H. C. *et al.* Functional brain networks and cognitive deficits in Parkinson's disease. *Hum Brain Mapp* **35**, 4620-4634, doi:10.1002/hbm.22499 (2014).

45 Berman, B. D. *et al.* Levodopa modulates small-world architecture of functional brain networks in Parkinson's disease. *Mov Disord* **31**, 1676-1684, doi:10.1002/mds.26713 (2016).

46 Borchert, R. J. *et al.* Atomoxetine and citalopram alter brain network organization in Parkinson's disease. *Brain Commun* **1**, fcz013, doi:10.1093/braincomms/fcz013 (2019).

47 Chen, X., Liu, M., Wu, Z. & Cheng, H. Topological Abnormalities of Functional Brain Network in Early-Stage Parkinson's Disease Patients With Mild Cognitive Impairment. *Front Neurosci* **14**, 616872, doi:10.3389/fnins.2020.616872 (2020).

48 Chen, S., Wang, S. H., Bai, Y. Y., Zhang, J. W. & Zhang, H. J. Comparative Study on Topological Properties of the Whole-Brain Functional Connectome in Idiopathic Rapid Eye Movement Sleep Behavior Disorder and Parkinson's Disease Without RBD. *Front Aging Neurosci* **14**, 820479, doi:10.3389/fnagi.2022.820479 (2022).

49 Chen, B. *et al.* Functional connectome automatically differentiates multiple system atrophy (parkinsonian type) from idiopathic Parkinson's disease at early stages. *Hum Brain Mapp* **44**, 2176-2190, doi:10.1002/hbm.26201 (2023).

50 Dan, X. J. *et al.* Reorganization of intrinsic functional connectivity in early-stage Parkinson's disease patients with probable REM sleep behavior disorder. *NPJ Parkinsons Dis* **10**, 5, doi:10.1038/s41531-023-00617-7 (2024).

51 De Micco, R. *et al.* Functional Connectomics and Disease Progression in Drug-Naïve Parkinson's Disease Patients. *Mov Disord* **36**, 1603-1616, doi:10.1002/mds.28541 (2021).

52 Devignes, Q. *et al.* Resting-State Functional Connectivity in Frontostriatal and Posterior Cortical Subtypes in Parkinson's Disease-Mild Cognitive Impairment. *Mov Disord* **37**, 502-512, doi:10.1002/mds.28888 (2022).

53 Diao, Y. *et al.* Acoustic assessment in mandarin-speaking Parkinson's disease patients and disease progression monitoring and brain impairment within the speech subsystem. *NPJ Parkinsons Dis* **10**, 115, doi:10.1038/s41531-024-00720-3 (2024).

54 Engels, G. *et al.* Clinical pain and functional network topology in Parkinson's disease: a resting-state fMRI study. *J Neural Transm (Vienna)* **125**, 1449-1459, doi:10.1007/s00702-018-1916-y (2018).

55 Fang, J. *et al.* Impaired brain network architecture in newly diagnosed Parkinson's disease based on graph theoretical analysis. *Neurosci Lett* **657**, 151-158, doi:10.1016/j.neulet.2017.08.002 (2017).

56 Filippi, M. *et al.* Longitudinal brain connectivity changes and clinical evolution in Parkinson's disease. *Mol Psychiatry* **26**, 5429-5440, doi:10.1038/s41380-020-0770-0 (2021).

57 Geng, L. *et al.* Functional activity, functional connectivity and complex network biomarkers of progressive hyposmia Parkinson's disease with no cognitive impairment: evidences from resting-state fMRI study. *Front Aging Neurosci* **16**, 1455020, doi:10.3389/fnagi.2024.1455020 (2024).

58 Göttlich, M. *et al.* Altered resting state brain networks in Parkinson's disease. *PLoS One* **8**, e77336, doi:10.1371/journal.pone.0077336 (2013).

59 Holtbernd, F. *et al.* The functional brain connectome in isolated rapid eye movement sleep behavior disorder and Parkinson's disease. *Sleep Med* **117**, 184-191, doi:10.1016/j.sleep.2024.03.012 (2024).

60 Hou, Y. *et al.* Impaired topographic organization in cognitively unimpaired drug-naïve patients with rigidity-dominant Parkinson's disease. *Parkinsonism Relat Disord* **56**, 52-57, doi:10.1016/j.parkreldis.2018.06.021 (2018).

61 Hou, Y. *et al.* Impaired topographic organization in Parkinson's disease with mild cognitive impairment. *J Neurol Sci* **414**, 116861, doi:10.1016/j.jns.2020.116861 (2020).

62 Hou, Y. *et al.* Disrupted topological organization of resting-state functional brain networks in Parkinson's disease patients with glucocerebrosidase gene mutations. *Neuroradiology* **65**, 361-370, doi:10.1007/s00234-022-03067-9 (2023).

63 Klobušiaková, P., Mareček, R., Fousek, J., Výtvarová, E. & Rektorová, I. Connectivity Between Brain Networks Dynamically Reflects Cognitive Status of Parkinson's Disease: A Longitudinal Study. *J Alzheimers Dis* **67**, 971-984, doi:10.3233/jad-180834 (2019).

64 Li, J. *et al.* Altered Brain Functional Network in Parkinson Disease With Rapid Eye Movement Sleep Behavior Disorder. *Front Neurol* **11**, 563624, doi:10.3389/fneur.2020.563624 (2020).

65 Li, N. *et al.* Disrupted functional brain network topology in Parkinson's disease patients with freezing of gait. *Neurosci Lett* **759**, 135970, doi:10.1016/j.neulet.2021.135970 (2021).

66 Li, N. *et al.* Brain network topology and future development of freezing of gait in Parkinson's disease: a longitudinal study. *J Neurol* **269**, 2503-2512, doi:10.1007/s00415-021-10817-x (2022).

67 Li, X. *et al.* Stage-dependent differential impact of network communication on cognitive function across the continuum of cognitive decline in Parkinson's disease. *Neurobiol Dis* **199**, 106578, doi:10.1016/j.nbd.2024.106578 (2024).

68 Lin, S. J., Baumeister, T. R., Garg, S. & McKeown, M. J. Cognitive Profiles and Hub Vulnerability in Parkinson's Disease. *Front Neurol* **9**, 482, doi:10.3389/fneur.2018.00482 (2018).

69 Lopes, R. *et al.* Cognitive phenotypes in parkinson's disease differ in terms of brain-network organization and connectivity. *Hum Brain Mapp* **38**, 1604-1621, doi:10.1002/hbm.23474 (2017).

70 Luo, C. Y. *et al.* Functional connectome assessed using graph theory in drug-naive Parkinson's disease. *J Neurol* **262**, 1557-1567, doi:10.1007/s00415-015-7750-3 (2015).

71 Ma, Q. *et al.* Altered modular organization of intrinsic brain functional networks in patients with Parkinson's disease. *Brain Imaging Behav* **11**, 430-443, doi:10.1007/s11682-016-9524-7 (2017).

72 Oltra, J. *et al.* Disrupted functional connectivity in PD with probable RBD and its cognitive correlates. *Sci Rep* **11**, 24351, doi:10.1038/s41598-021-03751-5 (2021).

73 Prajapati, R. & Emerson, I. A. Global and regional connectivity analysis of resting-state function MRI brain images using graph theory in Parkinson's disease. *Int J Neurosci* **131**, 105-115, doi:10.1080/00207454.2020.1733559 (2021).

74 Qian, L. *et al.* Frequency specific brain networks in Parkinson's disease and comorbid depression. *Brain Imaging Behav* **11**, 224-239, doi:10.1007/s11682-016-9514-9 (2017).

75 Qiu, Y. H. *et al.* Alterations in intrinsic functional networks in Parkinson's disease patients with depression: A resting-state functional magnetic resonance imaging study. *CNS Neurosci Ther* **27**, 289-298, doi:10.1111/cns.13467 (2021).

76 Ruan, X. *et al.* Impaired Topographical Organization of Functional Brain Networks in Parkinson's Disease Patients With Freezing of Gait. *Front Aging Neurosci* **12**, 580564, doi:10.3389/fnagi.2020.580564 (2020).

77 Sako, W. *et al.* Differences in the intra-cerebellar connections and graph theoretical measures between Parkinson's disease and multiple system atrophy. *J Neurol Sci* **400**, 129-134, doi:10.1016/j.jns.2019.03.022 (2019).

78 Sang, L. *et al.* Alteration of Brain Functional Networks in Early-Stage Parkinson's Disease: A Resting-State fMRI Study. *PLoS One* **10**, e0141815, doi:10.1371/journal.pone.0141815 (2015).

79 Sarasso, E. *et al.* MRI biomarkers of freezing of gait development in Parkinson's disease. *NPJ Parkinsons Dis* **8**, 158, doi:10.1038/s41531-022-00426-4 (2022).

80 Schill, J. *et al.* Parkinson's disease speech production network as determined by graph-theoretical network analysis. *Netw Neurosci* **7**, 712-730, doi:10.1162/netn_a_00310 (2023).

81 Shang, S. *et al.* Topological disruption of high-order functional networks in cognitively preserved Parkinson's disease. *CNS Neurosci Ther* **29**, 566-576, doi:10.1111/cns.14037 (2023).

82 Siva, K., Ponnusamy, P. & Ramanathan, M. Disrupted Brain Network Measures in Parkinson's Disease Patients with Severe Hyposmia and Cognitively Normal Ability. *Brain Sci* **14**, doi:10.3390/brainsci14070685 (2024).

83 Skidmore, F. *et al.* Connectivity brain networks based on wavelet correlation analysis in Parkinson fMRI data. *Neurosci Lett* **499**, 47-51, doi:10.1016/j.neulet.2011.05.030 (2011).

84 Sreenivasan, K. *et al.* Altered functional network topology correlates with clinical measures in very early-stage, drug-naïve Parkinson's disease. *Parkinsonism Relat Disord* **62**, 3-9, doi:10.1016/j.parkreldis.2019.02.001 (2019).

85 Sreenivasan, K. *et al.* Topological reorganization of functional hubs in patients with Parkinson's disease with freezing of gait. *J Neuroimaging* **33**, 547-557, doi:10.1111/jon.13107 (2023).

86 Suo, X. *et al.* Functional Brain Connectome and Its Relation to Hoehn and Yahr Stage in Parkinson Disease. *Radiology* **285**, 904-913, doi:10.1148/radiol.2017162929 (2017).

87 Suo, X. *et al.* Brain functional network abnormalities in parkinson's disease with mild cognitive impairment. *Cereb Cortex* **32**, 4857-4868, doi:10.1093/cercor/bhab520 (2022).

88 Tang, Y. *et al.* Altered Functional Brain Connectomes between Sporadic and Familial Parkinson's Patients. *Front Neuroanat* **11**, 99, doi:10.3389/fnana.2017.00099 (2017).

89 Tuovinen, N. *et al.* The reorganization of functional architecture in the early-stages of Parkinson's disease. *Parkinsonism Relat Disord* **50**, 61-68, doi:10.1016/j.parkreldis.2018.02.013 (2018).

90 van Balkom, T. D., van den Heuvel, O. A., Berendse, H. W., van der Werf, Y. D. & Vriend, C. Eight-week multi-domain cognitive training does not impact large-scale resting-state brain networks in Parkinson's disease. *Neuroimage Clin* **33**, 102952, doi:10.1016/j.nicl.2022.102952 (2022).

91 Vancea, R. *et al.* Cognitive performance in mid-stage Parkinson's disease: functional connectivity under chronic antiparkinson treatment. *Brain Imaging Behav* **13**, 200-209, doi:10.1007/s11682-017-9765-0 (2019).

92 Wang, H. *et al.* Disrupted topologic efficiency of brain functional connectome in de novo Parkinson's disease with depression. *Eur J Neurosci* **58**, 4371-4383, doi:10.1111/ejn.16176 (2023).

93 Wright, N. *et al.* Elevated caudate connectivity in cognitively normal Parkinson's disease patients. *Sci Rep* **10**, 17978, doi:10.1038/s41598-020-75008-6 (2020).

94 Wu, C. *et al.* Dynamic Network Connectivity Reveals Markers of Response to Deep Brain Stimulation in Parkinson's Disease. *Front Hum Neurosci* **15**, 729677, doi:10.3389/fnhum.2021.729677 (2021).

95 Yuan, J. & He, Y. Adoption of deep learning-based magnetic resonance image information diagnosis in brain function network analysis of Parkinson's disease patients with end-of-dose wearing-off. *J Neurosci Methods* **409**, 110184, doi:10.1016/j.jneumeth.2024.110184 (2024).

96 Zhang, D., Liu, X., Chen, J. & Liu, B. Distinguishing patients with Parkinson's disease subtypes from normal controls based on functional network regional efficiencies. *PLoS One* **9**, e115131, doi:10.1371/journal.pone.0115131 (2014).

97 Zhang, D., Wang, J., Liu, X., Chen, J. & Liu, B. Aberrant Brain Network Efficiency in Parkinson's Disease Patients with Tremor: A Multi-Modality Study. *Front Aging Neurosci* **7**, 169, doi:10.3389/fnagi.2015.00169 (2015).

98 Zhu, X. *et al.* Abnormal Topological Network in Parkinson's Disease With Impulse Control Disorders: A Resting-State Functional Magnetic Resonance Imaging Study. *Front Neurosci* **15**, 651710, doi:10.3389/fnins.2021.651710 (2021).

99 Diao, Y. *et al.* Individual Structural Covariance Network Predicts Long-Term Motor Improvement in Parkinson Disease with Subthalamic Nucleus Deep Brain Stimulation. *AJNR Am J Neuroradiol* **45**, 1106-1115, doi:10.3174/ajnr.A8245 (2024).

100 Guo, T. *et al.* Alterations of Brain Structural Network in Parkinson's Disease With and Without Rapid Eye Movement Sleep Behavior Disorder. *Front Neurol* **9**, 334, doi:10.3389/fneur.2018.00334 (2018).

101 Pereira, J. B. *et al.* Aberrant cerebral network topology and mild cognitive impairment in early Parkinson's disease. *Hum Brain Mapp* **36**, 2980-2995, doi:10.1002/hbm.22822 (2015).

102 Samantaray, T., Saini, J., Pal, P. K. & Gupta, C. N. Brain connectivity for subtypes of parkinson's disease using structural MRI. *Biomed Phys Eng Express* **10**, doi:10.1088/2057-1976/ad1e77 (2024).

103 Suo, X. *et al.* Topologically convergent and divergent morphological gray matter networks in early-stage Parkinson's disease with and without mild cognitive impairment. *Hum Brain Mapp* **42**, 5101-5112, doi:10.1002/hbm.25606 (2021).

104 Suo, X. *et al.* Disrupted morphological grey matter networks in early-stage Parkinson's disease. *Brain Struct Funct* **226**, 1389-1403, doi:10.1007/s00429-020-02200-9 (2021).

105 Tang, C. *et al.* Distinct serum GDNF coupling with brain structural and functional changes underlies cognitive status in Parkinson's disease. *CNS Neurosci Ther* **30**, e14461, doi:10.1111/cns.14461 (2024).

106 Wang, E. *et al.* Abnormal Topological Organization of Sulcal Depth-Based Structural Covariance Networks in Parkinson's Disease. *Front Aging Neurosci* **12**, 575672, doi:10.3389/fnagi.2020.575672 (2020).

107 Wu, Q. *et al.* Large-scale cortical volume correlation networks reveal disrupted small world patterns in Parkinson's disease. *Neurosci Lett* **662**, 374-380, doi:10.1016/j.neulet.2017.10.032 (2018).

108 Xie, Y. *et al.* Morphologic brain network predicts levodopa responsiveness in Parkinson disease. *Front Aging Neurosci* **14**, 990913, doi:10.3389/fnagi.2022.990913 (2022).

109 Xu, J. *et al.* Abnormalities in Structural Covariance of Cortical Gyrification in Parkinson's Disease. *Front Neuroanat* **11**, 12, doi:10.3389/fnana.2017.00012 (2017).

110 Xu, X. *et al.* Brain Atrophy and Reorganization of Structural Network in Parkinson's Disease With Hemiparkinsonism. *Front Hum Neurosci* **12**, 117, doi:10.3389/fnhum.2018.00117 (2018).

111 Yadav, S. K. *et al.* Gender-based analysis of cortical thickness and structural connectivity in Parkinson's disease. *J Neurol* **263**, 2308-2318, doi:10.1007/s00415-016-8265-2 (2016).

112 Yan, S. *et al.* Impaired topological properties of cortical morphological brain networks correlate with motor symptoms in Parkinson's disease. *J Neuroradiol* **51**, 101155, doi:10.1016/j.neurad.2023.09.007 (2024).

113 Bočková, M. *et al.* Cortical network organization reflects clinical response to subthalamic nucleus deep brain stimulation in Parkinson's disease. *Hum Brain Mapp* **42**, 5626-5635, doi:10.1002/hbm.25642 (2021).

114 Bosch, T. J., Espinoza, A. I., Mancini, M., Horak, F. B. & Singh, A. Functional Connectivity in Patients With Parkinson's Disease and Freezing of Gait Using Resting-State EEG and Graph Theory. *Neurorehabil Neural Repair* **36**, 715-725, doi:10.1177/15459683221129282 (2022).

115 Fogelson, N. *et al.* Functional connectivity abnormalities during contextual processing in schizophrenia and in Parkinson's disease. *Brain Cogn* **82**, 243-253, doi:10.1016/j.bandc.2013.05.001 (2013).

116 Formaggio, E. *et al.* Reduced Effective Connectivity in the Motor Cortex in Parkinson's Disease. *Brain Sci* **11**, doi:10.3390/brainsci11091200 (2021).

117 Hassan, M. *et al.* Functional connectivity disruptions correlate with cognitive phenotypes in Parkinson's disease. *Neuroimage Clin* **14**, 591-601, doi:10.1016/j.nicl.2017.03.002 (2017).

118 Li, Z. *et al.* Abnormal Functional Brain Network in Parkinson's Disease and the Effect of Acute Deep Brain Stimulation. *Front Neurol* **12**, 715455, doi:10.3389/fneur.2021.715455 (2021).

119 Mehraram, R. *et al.* Weighted network measures reveal differences between dementia types: An EEG study. *Hum Brain Mapp* **41**, 1573-1590, doi:10.1002/hbm.24896 (2020).

120 Peláez Suárez, A. A. *et al.* EEG-Derived Functional Connectivity Patterns Associated with Mild Cognitive Impairment in Parkinson's Disease. *Behav Sci (Basel)* **11**, doi:10.3390/bs11030040 (2021).

121 Rajagopal, K., Naseri, N., Parastesh, F., Ghassemi, F. & Jafari, S. Phase synchronization analysis of EEG functional connectivity in Parkinson's disease. *J Theor Biol* **598**, 111997, doi:10.1016/j.jtbi.2024.111997 (2025).

122 Revankar, G. S. *et al.* Prestimulus Low-Alpha Frontal Networks Are Associated with Pareidolias in Parkinson's Disease. *Brain Connect* **11**, 772-782, doi:10.1089/brain.2020.0992 (2021).

123 Stylianou, O. *et al.* Scale-Free Functional Brain Networks Exhibit Increased Connectivity, Are More Integrated and Less Segregated in Patients with Parkinson's Disease following Dopaminergic Treatment. *Fractal Fract* **6**, doi:10.3390/fractalfract6120737 (2022).

124 Utianski, R. L. *et al.* Graph theory network function in Parkinson's disease assessed with electroencephalography. *Clin Neurophysiol* **127**, 2228-2236, doi:10.1016/j.clinph.2016.02.017 (2016).

125 Vecchio, F. *et al.* Graph Theory on Brain Cortical Sources in Parkinson's Disease: The Analysis of 'Small World' Organization from EEG. *Sensors (Basel)* **21**, doi:10.3390/s21217266 (2021).

126 Wang, C. *et al.* Network disruption based on multi-modal EEG-MRI in α-synucleinopathies. *Front Neurol* **15**, 1442851, doi:10.3389/fneur.2024.1442851 (2024).

127 Yin, N. *et al.* A study of brain networks associated with Freezing of gait in Parkinson's disease using transfer entropy analysis. *Brain Res* **1821**, 148610, doi:10.1016/j.brainres.2023.148610 (2023).

128 Zhang, J., Villringer, A. & Nikulin, V. V. Dopaminergic Modulation of Local Non-oscillatory Activity and Global-Network Properties in Parkinson's Disease: An EEG Study. *Front Aging Neurosci* **14**, 846017, doi:10.3389/fnagi.2022.846017 (2022).

129 Zhang, W. *et al.* Analysis of Brain Functional Network Based on EEG Signals for Early-Stage Parkinson's Disease Detection. *Ieee Access* **10**, 21347-21358, doi:10.1109/access.2022.3150561 (2022).

130 Chen, D. *et al.* Brain Network and Abnormal Hemispheric Asymmetry Analyses to Explore the Marginal Differences in Glucose Metabolic Distributions Among Alzheimer's Disease, Parkinson's Disease Dementia, and Lewy Body Dementia. *Front Neurol* **10**, 369, doi:10.3389/fneur.2019.00369 (2019).

131 Ji, G. J. *et al.* Regional and network properties of white matter function in Parkinson's disease. *Hum Brain Mapp* **40**, 1253-1263, doi:10.1002/hbm.24444 (2019).

132 Ko, J. H., Spetsieris, P. G. & Eidelberg, D. Network Structure and Function in Parkinson's Disease. *Cereb Cortex* **28**, 4121-4135, doi:10.1093/cercor/bhx267 (2018).

133 Li, W. *et al.* The reconfiguration pattern of individual brain metabolic connectome for Parkinson's disease identification. *MedComm (2020)* **4**, e305, doi:10.1002/mco2.305 (2023).

134 Liu, C. *et al.* Brain Functional and Structural Signatures in Parkinson's Disease. *Front Aging Neurosci* **12**, 125, doi:10.3389/fnagi.2020.00125 (2020).

135 Olde Dubbelink, K. T. *et al.* Disrupted brain network topology in Parkinson's disease: a longitudinal magnetoencephalography study. *Brain* **137**, 197-207, doi:10.1093/brain/awt316 (2014).

136 Wang, M. B., Boring, M. J., Ward, M. J., Richardson, R. M. & Ghuman, A. S. Deep brain stimulation for parkinson's disease induces spontaneous cortical hypersynchrony in extended motor and cognitive networks. *Cereb Cortex* **32**, 4480-4491, doi:10.1093/cercor/bhab496 (2022).

137 Jin, C. *et al.* Altered Degree Centrality of Brain Networks in Parkinson's Disease With Freezing of Gait: A Resting-State Functional MRI Study. *Front Neurol* **12**, 743135, doi:10.3389/fneur.2021.743135 (2021).

138 Jiji, G. W., Rajesh, A. & Lakshmi, M. M. Diagnosis of Parkinson’s disease using EEG and fMRI. *Multimedia Tools and Applications* **82**, 14915-14928, doi:10.1007/s11042-022-14042-0 (2023).

139 Xiao, P. *et al.* Combined brain topological metrics with machine learning to distinguish essential tremor and tremor-dominant Parkinson's disease. *Neurol Sci* **45**, 4323-4334, doi:10.1007/s10072-024-07472-1 (2024).

140 Lu, W., Song, T., Li, J., Zhang, Y. & Lu, J. Individual-specific metabolic network based on (18)F-FDG PET revealing multi-level aberrant metabolisms in Parkinson's disease. *Hum Brain Mapp* **45**, e70026, doi:10.1002/hbm.70026 (2024).

141 Akgüller, Ö., Balcı, M. A. & Cioca, G. Functional Brain Network Disruptions in Parkinson's Disease: Insights from Information Theory and Machine Learning. *Diagnostics (Basel)* **14**, doi:10.3390/diagnostics14232728 (2024).